Probing the drug interactome by chemical proteomics

Eiwit-Medicijn Interacties bestudeerd met Chemical Proteomics

Probing the drug interactome by chemical proteomics

Eiwit-Medicijn Interacties bestudeerd met Chemical Proteomics

(met een samenvatting in het Nederlands)

Proefschrift

ter verkrijging van de graad van doctor aan de Universiteit Utrecht
op gezag van de rector magnificus, prof.dr. J.C. Stoof, ingevolge
het besluit van het college voor promoties in het openbaar te
verdedigen op donderdag, 29 oktober 2009 des middags te 12.45
uur

door

Poupak Dadvar

geboren op 14 september 1976, te Teheran, Iran

Promotor: Prof. Dr. A.J.R. Heck

The work described in this thesis was financially supported by Pfizer Global Research and Development, Sandwich, United Kingdom.
Financial support from the J.R. Jurriaanse Stichting and UIPS for printing this thesis is kindly acknowledged.

To my Parents

On the cover: A painting made by Poupak from the vase with irises of Van Gogh

contents

Chapter 1 Introduction 9

Chapter 2 A chemical proteomics based enrichment technique targeting the interactome of the PDE5 inhibitor PF-4540124 43

Chapter 3 Phosphatidylethanolamine binding proteins, including the Raf kinase inhibitor protein exhibit affinity for the phosphodiesterase-5 inhibitor PF-3717842 65

Chapter 4 Target profiling of a small library of PDE5 inhibitor derivatives using chemical proteomics 85

Chapter 5 Summary/Samenvatting 105

Dankwoord 115

Curriculum Vitae 119

Chapter 1

General Introduction

I. PDE family and PDE5 inhibitors 10

II. Identification of drug interactome 26

III. Scope and outline of this thesis 38

I. PDE family and PDE5 inhibitors

Cyclic nucleotides: Structure, physiological function in NO signaling

Cellular metabolism and regulation of gene expression are important results of extracellular signals. These signals are composed of different chemical origins such as polypeptides, steroids and amino acids, which interact with their cognate receptors. Hormone signals are commonly converted at the cell membrane to second messengers. The second messenger concept was coined after the discovery of the cyclic nucleotides 3′,5′-cyclic monophosphate (cAMP) and guanosine 3′,5′-cylcic monophosphate (cGMP) in 1957 and 1963, respectively. These cyclic nucleotides are introduced as ubiquitous intracellular second messengers and mediate the response of cells to a variety of extracellular stimuli. They activate a cell signaling cascade through the activation of cyclic nucleotide-dependent protein kinases (PKA and PKG), cyclic nucleotide gated ion channels (CNG), GTP-exchange factors (Epac) and their downstream effector systems[1]. A number of second messenger-synthesizing and -degrading enzymes regulate second messenger levels[2]. Adenylyl and guanylyl cyclases (AC and GC) synthesize cAMP and cGMP, from ATP and GTP, respectively, whereas 3′,5′-cyclic nucleotide phosphodiesterases (PDEs) degrade cyclic nucleotides. Conclusively, AC/GC and PDEs control the amplitude and duration of cyclic nucleotide signals[1]. Endothelial-derived relaxant factor (EDRF) was discovered as a small molecule, which is produced in endothelial cells and causes the relaxation of the adjacent smooth muscle[3]. This discovery was followed by the exploration of the cGMP production system[4,5]. Later recognition of arterial natriuretic peptide (ANP) as stimulus for cGMP production was established as well. EDRF, later surprisingly identified as nitric oxide, (NO) activates the soluble form of guanylyl cyclase (sGC), whereas ANP is the stimulus for the transmembrane form of guanylyl cyclase (pGC) (Figure 1). In the NO/cGMP signaling pathway,

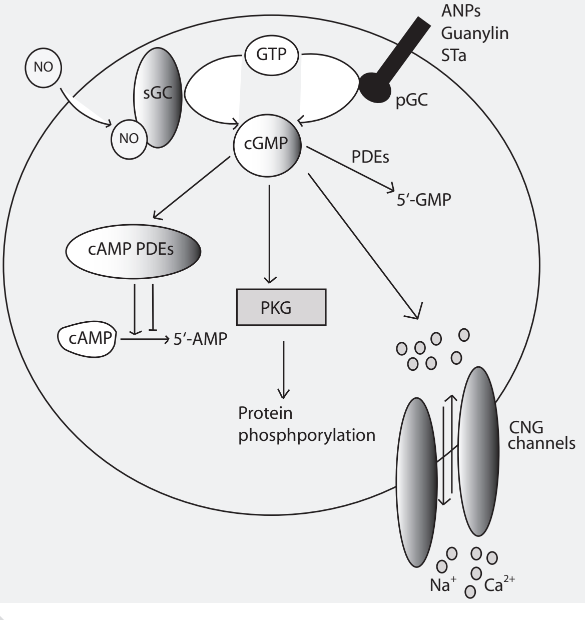

Figure 1. Basic mechanism of cGMP regulation and function. This cartoon shows the synthesis and regulatory pathway of cGMP metabolism. The main mechanism of the synthesis of cGMP by guanylyl cyclases (sGC and pGC), its regulation by PDEs and the main receptors of cGMP are depicted. cGMP is degraded by specific PDEs and when cGMP is present at high concentration, it stimulates the PDEs' activity by allosteric binding to their regulatory domain in a negative feedback mechanism[1].

NO is endogenously produced by NO synthases[6]. Upon activation of sGCs and/or pGC, synthesis of cGMP from GTP is increased. sGC is activated by NO, whereas pGC is activated by the binding of specific peptides such as arterial natriuretic peptide (ANP), guanylin and heat-stable enterotoxin of E. coli (STa)[6] (Figure 1). The resultant cGMP regulates three kinds of effector proteins including PKG, CNGs and PDEs. These mediate protein phosphorylation, cation influx across the plasma membrane, and cyclic nucleotide catabolism, respectively. The most prominent physiological consequence of this signaling pathway is vasodilation caused by smooth muscle relaxation[7]. Other consequences of NO/cGMP signaling are inhibition of platelet aggregation, regulation of neurotransmission, immune defense, and stimulus-secretion coupling. After a general introduction about cyclic nucleotides, their downstream effectors and their role in the vasodilation of the vascular smooth muscle cells, the first part of this thesis will focus on one specific PDE namely PDE5, and PDE5 inhibitors involved in regulation of smooth muscle relaxation and penile erection. The emergence of PDE5 inhibitors as effective therapy for erectile dysfunction, emphasizes the potential of specific PDEs to serve as important therapeutic targets. However, the unbiased profiling of the interaction of these inhibitors in a target cell/tissue is essential to further improve the selectivity and potency of these inhibitors. The introduction ends with a description of emerging sensitive chemical proteomics techniques, which indeed may be used to probe drug interaction profiles.

Molecular targets of cAMP and cGMP

Cyclic nucleotides have a few targets in the cell, primarily the family of phosphodiesterases (PDEs), cAMP dependent kinase (PKA), cGMP dependent kinase (PKG), exchange protein directly activated by cAMP (Epac), and several cyclic nucleotide-gated channels (CNGs). Most studies to date have focused on PKA and PKG, that are directly activated by cAMP and cGMP, respectively[6]. These kinases control diverse functional cellular responses such as intracellular calcium, cell proliferation, inflammation, and transcription. The localization of PKA and PKG is largely determined by scaffold proteins called A kinase anchoring proteins (AKAPs) or G kinase anchoring proteins (GKAPS), which participate in intracellular signaling compartmentalization. CNGs transduce changes in intracellular concentrations of cyclic nucleotides into changes in membrane potential and Ca^{2+}concentration[8]. In an attempt to find the cAMP-mediated regulation of Ras – proximity 1 (Rap1), (a member of the Ras family of small guanine triphosphatase (GTPases)), Epac was identified. Epac mediates several cAMP signaling pathways in cells. Cellular actions of cAMP which are mediated by Epac, include regulation of exocytosis, the control of cell adhesion, growth, division and differentiation[9]. Although PKA and Epac may function independently as cAMP effectors, they provide a mechanism to accurately control the cAMP signaling pathway in an integrated fashion[10]. An important biological function of PKG is vasodilation of smooth muscle cells as described in more detail in the following part.

cGMP and PKG influence vasodilation in vascular smooth muscles cells (VSMCs)

Hormonal and neural stimuli regulate the contractility of vascular smooth muscle cells (VSMCs) in a dynamic fashion, which in turn determines local blood pressure. The cytosolic Ca^{2+}-concentration, $[Ca^{2+}]_{cyt}$, directly controls VSMC tension. Contraction is initiated by a rise in $[Ca^{2+}]_{cyt}$, whereas a decrease in $[Ca^{2+}]_{cyt}$ results in relaxation. Two sources of Ca^{2+} include: (I) Ca^{2+} released from the endoplasmic reticulum (ER) via Inositol 1,4,5-Triphosphate (IP_3) or ryanodine receptors, and (II) extracellular Ca^{2+} imported via Ca^{2+} chanals. When the $[Ca^{2+}]_{cyt}$ is increased, the ubiquitous Ca^{2+}-interactor calmodulin (CaM) is activated. The latter activated molecule in turn activates myosin light chain kinase (MLCK), which causes phosphorylation of the regulatory myosin light chain (rMLC). The resulting phosphorylated molecule causes contraction. Phosphorylation/dephosphorylation of the 20 kDa rMLC is the major regulatory mechanism of smooth muscle tension (Figure 2)[11]. Myosin light chain phosphatase (MLCP) dephosphorylates rMLC, which leads to relaxation of VSMCs. Two pathways are known for MLCP inhibition: (I) through the small

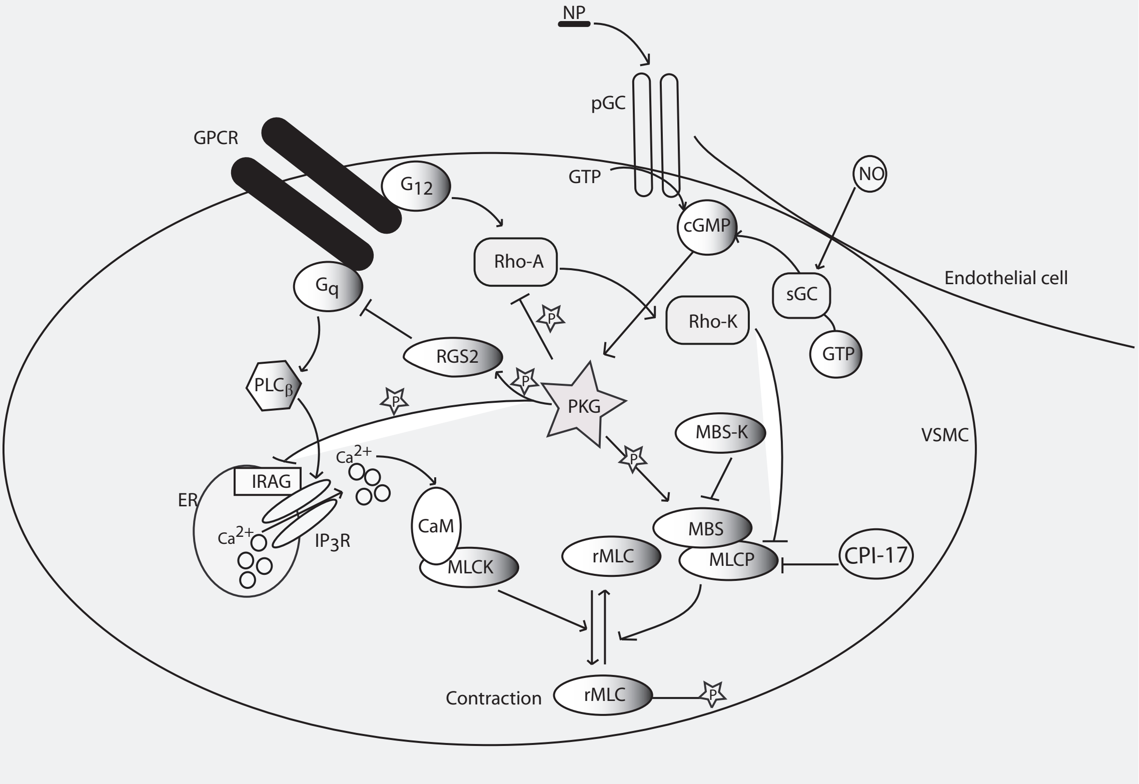

Figure 2. Vasodilatory effects of cGMP and PKG in the regulation of vascular smooth muscle function. The influence of cGMP and PKG to regulate the balance between phosphorylated and de-phosphorylated rMLC is present at multiple levels. Phosphorylation of the regulatory myosin light chain (rMLC) by the respective kinase leads to the vasoconstriction, whereas dephosphorylation of rMLC by the phosphatase MLCP causes vasorelaxation[131-135].

GTPase Ras homolog gene family (RhoA), when translocation of GTP-bound RhoA to the plasma membrane leads to the activation of Rho-kinase (Rho-K). The latter kinase inhibits MLCP by acting on its regulatory subunit, and (II) phosphorylation of a novel heat-stable protein termed 17 KDa peptide namely protein-kinase C-potentiated myosin phosphatase inhibitor (CPI-17), which inhibits the catalytic subunit of MLCP (i.e. PP1c)[12,13]. Besides these other proteins such as protein kinase C, calmodulin-dependent kinase II, integrin-associated kinase, and mitogen-activated protein kinase control the steady-state level of rMLC phosphorylation at a constant [Ca^{2+}]cyt[11]. Alternatively, a direct effect enhances Ca^{2+} sensitivity of the contractile apparatus (i.e. 'Ca^{2+} sensitization'). Figure 2 also shows two phosphorylation events that prevent the inactivation of MLCP. These events involve the phosphorylation of the myosin binding subunit (MBS). MBS-kinase (MBS-K) controls MBS by phosphorylation, leading to inactivation of MBS. The inactivated state of MBS leads to inactivation of MLCP and hence contraction. In the aforementioned mechanism, when PKG phosphorylates MBS, this prevents phosphorylation of MBS by MBS-K that would inhibit rMLC phosphorylation, thereby causing vasodilation[14]. Another vasodilatory pathway controlled by PKG, is via the phosphorylation of RhoA/RhoA-K, thereby inhibiting MLCP. PKG can also influence vasodilation through inhibition of Ca^{2+}-release from the ER (Figure 2). IRAG (IP$_3$R associated PKG substrate) described as a PKG-anchoring protein (GKAP) binds to PKG and IP$_3$R to induce IP$_3$R phosphorylation by PKG. Upon phosphorylation of IP$_3$R, the molecule is inactivated and Ca^{2+} outflow in the cytosol is decreased. Another pathway depicted in figure 2, involves regulation of G-protein signaling 2 (RGS2), which is phosphorylated by PKG and subsequently terminates the G-protein coupled receptor (GqPCR) signaling through extracellular contractile agonists and IP$_3$[15].

The superfamily of phosphodiesterases (PDEs)

Cyclic nucleotide phosphodiesterases are a family of related phosphohydrolases that selectively catalyze the hydrolysis of the 3' bond of adenosine/guanosine 3',5'cyclic monophosphates (Figure 3). The enzymes hydrolyzing the 3' bonds are grouped into class I PDEs, whereas class II enzymes can additionally catalyze

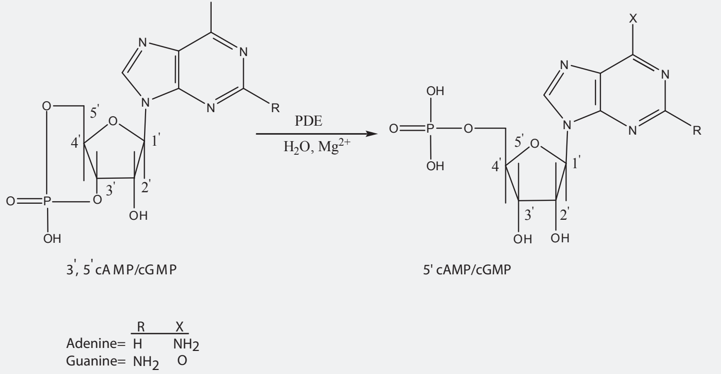

Figure 3. Cyclic nucleotide hydrolysis by phosphodiesterase. The hydrolysis of the 3′ cyclic phosphate bond of adenosine or the guanosine's 3′,5′ cyclic monophosphate is depicted.

Table 1. Biochemical and pharmacological characteristics of cyclic nucleotide phosphodiesterase (PDE) isoenzymes.

Family	Gene	Substrate	Tissue localization	Inhibitor	IC50 (µM)	Regulators	Consequence of inhibition
PDE1	PDE1A	cAMP/cGMP	Brain, heart	Vinpocetine,	20	Ca^{2+}-CaM	Hypotention
	PDE1B		smooth muscle	8-methoxy methyl-IBMX	4	PKA, CaMKII	
	PDE1C		olfactory cilia, testis	IC224	0.08		
				SCH51866	0.013 to 0.1		
PDE2	PDE2A	cGMP\cAMP	Adrenal Cortex, brain	EHNA	1	cGMP	Unknown
			heart	Trequinsin,	0.64-2		
				BAY 60-7550	0.0047		
				IC933	0.004		
				PDP	0.0006		
PDE3	PDE3A	cAMP>cGMP	Heart, adipose tissue	Cilostamide	0.005	cGMP, PKA	Inotrope, arrhythmia
	PDE3B		pancreas, platelets	Enoximone	1	PKB	
				Cilostazol	0.12		
				Imazodan	6		
				OPC-33540	0.0003 to 0.0015		
				Trequinsin	0.0003		
				Milrinone	0.3		
PDE4	PDE4A	cAMP	many tissues	Rolipram	2	PKA, PKC	anti-inflammatory
	PDE4B			Roflumilast	0.0008		
	PDE4C			AWD 12-281	0.0097		
	PDE4D			YM976	0.002		
				Ro 20-1724	0.002		
				Cilomilat	0.12		
				V-11294A	0.405		
				SCH351591	0.058		
PDE5	PDE5A	cGMP	Lung, platelets, smooth	Sildenafil (Viagra)	0.004	PKA, PKG,	Vascular relaxation
			muscle, corpus	Vardenafil (Levitra)	0.0007	cGMP	
			cavernosum	Tadalafil (Cialis)	0.005		
				Dipyridamole	0.9		
				Zaprinast	0.76		
				DA-8159	0.006		
				T-1032	0.001		
				T-0156	0.0002		
				DMPPO	0.003		
PDE6	PDE6A	cGMP	Rod and cone	Sildenafil (Viagra)	0.074	Transducin	Visual disturbance,
	PDE6B		photoreceptor outer	Vardenafil (Levitra)	0.011	PDE6 γand α	retinitis pigmentosa
	PDE6C		segments	Tadalafil (Cialis)	5.1	subunits	
				Zaprinast	0.15		
				Dipyridamole	0.38		
PDE7	PDE7A	cAMP	Skeletal muscle, T-cells,	Dipyridamole	9 to 42	Unknown	Inhibition of T-cell activation
	PDE7B		B-cells	BRL 50481	0.62		
				IC242	0.37		
PDE8	PDE8A	cAMP	Testis, liver, thyroid	Dipyridamole	4.5	Unknown	Unknown
	PDE8B						
PDE9	PDE9A	cGMP	kidney	Sildenafil,	7	Unknown	Unknown
				Zaprinast	29		
				BAY 73-6691	0.055		
PDE10	PDE10A	cAMP/cGMP	Testis, brain	Dipyridamole	1.1	PKA	Unknown
PDE11	PDE11A	cAMP/cGMP	Skeletal muscle, prostate	Dipyridamole	0.82-1.8	Unknown	Unknown
				Zaprinast	5 to 28		

the hydrolysis of the phosphodiester bond. The substrate selectivity of class I and class II enzymes is significantly different[16]. The PDEs form a superfamily of at least 21 different gene-families (Table 1) comprising more than 50 different gene products[17]. Due to alternative splicing or alternative start site variants, there are even more PDE linked mRNAs which have yet not been annotated. The major families of PDE, listed in table 1 have been delineated based primarily on two criteria: (1) the specific kinetic properties of the enzymes for hydrolyzing cAMP and cGMP, and (2) the mechanism for regulation of PDE activity[18,19]. The kinetic properties are partly determined by the selective affinity of the PDEs for cAMP or cGMP, which are related to the Michaelis Menten constant (K_m) values. Functions of PDEs are not only restricted to control the intracellular level of cyclic nucleotides, PDEs can additionally serve as scaffolding proteins in multiprotein complexes wherein they can affect protein-protein interactions through allosteric interactions. Besides genetic differences in the PDEs, they can also be differentially regulated by biochemical mechanisms such as phosphorylation/dephosphorylation, cGMP/cAMP binding to the regulatory domain, binding of Ca^{2+}/calmodulin, and other PDE-protein interactions. Some examples for mechanism of regulation by protein association include activation of PDE1 and PDE6 by Ca^{2+} /calmodulin (CaM) binding and transducin, respectively[20, 21]. Three PDE families that are primarily regulated by cGMP include PDE2, PDE3, and PDE5[16, 22]. PDE2 and PDE3 are found in cells in both soluble and membrane-associated forms, whereas PDE5 has so far only been observed as a soluble enzyme. PDEs that hydrolyze cGMP with high affinity include PDE5 and PDE6. The PDE5 and PDE6 isoenzymes also known as cGMP-specific PDEs display a much higher selectivity for cGMP over cAMP. Although both of these PDEs have high affinity for cGMP, they exhibit distinct structures, function and different tissue distributions. PDE5 is a homodimer containing both regulatory and catalytic domains, while PDE6 is a heterotetramer containing one α-subunit (PDE6A), one ß-subunit (PDE6B), and two γ-subunits[23]. PDE5 is mostly expressed in smooth muscle, including lung and corpus cavernosum, whereas PDE6 is quite specifically found in the retina. Generally, PDEs have been linked to various diseases such as inflammation, asthma, vascular disease, diabetes, erectile dysfunction[24] and are therefore considered to be attractive targets for pharmacological intervention.

Phosphodiesterase type 5 (PDE5), domains organization and regulation

PDE5, which has also been named cGMP-PDE, cGMP-binding cGMP-specific phosphodiesterase (cG-BPDE), or PDE V was originally identified, isolated and characterized as a cGMP binding protein co-purifying with a cGMP-phosphodiesterase from rat platelets[25, 26] and later also detected in rat lung tissue [27,28]. As mentioned above PDE5 is a homo-dimer of two 93 kDa subunits, which are composed of 3 distinct domains, a catalytic domain and two highly homologous regulatory domains, so called GAF domains (GAF-A and GAF-B) as schematically depicted in figure 4A. The GAF-A domain of PDE5 is characterized as the high-affinity cGMP binding domain (KD < 40 nM)[29] and binds 100 times more selective

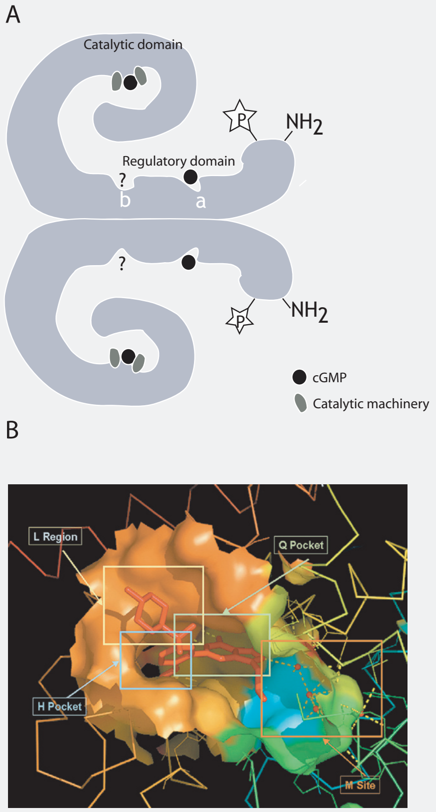

Figure 4. Schematic model of PDE5 and surface representation of the active site of PDE5 occupied by PDE5 inhibitor sildenafil. **A**) Each PDE5 subunit contains a catalytic domain and a regulatory domain. The regulatory domain in the amino terminal portion contains the phosphorylation site and two GAF subdomains. The catalytic domain contains two Zn^{2+} binding motifs (shown as catalytic machinery) and a cGMP-binding substrate site. **B**) The active site of binding is divided into four subsites: a metal-binding site (M site), core pocket (Q pocket), hydrophobic pocket (H pocket) and lid region (L region) (adapted from reference[24]).

to cGMP than cAMP. Rybalkin et al.[22] have suggested a vital role of GAF-A in ligand binding, modulating activity of the enzyme. Phosphorylation of a proximate serine (serine 92 in the bovine enzyme) by PKG would stabilize binding of cGMP to this domain[30, 31]. Actually, cGMP binding to PDE5 stimulates phosphorylation hence stabilizing the catalytic activity of this enzyme[30-33]. Phosphorylation can also occur when cGMP levels are high, which results in an increase of the cGMP affinity to the GAF-A domain. A conserved sequence, namely NK/RX(5-14)FX3DE contributes to cyclic nucleotide binding in the GAF domains[34, 35]. N and C-terminal truncation mutagenesis studies have shown that the GAF domains take part in the PDE5 dimerization[36]. It was later suggested that GAF-A is the only site for cGMP binding in PDE5A. Mutational analysis also indicated the crucial role of F205 for cGMP binding to the GAF-A domain[37]. PDE5 activation was prevented and basal activity was decreased when a monoclonal antibody specific for the GAF-A domain prohibited cGMP binding, therefore non-activated cGMP free PDE5 seems to have low intrinsic catalytic activity[22]. In addition, the NMR solution structure of the cGMP-bound PDE5A GAF-A domain revealed the importance of the Asp-196 residue (PDE5A, mouse) for nucleotide binding[38]. Much less is known about the specific role of the GAF-B domain, but this domain seems to play a role in the dimerization, the sequestration of the phosphorylation site and the inhibition of cGMP binding to the GAF-A domain[39]. However, recombinant PDE5-

GAF-B (a glutathione S-transferase fusion protein) was not able to bind cGMP[40]. The catalytic domain (human PDE5) contains three helical sub-domains, an N-terminal cyclin–fold region, a linker part and a C-terminal helical bundle[41]. Four main sub-sites in the catalytic domain include (1) the hydrophobic pocket (H pocket), (2) the core pocket (Q pocket), (3) the metal-binding site (M site), and (4) the lid region (L region). cGMP binding to the catalytic site shares little similarity with the allosteric binding. Scanning mutagenesis studies revealed the importance of nine residues (His603, Asn604, His607, His643, Asp644, His647, Glu672, Asp714, and Asp754) for catalysis in PDE5 (from bovine lung)[42], while Tyr602 and Glu775 are involved in cGMP binding. Some divalent metal cations such as Zn^{2+}, Mn^{2+}, Co^{2+}, and Mg^{2+} increase the catalytic activity of PDE5, from which Zn^{2+} already at lower concentrations enhances the activity[42]. Phosphorylation has been reported to be able to further regulate PDE5 activity. After phosphorylation of PDE5 by PKA/PKG at Ser 102 (in human PDE5) and a change in the conformation of the enzyme, the in vitro activity was observed to be increased (Figure 5)[31].

The structural basis for PDE5 selectivity and binding of inhibitor

The molecular mechanism of cyclic nucleotide specificity (cAMP versus cGMP) has been an important subject in structural studies on PDE5. Apparently, an invariant glutamine (Gln) residue is the key specificity determinant in several PDEs, wherein it stabilizes the binding of the purine ring in the binding pocket[43]. The γ-amino group of the conserved Gln residue can adopt two different orientations. Free rotation of this glutamine seems to be important for appropriate hydrogen binding between PDEs and cyclic nucleotides. In PDEs with high selectivity for cAMP (e.g. PDE1B), this glutamine is oriented in a way that cAMP binding is favored, whereas in cGMP selective PDEs (e.g. PDE5A) the position of the glutamine is turned into an orientation (rotated by nearly 180 degrees) more appropriate for cGMP interaction (Figure 6). Glutamine should be capable of free rotation in dual selective PDEs. Sildenafil (Viagra) was the first phosphodiesterase-5 (PDE5) inhibitor approved by the Food and Drug Administration (FDA). The crystal structure of PDE5 bound

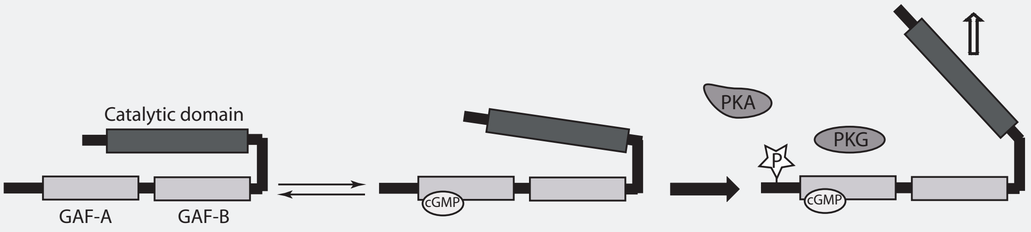

Figure 5. Regulation of enzymatic activity in PDE5. The conformational change of PDE5 shows alteration of enzymatic activity. Upon the allosteric binding of cGMP, phosphorylation by PKA and PKG is promoted, which activates the catalytic function. This activation is indicated by the open upward arrow[17].

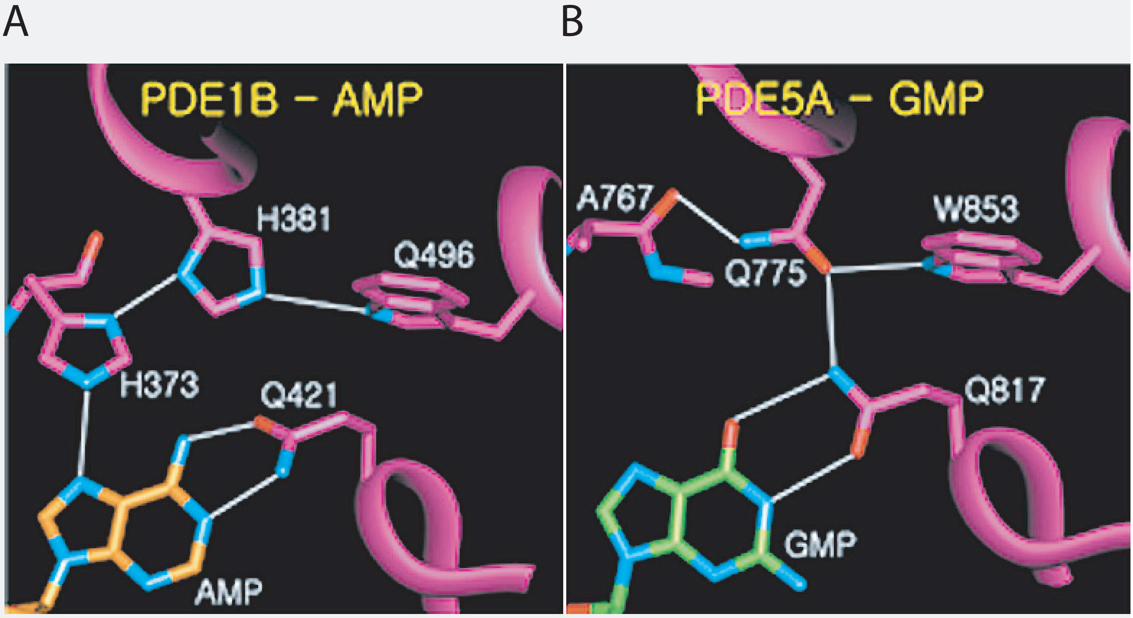

Figure 6. The glutamine switch mechanism recognizes the purine moiety in cAMP or cGMP. (A) Q421 recognizes AMP in the model of cAMP bound to PDE1B. (B) Q817 recognizes cGMP in PDE5[24].

to sildenafil, a competitor of cGMP, was resolved to get insight into the binding mode of sildenafil. According to the crystal structure[43], the core pocket (Q pocket) in the catalytic domain of PDE5 contains the described Gln residue and the pyrazolopyrimidinon group of sildenafil binds to this Q pocket (Figure 4B). The pyrazolopyrimidinon group of sildenafil mimics the guanosine group in cGMP and has the same characteristics of a bidentate hydrogen bond with Q817 (the invariant glutamine) through its amide moiety. The hydrophobic H pocket accommodates the ethoxyphenyl moiety of sildenafil and the L-region of PDE5A interacts with the methylpiperazine group. The high-resolution crystal structure of PDE5 bound to sildenafil revealed that the pyrazolopyrimidinon group of sildenafil stacks against Phe820 and contacts residues Tyr612, Val782, Ala767, and Gln817. The O1 and N4 atoms in this moiety form two hydrogen bonds with Nε2 and Oε1 of Gln817, respectively. The ethoxyphenyl moiety has van der Waals interactions with Val782, Ala783, Phe786 and Leu804. The methylpiperazine group interacts with Met816, Ala823, Tyr664 and Gly819. The oxygen atoms of the sulfonyl group contacts mainly Phe820 (Figure 7)[41, 44]. High affinity interaction of the PDE5 inhibitors is influenced/regulated by many different amino acids. Using titrations with ^{3}H-labeled catalytic site specific inhibitors (i.e. sildenafil, vardenafil and tadalafil), it was found that upon substrate (or inhibitor) binding PDE5 may adopt another conformation, whereby the low affinity substrate binding site converts to a high affinity binding site. Hence, the PDE5 inhibitor not only directly converts the catalytic site of PDE5 into a higher affinity site but also blocks cGMP hydrolysis, which leads to the intended increased level of cGMP[45-47].

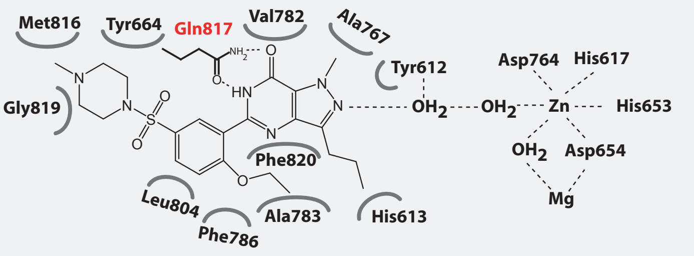

Figure 7. The structure of bound sildenafil to the PDE5 active site. The PDE5 interacting residues with each moiety in sildenafil are represented. The side chain of Gln 817 is shown interacting with the pyrimidone moiety via the hydrogen bonds. Bound water molecules bridge sildenafil to the metals[41].

Biological function of PDE5

PDE5 has an important role in the control of intracellular levels of cGMP by converting it to GMP, thereby mediating the NO/cGMP relaxing effect. Furthermore, PDE5 is involved in the control of pulmonary resistance and has been identified in the pulmonary artery[48]. Activation of this enzyme in pulmonary hypertention was observed by Hanson et al.[49]. PDE5 expression is high in the lung, followed by the heart and cerebellum (localized in cerebellar purkinje neurons) as revealed by western blot analysis in mouse tissues[6]. PDE5 was also found in isolated cardiomyocytes and in dog and human platelets [50-52]. An important role in regulation of platelet aggregation has been suggested for this enzyme[53, 54]. In the human genome three closely related PDE5 genes have been annotated, of which one has been experimentally unambiguously identified at the protein level. The three variants in the genome are named PDE5A1, PDE5A2 and PDE5A3, each especially differing in their N-terminal region (Figure 8). They share identical first exones and a sequence of 823 amino acids. Two different promoters have been recognized as the regulators of PDE5A1 and PDE5A2. It seems that the exon of PDE5A3 is transcribed by the same promoter as PDE5A1[55, 56]. Transcripts of PDE5A1 and PDE5A2 have been detected in a wide variety of tissues, but significant PDE5A3 expression has only been found in vascular smooth muscle[56]. With such little information, it is not surprising that little is known about the specific function of these PDE5 isoforms.

Why are PDEs potential drug targets?

PDEs are important regulators of second messenger levels and the rate of cyclic nucleotides degradation is higher than their maximum rate of synthesis. This higher maximum degradation velocity enhances the effect of PDE targeting. PDEs exhibit a broad range of expression in different tissues and possess each a unique architecture around their active site that makes specific target

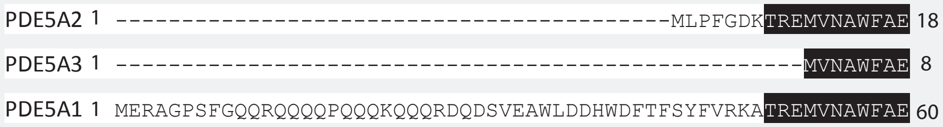

```
PDE5A2 1 ------------------------------------------MLPFGDKTREMVNAWFAE 18

PDE5A3 1 ----------------------------------------------------MVNAWFAE  8

PDE5A1 1 MERAGPSFGQQRQQQQPQQQKQQQRDQDSVEAWLDDHWDFTFSYFVRKATREMVNAWFAE 60
```

Figure 8. Multiple sequence alignment of PDE5A1-3 (human). The N-terminal part differs by three isozymes and the rest of the proteins are identical. This alignment was obtained using CLUSTALW protein sequence alignment tool.

inhibition possible. The latter property is of great importance in the design and synthesis of PDE selective inhibitors. Concentration of PDE substrates (cyclic nucleotides) in the cell is in the range of 1-10 µM, which indicates that a competitive inhibitor does not need to be present at high concentrations to compete with the substrates[16]. As mentioned before the PDE family of enzymes has been linked to a broad range of pathological conditions such as sexual dysfunction (PDE5), neurodegenerative diseases (PDE1), vascular disease and diabetes (PDE3) and rheumatoid arthritis and osteoporosis (PDE4)[24]. These links make the PDEs attractive pharmacological targets.

PDE5 inhibitors

Already in the late 1950s, Sutherland and Rall[57] investigated the mechanism on how caffeine increased the effect of glucagon (i.e. a stimulator of adenylyl cyclase) on cAMP accumulation and glycogenolysis in the liver, suggesting inhibition of PDE activity. Since that time, synthesis of caffeine analogues as nonselective PDE inhibitors, such as IBMX, began. Important herein was the quest to enhance the selectivity of such inhibitors to a distinct PDE. Nowadays, It is known that the inhibitory effect of caffeine is partly due to its similar structure to cGMP, which is a natural substrate of some PDEs (Figure 9). Quite a variety of PDE inhibitors have been developed that target specific PDEs, summarized in Table 1. As shown in Table 1, a few inhibitors display cross-talk against several PDEs, such as sildenafil and vardenafil for both PDE5 and PDE6, which is likely due to the high homology of the respective binding domains. In the mid-1980s, discovery and clinical development of different vasodilators was initiated being part of a cardiovascular research program of Pfizer in Sandwich, UK[58]. Somewhat later, in a research program to find drugs for angina pectoris, novel pyrazolopyrimidines were identified as potent inhibitors of PDE5. The novel compounds did not show the expected therapeutic effects in angina but seemed to have an attractive therapeutic effect in erectile dysfunction caused by selective PDE5 inhibition. PDE5 inhibitors bind to the catalytic domain of PDE5 and block cGMP degradation. Moreover, PDE5 inhibitors ensure maximal erectogenesis and stimulate their own potencies[59-61]. This is achieved via a positive feedback mechanism, as PDE5 inhibition also prohibits cGMP allosteric binding[62]. PDE5 inhibitors also increase platelet cGMP levels, hence the inhibitory effect of NO on platelet aggregation and secretory function is reinforced[53, 54]. Due to differences in pharmacokinetic profiles of clinically used PDE5 inhibitors different patients are best treated by one drug over the other[63]. Despite the high prevalency of erectile dysfunction, relatively few men had sought treatment for erectile dysfunction before the introduction of sildenafil[64]. Nowadays, sildenafil, vardenafil and tadalafil are three related drugs, approved by the FDA, to treat erectile dysfunction (Figure 9). Vardenafil has a rather similar chemical structure to sildenafil. The pyrazolopyrimidinon in sildenafil is modified to imidazotriazinone in vardenafil and also vardenafil

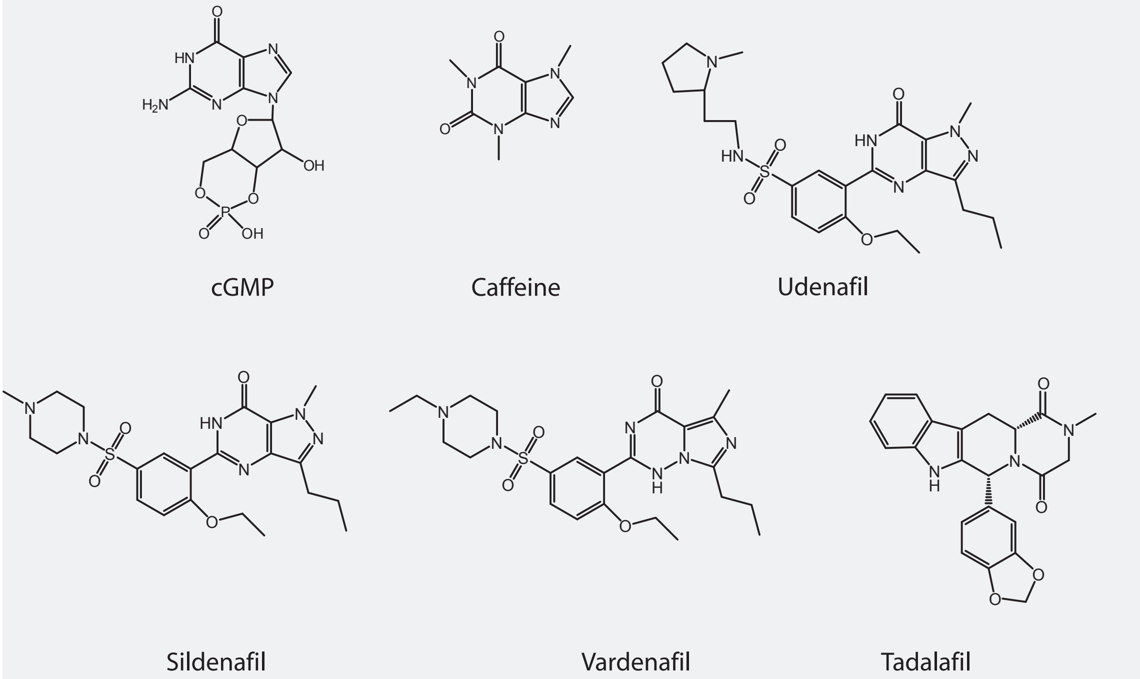

Figure 9. The chemical structure of caffeine, cGMP, sildenafil, vardenafil, tadalafil and udenafil. Caffeine compares in structure to the guanidine in cGMP. Sildenafil and vardenafil have a similar chemical structure, whereas the structure of tadalafil is different, showing more rigidity. A new PDE5 inhibitor namely udenafil is also depicted, which has a very similar structure to sildenafil and vardenafil.

contains an ethylpiperazin moiety in place of a methylpiperazine of sildenafil. Tadalafil has quite a different chemical structure and contains a more heterocyclic rigid structure. Evidently, the pharmacokinetics and pharmacodynamics of these drugs are affected by these chemical differences[65]. Although sildenafil, vardenafil and tadalafil are structurally different, all target PDE5 at approximately the same binding site and competitively inhibit cGMP hydrolysis resulting in the relaxation of vascular smooth muscle. Relative potencies in vitro have been demonstrated to be vardenafil > tadalafil > sildenafil[47]. The higher potency of vardenafil over sildenafil is most likely due to differences in the heterocyclic rings[47] and the stronger hydrophobic bonds between Tyr612 and vardenafil[66]. Another determinant of vardenafil potency and of influence for the observed selectivity between vardenafil and sildenafil is Gln817, which emphasizes the particular importance of a bidentate H-bond with the inhibitors[67]. Tadalafil has a different binding mode in comparison with sildenafil and vardenafil. Tadalafil does not make any interaction with the L region of PDE5 and makes also different interactions with the Q pocket of PDE5. However, in tadalafil binding the side chain of Gln 817 makes a single, not bidentate, hydrogen bond with the NH group[41].

Erectile dysfunction and PDE5 targeting

Erectile dysfunction (ED) is a highly prevalent disorder in middle-aged men and is strongly related to other health factors. Erection is a hemodynamic event and is regulated by vascular tone and blood-flow balance in the penis. Nitric oxide (NO) is the principal neurotransmitter that mediates penile erection. Local release of NO occurs in the nerves terminating in the penile tissue and also in the vascular and sinusoidal endothelium of the penis[60, 68]. Upon stimulation of a man either physically or psychologically, nitric oxide (NO) is released from endothelial cells, non-cholinergic, and non-adrenergic neurons in the penis. Soluble guanylyl cyclase is activated by the diffused NO and produces cGMP from GTP. Elevated cGMP levels cause PKG (cGMP-dependent protein kinase) activation, thereby initiating several phosphorylation cascades, as outlined earlier and shown in Figure 10. These signaling pathways could ultimately lead to a decrease in intracellular calcium concentration and dilation of the arteries bringing blood to the penis and compression of the spongy corpus-cavernosum tissue. The resulted contracted veins, reduce the outflow of blood and increase intracavernosal pressure, resulting in penile erection[69-71]. Nitric oxide signaling is mediated by cGMP and therefore indirectly poised by PDE5. PDE5 is a highly expressed protein in the corpus cavernosum and its cGMP hydrolyzing activity, has a direct effect on cGMP availability[60]. PDE5 is involved in the opposite function of corporal smooth muscle contraction, inducing penile flaccidity. Upon binding of an inhibitor to PDE5, cGMP levels are elevated leading to a decrease in intracellular calcium concentration and enhanced relaxation of smooth muscle and ultimately an increased arterial inflow followed by venous congestion causing erection[72].

Therapeutic effects of PDE5 inhibition in pulmonary and cardiovascular diseases

Pulmonary Arterial Hypertension (PAH) is defined as a persistent elevation in pulmonary arterial pressure (PAP) with normal left-sided pressures. PAH is characterized by increased pulmonary vascular resistance due to increased vascular tone and structural remodeling of pulmonary vessels[73]. PDE5 and PDE1 are the main enzymes that are necessary for inactivation of cGMP in vascular smooth muscle cells[22]. PDE5 is a highly expressed enzyme in pulmonary vascular smooth muscle of pulmonary arteries and veins, bronchial blood vessels and airway smooth muscle[74]. Increased abundance of PDE5 in the vessels of hypertensive lungs suggests that PDE5 limits vasodilation in hypertensive lungs. Consequently, when sildenafil inhibits PDE5, pulmonary vascular resistance can

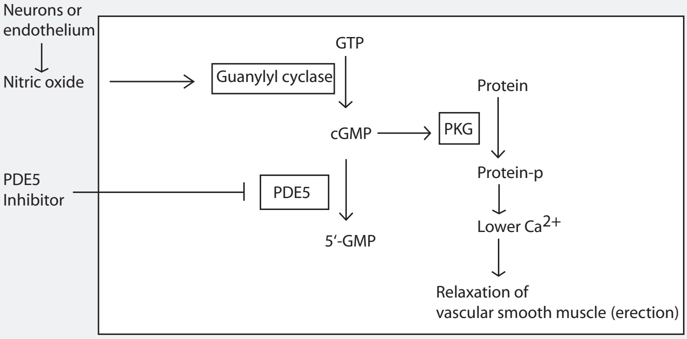

Figure 10. The basic mechanism of NO/cGMP signaling leading to the relaxation of vascular smooth muscle cell and erection. Nitric oxide is a physiologic signal molecule essential to penile erection, which stimulates guanylyl cyclase to synthesize cGMP. cGMP in turn activates PKG leading to the activation of a phosphorylation cascade and erection. PDE5 inhibitor selectively increases cGMP in penile erectile tissue by inhibiting PDE5.

be reduced in subjects with hypoxic-induced pulmonary hypertention or severe pulmonary hypertension[75]. In 2005, sildenafil was approved under the trade name revatio by the FDA as a treatment of PAH. Pulmonary hypertension can introduce some difficulties in the management of patients undergoing cardiac surgery[76]. Interestingly, when sildenafil was added to a pre-existing regiment of nitrosovasodilation in patients with pulmonary hypertension following cardiac surgery, marked pulmonary vasodilation occurred[76]. On the other hand, hypoxic pulmonary hypertension and vascular remodeling are features of moderately severe Chronic Obstructive Pulmonary disease (COPD). As PDE5 inhibition with sildenafil and stimulation of the cGMP pathway of pulmonary artery smooth muscle cells inhibited cell proliferation and promoted apoptosis of these cells, this could have some beneficial effects on vascular remodeling[77]. Therefore, PDE5 inhibitors may offer some therapeutic effects in COPD. An extra therapeutic effect of sildenafil has been reported and clinically approved in heart failure and cardiac hypertrophy. Hypertrophy and pathological remodeling are induced by sustained cardiac pressure overload. Takimoto et al. have shown that sildenafil could suppress chamber and myocyte hypertrophy in mice due to blocking of the intrinsic catabolism of cGMP[78]. Hence, they propose that PDE5 inhibition may provide a new treatment strategy for cardiac hypertrophy and remodeling.

Principles in drug action

Most drugs affects the rate at which an existing biological function (e.g. enzymatic reaction) proceeds. Two basic concepts in the full understanding of clinical drug action are pharmacokinetics and pharmacodynamics. Pharmacokinetics is the study of ‘what the body does to the drug’. In detail, pharmacokinetics describes the time course of the drug concentration in the body after administration of a certain dosage regimen. In general, after administration of a drug into the body, it is delivered into the systemic circulation (absorption). Subsequently it is then transported and taken up into different organs and tissues (distribution). The chemical alteration of a drug known as metabolism may occur rather early, before the drug performs its action or later after they have reached the specific tissue/organs. The final removal of a drug from the body is defined as excretion[65]. Another element described often in pharmacokinetics is the volume of distribution, which is the theoretical volume of fluid into which the total administrated drug would have to be diluted to produce the concentration in plasma. Pharmacodynamics explains ‘what the drug does to the body’ and it describes the intensity of a drug effect (at the target site) in relation to the concentration in the body fluid[65].

Pharmacokinetics of sildenafil, vardenafil and tadalafil

Absorption and distribution

The absorption rate of all three above described PDE5 inhibitors is fast. Vardenafil reaches peak concentrations earlier in comparison with the other.

After inhibitor administration, the onset time is usually 30-120 min for sildenafil and vardenafil. An onset time of 30-120 min post-dose has also been reported for tadalafil. While the necessary time to reach the maximum concentration is slightly longer compared with sildenafil and vardenafil, the rate and extent of absorption of tadalafil seems not to be affected by the use of a high-fat meal. Consumption of a high-fat meal decreased the rate of absorption for the other two drugs. The volume of distribution of the inhibitors is high and exceeds total volume of body water, which indicates possibly binding to extravascular proteins. After intravenous administration, the mean volume of distribution has been reported to decrease in the order from vardenafil > sildenafil > tadalafil. All three inhibitors can be bound to some highly abundant plasma proteins, namely albumin, α1-acid glycoprotein and lipoproteins[65].

Metabolism and elimination

In the metabolism of PDE5 inhibitors the cytochrome P-450 (CYP) system, which metabolizes drugs by oxidative pathways, plays a major role. CYP enzymes are located in the liver, intestine, lungs but also in other organs. The cyp3A subfamily found in the human liver and intestine can metabolize sildenafil, vardenafil and tadalafil. There are some extra enzymes participating in the metabolic pathway of some of these inhibitors. The main active metabolite of sildenafil is N-desmethyl sildenafil (UK-103320) that still possesses 50% of the sildenafil inhibitory potency (for PDE5). The main active metabolite of vardenafil possessing 28% of the inhibitory potency of the original compound is called M1. Methylcatechol glucuronide is the major circulating metabolite of tadalafil and has 10000-fold less affinity for PDE5 compared to tadalafil. Hepatic metabolism, is the main route in the elimination of all PDE5 inhibitors, while renal excretion contributes to 1% of the elimination pathway. All three mentioned inhibitors become extensively metabolized after oral administration. These metabolites are mainly excreted in the feces and to a lesser extent in the urine. Drug clearance is defined as the volume of plasma that would contain the amount of drug excreted per a unit of time. The total body clearance rates of sildenafil and vardenafil are nearly the same being 41 l/h and 56 l/h, respectively. Tadalafil clearance is much lower, i.e. 2.5 l/h, determined in healthy subjects. Tadalafil is, in contrast to sildenafil and vardenafil, classified as a drug with low hepatic extraction ratio. Half-life is another pharmacokinetic property of a drug which accounts for the required time for the plasma concentration to decrease by one-half. The half lives of elimination for sildenafil and vardenafil are in the same range as 3-5h and 4-5 h, respectively, while tadalafil possesses the longest half life, namely 14.5h. Due to the long half life, tadalafil is detected in plasma even 5 days after oral administration. Doses of these inhibitors can be adjusted based on efficacy and tolerability. The recommended dose for sildenafil is about 25 mg to 100 mg. Vardenafil and tadalafil can be taken in the range between 5 to 20 mg. The recommended administration time for all three is about 60 min before sexual activity[65, 79].

Pharmacodynamics of sildenafil, vardenafil and tadalafil

The pharmacodynamics of these three inhibitors depends on their potency and selectivity towards PDE inhibition. Based on the variable potency and selectivity for PDEs, the inhibitors may show differences in their side effect profiles. Among them, vardenafil has the highest potency to inhibit PDE5 as the reported IC50 value (the drug concentration needed to inhibit half of the maximum of PDE5 activity) was relatively high. The IC50 values for sildenafil and vardenafil were measured as 3.5-8.5 nM and 0.1-0.7 nM, respectively. Selectivity is a more predominant characteristic as it may have a direct relationship with the side effects of the drug. As shown in table 1, weak affinity of PDE5 inhibitors to the other PDE targets PDE6, PDE1 and PDE11 could cause some side effects such as transient abnormal vision, flushing and myalgia (muscle pain). Sildenafil and vardenafil may obviously bind easier to PDE1 than tadalafil (see table 2). Moreover, tadalafil shows also less selectivity towards PDE6, which is highly desired in these kind of drugs as sildenafil (the first marketed drug for erectile dysfunction) suffers from its selectivity for this isozyme causing visual side effects[80,81]. The PDE inhibition profile of tadalafil, the most selective PDE5 inhibitor, may be the cause for the diminished visual side effects compared with sildenafil and vardenafil. Consumption of tadalafil can induce myalgia and back pain, which is apparently due to its higher affinity for PDE11 (which is highly abundant in skeletal muscle tissue). In general, the side effects of clinically approved PDE5 inhibitors are described as headache, flushing, rhinitis, dyspepsia and myalgia, which are a reflection of the vasodilatory effects on the capillary smooth muscle in other parts of the body[81-84]. Lower doses of PDE5 inhibitors are therefore recommended after concomitant medications namely, ketoconazole, itraconazole, erythromycin, clarithromycin, cimetidine and HIV protease inhibitors. There are also some medications such as rifamin, rhenobarbital, phenytoin and carbamazepin that demand consumption of higher doses of PDE5 inhibitors. Generally different PDE5 inhibitors provide a versatile spectrum and side effects and therefore patients who fail with their initial choice of treatment, will not necessarily fail with higher or lower doses of one of the other inhibitors[85].

Novel alternative PDE5 inhibitors

Next to the three well-known inhibitors of PDE5 still new compounds are synthesized with similar activity. An example of a new PDE5 inhibitor is udenafil

Table 2. Selectivity of PDE5 inhibitors. Selectivity of PDE5 inhibition is expressed as a ratio between the IC50 for a given PDE and the IC50 for inhibition of PDE5. Tadalafil is clearly more selective than sildenafil or vardenafil towards PDE5 relative to PDE6 inhibition[65].

	Selectivity ratio of PDE family										
Drug	PDE1	PDE2	PDE3	PDE4	PDE5	PDE6	PDE7	PDE8	PDE9	PDE10	PDE11
Sildenafil	41	>1000	>1000	>1000	1	7.4	>1000	>1000	>1000	447	203
Vardenafil	136	>1000	>1000	>1000	1	15	>1000	>1000	>1000	>1000	346
Tadalafil	>1000	>1000	>1000	>1000	1	780	>1000	>1000	>1000	>1000	7.1

(DA-8159)[86], which is available in South Korea and is synthesized based on the sildenafil chemical structure, in which the ethoxyphenyl moiety is replaced by the propoxy phenyl moiety and methylpiperazin group was modified to 1-methyl-2-pyrrolidinyl-ethylamine. Udenafil is a long-acting drug with a half life of 11-13 hours and also has a similar selectivity profile to sildenafil. It has been reported by Lee et al.[87] that udenafil does not inhibit PDE11, which is involved in myalgia and testicular toxicity. Other new developed (pro)-drugs for PDE5 inhibition include mirodenafil, lodenafil, lodenafil carbonate, avanafil, and SLX-2101. Discussion about their pharmacological properties is beyond the scope of this thesis. Next to the inhibition of PDE5 other key-players in the NO signaling pathway could be targeted, especially as the basic cause of erectile dysfunction could also lay on the deficiency of other members of NO signaling pathway such as the calcium-activated potassium channels (BKca). In an animal study, after injection of the complementary DNA for BKca channels, an enhanced erection event could be detected[88], which shows the importance of each molecular target of NO in the efficient occurrence of the erection. Such observations provide new insights to consider the targeting of other members of cGMP signaling pathway to reach new therapeutic strategies, that are beyond inhibition of PDE5.

II. Identification of drug interactome

Important properties of drugs

Potency and efficacy

Potency describes the amount of drug (drug dose) required to produce an effect. For instance, if 5 mg of drug A reduce the blood pressure as effectively as 10 mg of drug B, drug A is twice as potent as drug B. Efficacy is related to the potential maximum therapeutic response that a drug can produce. For instance, if drug A eliminates much more salt and water through urine than drug B, it means that drug A has greater efficacy than drug B. However, greater potency or efficacy could not always be interpreted in a higher preferability. Considerable factors in choosing a drug are; side effects, potential toxicity, duration of effect and costs.

Selectivity, specificity, and sensitivity

The words selectivity, specificity, and sensitivity are terms often used simultaneously and/or inconsistently in pharmaceutical literature. Each of these terms represents a different phenomenon and should not be used interchangeably. Mencher et al. defined these terms as described below[89]. Selectivity indicates the ability of a drug to affect a particular population; for example a gene, protein, a signaling pathway or a cell, in preference to others. Therefore, a selective drug is capable to discriminate between, and affect only, one population, which then produces an event. Specificity describes the capacity of a drug leading to a particular action in a population. Therefore, a drug of absolute specificity of action might either decrease or increase a specific function of a given gene or protein or cell type. In contrast to the two aforementioned terms, sensitivity is the capacity of a population, to respond to a drug's ability at a specified dose. The sensitivity of a responding system is high, when a smaller dose is required to produce an effect. Among the explained properties of a drug, selectivity is highly desired in drug discovery and development. For example, a chemotherapy drug used to treat prostate cancer should be highly selective meaning that the drug should affect prostate cancer cells and not affect nearby healthy prostate cells and other normal tissues. Another example includes the drugs treating erectile dysfunction, which should be highly selective for the PDE5 protein among the other members of the PDE family because PDE5 plays a specific role in the signaling of erectile function. An important class of drug targets in oncology and inflammation are protein kinases[90]. The study of new multi-kinase drugs has shown that kinase inhibitors can be conformation specific and also have multiple targets[91-94], but most of these drugs target the relatively conserved ATP-binding site of protein kinases and have been screened against a small group of many human protein kinases[95]. Therefore, there is a need to map the selectivity of protein kinase inhibitors in drug development programs. Selectivity is a critical issue for small-molecule kinase inhibitors[96-99], and the relationship between selectivity, kinome interaction patterns and biological activity needs to be elucidated during development of inhibitors[100]. Pharmaceutical industries use classical selectivity panels based on sequence homology considerations and speculate that sequentially similar kinases share inhibitor binding capabilities. It has been shown that sequence similarity among kinases does not correlate with inhibitor binding but structural homology from a compound's perspective could be taken into account to classify kinases as similar in their ligand binding profile[95]. Low selectivity to a desired target leads to the occurrence of side effects. Hence, it is of great importance to identify a drug interactome and be able to selectively rank the identified drug interactors. State-of-the-art chemical proteomics methods are now widely applied in the unbiased evaluation of selectivity on a proteome-wide scale.

Chemical proteomics

Identification of a drug's interactome followed by unraveling the selective interactions to understand the biological action of a drug and for further optimization of available drugs is a key consideration for pharmaceutical industries. A plethora of approaches and tools, such as recombinant protein array[101] and reverse docking approach[102], have been developed to facilitate this process. The absence of biological contexts in such methods results in the generation of an incomplete characterization of the drug's interactome. In recent years mass spectrometry-based chemical proteomics has been applied to profile the drug interactome in a more unbiased manner under more physiologically relevant conditions. Chemical proteomics combines affinity purification of targeted proteins with mass spectrometric analysis for identification of the captured proteins.

Chemical proteomics approaches for identification of a drug interactome can be divided in to two main categories: (I) immobilized molecules, which can be used for selective enrichment of the target interactome; (II) activity based protein profiling (ABPP), for which specific small molecular probes containing the drug structure are applied to covalently capture a distinct class of enzymatic proteins. The major sequential elements of chemical proteomics using immobilized molecules include: (1) enrichment of the total interactome of a drug using the immobilized modified drug on an affinity matrix directly from tissue/cell extract; (2) digestion of the captured interactome; (3) identification of the retrieved proteome by LC-MS/MS. The latter approach is the method of choice in our research and we will focus on it by giving some examples that explain its applicability in drug discovery. Hidaka and co-workers immobilized isoquinoline H-9 and successfully enriched for protein kinase C and cAMP- and cyclic GMP-dependent protein kinases (PKA and PKG)[103]. Later, flavopiridol, a CDK inhibitor, was immobilized on beads resulting in the identification of aldehyde dehydrogenase and glycogen phosphorylase as potentially novel target enzymes of this inhibitor[104,105]. SB 2033580, a p38 kinase inhibitor, was established as a rather selective inhibitor based on kinase selectivity panels[106,107]. Daub et al. used an affinity column with immobilized SB 203580 and after required optimization, selective separation of P38 inhibitor targets was achieved in different cell lines. They stated that the larger the amount of biological starting material (i.e. cells), the higher the probability to detect targets of low cellular abundance[95]. Kinase activity assays indicated that the newly identified targets such as Rip-like interacting CLARP kinase (RICK) were inhibited potently by SB 203580 in vitro. Conclusively, SB 203580 selectivity was highly overestimated based on derived data from kinase selectivity panels[106]. Chemical proteomics studies have provided an important means to unravel the inhibitor interacting proteins, but they do suffer from general limitations. It is worth mentioning that the obtained results for the immobilized molecule may not directly reflect the inhibitor selectivity because of the possible altered potency and selectivity due to the attachment of the linker. Moreover, the resulting binding profiles are biased towards abundant proteins[108].

Technical aspects of chemical proteomics

The first step in chemical proteomics is the enrichment of a drug interactome by using a pull-down affinity assay. This assay is based on specific and reversible molecular interactions between a biologically active structure (e.g. drug) and their binding proteins and enables isolation and analytical characterization of various purified interacting proteins[109]. Two essential prerequisites for this assay are: 1) A modified drug (drug candidate) with specific affinity to distinct interactors. 2) An affinity support suitable for the affinity isolation. An appropriate chemical reaction is necessary to couple the modified drug/inhibitor onto the beads. To enrich a drug interactome, the drug is modified and immobilized on the affinity support. The retained activity of the drug after modification and immobilization on the support is necessary for identification of true interactors. The resulting affinity bead binds to the interacting proteins in a cell/tissue extract and allows the isolation of a sub-proteome as the total drug interactome[110]. The captured interactome could be released from the beads by an elution step. A simple overview of affinity chromatography is illustrated in figure 11. The great advantage of this assay is that the selective capturing of the interacting proteins improves the dynamic range, which increases the possibility of the identification of the low abundant specific interactors in following MS analysis. Besides that, all types of cell/tissue could be used as the protein source for pull-down, in which the immobilized drug interacts with its endogenous targets.

Immobilization of affinity bait and the essential role of its concentration

One of the important factors affecting the bait-target binding is the covalent immobilization of the affinity bait on the affinity support. The presence of the affinity support should neither cause steric hindrance nor limitation in drug flexibility upon binding to the prey protein. A prerequisite for immobilization is the attachment of a reactive group to the bait by matrix coupling chemistries. Common activation methods for polysaccharide matrices include cyanogen bromide, epoxy, divinylsulfone, carbonyl diimidazole, organic sulphonyl chlorides, and N-hydroxy succinimide. Baits which contain amino groups, carboxyl groups, and phenolic groups can easily be coupled to the beads. With these generic chemistries, the coupling often results in random orientation and spacing of the immobilized bait. Drugs often contain moieties essential for activity, but also nonbinding groups in their structure. The non-binding sites can be used for covalent coupling. The information related to these non-binding moieties can be obtained from the 3D X-ray crystal or NMR structure of the drug bound to the target(s). When no high resolution structural data is available, the structure-activity relationship (SAR) data is usually sufficient to guide functional compound immobilization[95]. When the nonbinding domain of the drug does not offer sufficient molecular spacing between the binding domain (drug) and the affinity support, the covalent attachment of a spacer to the nonbinding domain of the drug is necessary. The spacer arm creates a link between the affinity support and

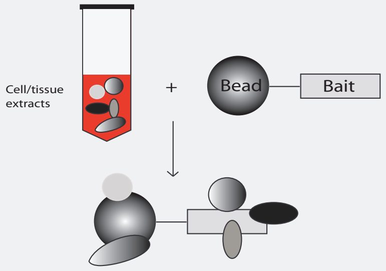

Figure 11. Overview of the chemical proteomics experiments. Cell/tissue extract is incubated with the bait and the total bait interactome is pulled down.

the drug. When the binding pockets are partially buried inside the inner structure of the protein the use of a spacer arm can increase the binding efficiency between the immobilized bait and the protein binding domain. Another important factor in bait-target binding is the concentration of the immobilized bait on the affinity support. A high bait density can encumber target binding between proximally immobilized baits due to the increased nonspecific adsorption, as this could lead to the formation of an anionic exchange support. Additionally, a low density of the immobilized bait gives space for non-specific interactions (Figure 12). The increased nonspecific adsorption of contaminant proteins onto the affinity support could diminish the purification efficiency due to co-elution of massive impurities with the specific interactors. On the other hand steric hindrance promoted by the interaction between each individual immobilized bait and the related binding pocket in the prey protein, disturbs the specific adsorption of the target protein (Figure 12)[111].

Different approaches to reduce and recognize nonspecific binding

The total interactome identified from a pull-down assay using a drug immobilized bead after MS analysis include; (I) a nonspecific interactome, which does not have any binding affinity to the drug, (II) a less specific interactome with a high initial abundance which has a weak affinity (in the high micromolar range) to the drug and (III) the specific interactome with a low initial abundance, which has a high affinity (nanomolar range) to the drug. Nonspecific interacting proteins in pull-down assays can be defined in two categories; (I) proteins which bind to affinity resins or spacer because of physical adsorption rather than specific binding. Seemingly, they interact with the resin through hydrophobic interactions[112], (II) high abundant proteins, housekeeping and structural proteins that stick to the captured proteins. As the reduction of nonspecific binding in chemical proteomics is of central importance in the identification of specific low abundant drug interactors, some strategies have been developed to circumvent or identify nonspecific binding events to the immobilized affinity beads. Tamura et al. have shown that a linear relationship exists between the amount of nonspecific protein binding and a descriptor of a compound's hydrophobicity (CLOGP). This factor could be calculated by the CLOGP program and was used to estimate the amount of nonspecific binding of tubulin to a specific affinity support. Based on this calculation, they designed a novel hydrophilic poly ethylene glycol (PEG) spacer to reduce nonspecific binding[112]. Additionally nonspecific binders tend to stick to hydrophobic affinity supports. Introduction of hydrophilicity on the surface of affinity resins is an alternative way to reduce nonspecific binders. After investigation of different affinity beads such as AffiGel, Toyoperal and Tenta Gel, the AffiGel support exhibited much less nonspecific binding attributed to the more hydrophilic characteristic of the AffiGel support[112]. Other options include using a buffer with a higher ionic strength or detergents to decrease background protein binding. A major disadvantage of

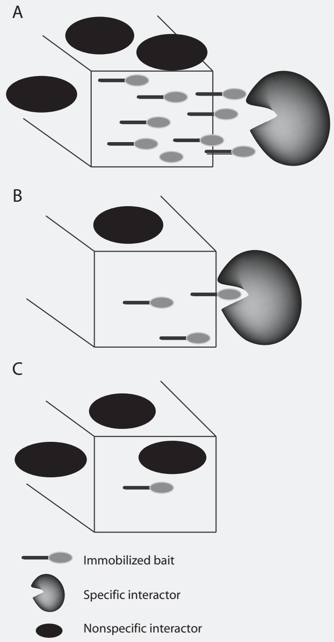

Figure 12. Effect of the density of the immobilized bait on the interaction of target proteins.
(A) High density immobilized bait, which avoids target binding and results in increased nonspecific binding. (B) Appropriate density of immobilized bait. (C) Too low density of immobilized bait, that leads to an increase in nonspecific binding.

these additives is that proteins could be denatured or dissociated from the bait compound. Competitive elution is another approach to reduce nonspecific binding in the target interactome. This method involves an aqueous solution of the active unimmobilized drug (free drug), which solely disturbs the specific interaction with the affinity resin competitively, but doesn't affect the nonspecific interaction. However, it is only applicable when the drug has a high solubility in an aqueous solution and the interaction has fast dissociation kinetics[113]. A schematic representation of competitive elution is shown in figure 13. Another alternative method for reduction of nonspecific binding is an affinity purification in a wider scale followed by the competitive elution of high affinity targets by 'free' inhibitor. Brehmer et al. applied a γ-phosphate-linkedATP-Sepharose to isolate all cellular purin binding proteins. Subsequently the relevant targets were competitively eluted by the kinase inhibitor of interest[114]. High throughput is a distinct advantage of this approach, but it avoids the identification of kinases with low affinity for ATP[115]. Sequential elution was introduced by Scholten et al. when they investigated the specific interactome of cGMP. An analogue of cGMP, 2-AH-cGMP (2′-(6-aminohexyl) guanosine-3′, 5′-cyclic monophosphate) was immobilized on sepharose beads followed by incubation with a HEK293 lysate or various tissue lysates. The ADP and GDP interacting proteins, which are known proteins with lower affinity to cGMP but with higher abundance, were sequentially pre-eluted using high concentrations of these nucleotides. Finally, the remaining high affinity interactome of cGMP on the beads was eluted by the SDS-sample buffer. PKGIα and PKA-RIα were identified as the specific bait interactors[116]. Another efficient approach to recognize binding of nonspecific interactors introduced by Yamamoto et al. is serial affinity chromatography. In this method, the affinity resin is added to the lysate and after removal of the first bead fraction, the same amount of fresh affinity resin is added to the lysate. Due to the low affinity and high abundance of nonspecific binders to the beads, the amount of nonspecific protein identified on the two resins is similar, while the amount of specific low-abundant interactors would significantly decrease in the second and/or third pull-down[113]. The prerequisite of this approach is the high affinity for the bait and low abundant prey protein. It is noteworthy that the amount of immobilized bait on the affinity support should be greater than the amount of specific binding protein. Using this approach, the interactome of FK506 affinity resins was analyzed and nonspecific binding proteins could be confidentially recognized[113]. One of the best approaches for recognition of nonspecific interactions is a comparative study using the small active structure of a drug and its inactivated structure as a negative control. The total interactome containing the specific and nonspecific interactors bind to the active drug, whereas the inactivated structure absorbs solely the nonspecific interactors. The specific interactome can be recognized by subtraction of interactome of the control from the total interactome. Although such an subtractive approach is quite ideal it is often not possible as the crystal structure of the active protein-drug complex is not often available, and the synthesis of such complex organic compounds can be difficult.

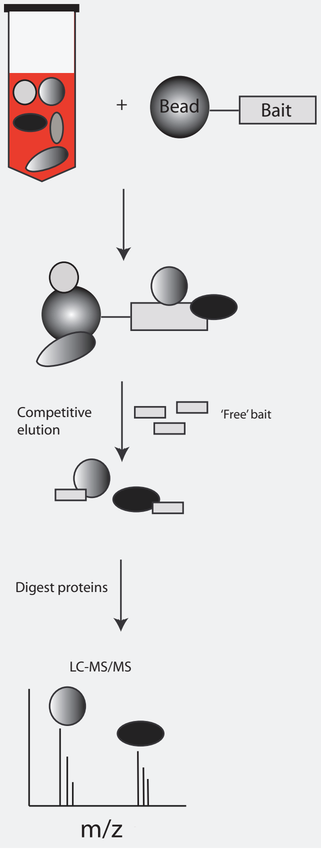

Figure 13. Competitive elution using an appropriate concentration of the free bait . After pull-down assays, a concentration of 'free' bait is added to the beads. The eluted proteins are proceeded to MS analysis for identification.

As a positive example, in an effort to identify ampicillin-binding proteins using a pull-down assay, an inactivated ampicillin was synthesized as a negative control by treatment of the drug with beta-lactamase, which opens the beta-lactam ring of ampicillin. This approach helped in the recognition of nonspecific interactors when a mild denaturing agent (sarcosyl) was used for elution of proteins bound to the inactivated ampicillin control beads[117].

Quantitative based approaches for recognition of specific drug interactomes

Identification of specific interactions with small molecules involves a delicate balance between selectivity and affinity. Stable isotope labeling is an accurate approach to distinguish specific from nonspecific background interacting proteins[118]. Stable isotope labeling can be carried out through metabolic labeling (SILAC) or chemical labeling (i.e. peptide/protein derivatization), both techniques are briefly introduced in the following part.

Stable Isotope Labeling by Amino acids in Cell culture (SILAC) in combination with pull-down affinity chromatography

Metabolic labeling was initially developed for total labeling of bacteria using ^{15}N-enriched cell culture medium[119] and later became more well-known by Mann and co-workers in the form of the stable isotope labeling by amino acids in cell culture (SILAC)[120]. SILAC involves growing two populations of cells, one in a medium which contains a ‘light’ (normal) amino acid and the other in a medium which contains a ‘heavy’ amino acid. Essential amino acids are chosen for the labeling to ensure that cells only incorporate the added, labeled amino acid into their proteome. The heavy amino acid can contain ^{2}H, ^{13}C, and ^{15}N in place of ^{1}H, ^{12}C, and ^{14}N, respectively. The result of incorporation of the heavy amino acids into a protein is a predicted mass shift of heavy labeled peptide compared to the light labeled peptide. The light and heavy labeled peptides only differ in their masses, therefore the peak intensities in the mass spectrometer directly reflect the relative abundance of the related peptides in their original sample. SILAC is used to monitor quantitative differences at the protein level between different conditions. An important advantage of SILAC metabolic labeling is that mixing of labeled and unlabelled proteomes occurs in the early stage before fractionation and purification steps, which does not result in the introduction of any error in quantification. Interestingly, a combination of SILAC and affinity pull-down assays has been reported by Schulze et al. in an approach to identify the interactome of immobilized peptides. The tyrosine-containing peptides mimicking a small part of the EGF receptor in the phosphorylated and unphosphorylated state were immobilized as active and inactive bait. The active and inactive bait were incubated with the same amount of heavy and light SILAC cell extracts, to pull-down interactors. Finally, differentially labeled forms of tryptic peptides originating from two interactomes were measured by mass spectrometry and the specific interacting proteins with the active bait were recognized by their large difference in peak intensities[121]. Later on, Ong et al. described the combination of SILAC and affinity pull-down chromatography for unbiased identification of small-molecule (SM)-protein interactions within cellular proteomes[120]. SILAC labeled lysates were used in pull-down experiments with SM-immobilized affinity beads in the presence or absence of 'free small molecule' to compare the relative enrichment of target proteins. Although the small molecules used here were kinase inhibitors, for which they identified specific protein targets, the technique seems amenable for other kind of inhibitors and/or drugs to unravel their specific interacting proteins. Conclusively, SILAC combined with modification-based affinity purification is a useful approach to recognize the nonspecific interactome of a drug, assisting in detection of the bonafide interactome.

Isotope labeling by chemical derivatization

In an alternative approach, peptides or proteins in a sample can be chemically labeled via derivatization of functional groups within their structures using stable isotope containing reagents. The samples are pooled and analyzed by mass spectrometry, after labeling. Reactive groups in proteins or peptides including the C and N-terminus, ε-amino groups of lysine residues, the carboxylic groups of the side chains of aspartic acid and glutamic acid residues or the thiol of the cysteine could be specifically labeled. Based on the available stable isotope containing reagents producing labeled species with a resolvable mass difference in the mass spectrometer, the differential isotopic labeling between two, three or four samples are possible. Chemical derivatization is applicable to any protein sample, including extracts from tissues or body fluids, whereas application of SILAC is only limited to the cells or mice as the protein source. Chemical labeling is also compatible to the used separation methods in proteome studies. One disadvantage of chemical labeling is that labeling and mixing of labeled and unlabelled proteomes occurs in the later stage in comparison with SILAC, which can introduce errors in quantification. For example, the ICAT approach is based on differential isotope labeling of the cystein residues in proteins with biotin containing tags, which allows the isolation of modified peptides by avidin affinity chromatography. Although this step reduces complexity by 10-fold, it reduces the sequence information of the proteins by almost the same factor[122]. In a relatively new approach termed isotope coded protein labeling (ICPL), all free amino groups in proteins can be isotopically labeled. Schmidt et al. have reported high accuracy and reproducibility of quantitation using this approach[123]. The iTRAQ labeling approach is based on the quantification of peptides by their MS/MS fragment of reporter ions. The iTRAQ molecule is composed of a reporter group, a mass balance group and a peptide reactive group. The overall mass of the reporter and balance components are kept constant resulting in an equal total mass of the isotopic iTRAQ molecules. Upon the fragmentation, the balance moiety is lost and the charge is retained by the reporter fragment[124].

An efficient isotope labeling method, which is nowadays used in combination with affinity pull-down experiments is stable isotope dimethyl labeling, which is further described below.

Stable-isotope dimethyl labeling

Reductive amination, also termed reductive alkylation, involves condensation of an aldehyde or ketone with an amine in the presence of a reducing agent. The reductive dimethylation of free amino groups uses formaldehyde as a tagging reagent and sodium cyanoborohydride as a reducing reagent. Formaldehyde reacts with the N-terminus, or an epsilon-amino group of a lysine residue of a peptide and produces the intermediate shiff base. Sodium cyanoborohydride reduces the intermediate product to a secondary amine, which subsequently follows an extra reductive alkylation to form a tertiary amine. Some of the proteolytic peptides (after tryptic enzymatic cleavage) contain lysine(s) in their structures (due to miss cleavages), resulting in the creation of two (or more) appropriate sites for dimethylation. This labeling strategy was first applied by Chen and co-workers for quantitative proteomics[125]. The N termini and lysine side chains of a peptide can be labeled by isotopomers of formaldehyde (i.e. d0- and d2-formaldehyde), which results in a mass shift of 28 or 32 Da per modified amino group (Figure 14). Upon dimethyl labeling, slight differences in chromatographic elution times were observed between d0- and d2-formaldehyde-treated peptides (i.e. isotopic effect), which could be due to the reduced interaction of the labeled peptide with the chromatographic support[126], however in daily use, these are minimal. Using stable isotope dimethyl labeling, Aye at al. showed that an immobilized cAMP analogue namely 8-AHA-2'-OMe-cAMP can selectively enrich for PKA-R type I rather than PKA-R type II. Using the dimethyl labeling approach allowed them to differentiate between specific and dual-specific AKAPs bound as the secondary interactors to the cAMP-immobilized affinity beads[127]. Interestingly, the dimethyl labeling method can provide quantitative analysis of three different states by employing three different isotopomers of formaldehyde. Boersema et al. have expanded the dimethyl labeling strategy applying two isotopomers of formaldehyde (d0- and d2-formaldehyde) to a method applying three formaldehyde isotopomers (d0- and d2- and d2,^{13}C-formaldehyde) to incorporate dimethyl labels at the alpha and epsilon-amino groups of the proteolytic peptides (Figure 14). In this way peptide triplets can be observed in the mass spectrum, displaying a mass difference of 4 Da for each amine site. This approach was also applied to distinguish the specific interactome of cAMP immobilized beads from nonspecific interactors, in three different conditions. As a result, PKA-RIIα was identified as the specific target of the cyclic nucleotide, whereas myosin 4 was identified as a non specific binder[128]. Furthermore, Hsu and the co-workers extended the binary dimethyl labeling method further to a set of four isotopic labeles. Multiplex labeling allows simultaneous monitoring of several time points, thereby facilitating the research of the dynamic events[126]. Overall the dimethyl labeling approach can be used to identify and quantify

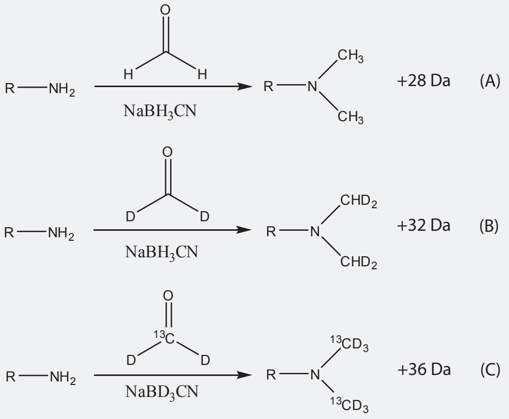

Figure 14. Overview of the dimethylation labeling strategy used to recognize the specific interactome of a drug. The labeling reagents are formaldehyde and sodium cyanoborohydride or their isotopomers. For quantitative comparison of two samples, steps A and B are used resulting in light labeled and heavy labeled peptides with 4 Da mass differences. For quantitative comparison of three samples, steps A,B and C are used producing light, intermediate and heavy labeled peptides with 4 Da mass differences[128].

important low abundant proteins.

Chemical proteomics, a promising strategy for generic drug target profiling

To help accelerate the development of new drugs, pharmaceutical companies have embraced a variety of new technologies. The clinical relevance and therapeutic efficacy of an inhibitor is determined by high selectivity and potency of the compound. Hence, it is of great importance to identify the selectivity profile of a discovered lead compound before optimization and development. Major challenges for this purpose are related to the sensitivity and the dynamic range. Bantscheff and colleagues recently developed an innovative approach for unbiased validation of kinase inhibitor selectivity[108]. They used several immobilized broad-selectivity kinase inhibitors, named Kinobeads™, to enrich a broad range of kinases from whole-cell lysates. A mixture of seven kinase inhibitors were immobilized on a sepharose affinity matrix and individually exposed to different cell/tissue lysates. A multitude of kinases was retrieved, but also abundant non-kinase proteins were recovered. A selectivity profile was defined for the identified kinases based on the number of spectrum-to-sequence matches as a quantitative metric. To accurately profile the drug target binding quantitatively, they used a competition assay using addition of incremental concentrations of a to be investigated drug to cells (or cell lysate). After pull-down, each captured interactome was labeled with iTRAQ reagents to quantify the reduction in proteins binding to the Kinobeads™, caused by competition with the free drug in solution. An example of this kind of quantitative competition assay is shown in figure 15. To quantify the selectivity of inhibitor-kinase interactions, Karaman and co-workers[100], introduced the concept of a selectivity score based on a previously described in vtiro competition binding assay[129]. The binding assays were active-site directed, therefore they did not reveal potential allosteric interactions. The methodology here is the combination of phage display and affinity chromatography, which has been previously described to elucidate the FK506 interacting proteins. They determined a quantitative dissociation constant (K_d) for each observed interaction providing a qualitative overall impression of selectivity. The selectivity score was calculated to describe a quantitative description by dividing the number of kinases found to bind with a K_d less than 3 μM (cut-off) by the total number of distinct kinases tested. To obtain a broader range of the selectivity profile, one can chose a higher Kd as the cut-off. Based on these criteria, the quantitative selectivity profile was determined for 38 kinase inhibitors against a panel of 287 distinct human protein kinases. As this approach is based on a cell-free in vitro binding assay with (parts of) recombinant kinases, the resulting activity of compounds here does not exactly reflect the real-life biological activities of these inhibitors[130]. When, the identified alternative targets are of validated clinical relevance, chemical proteomics facilitates the application of once established kinase inhibitor principles for additional target kinases, resulting in a more efficient approach to characterize highly selective, preclinical candidates[95].

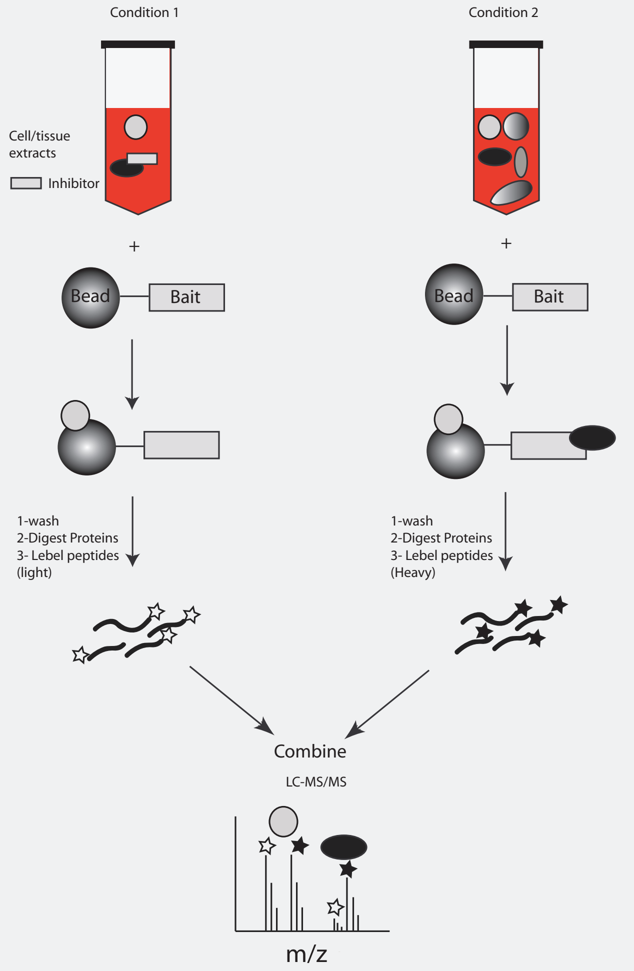
Condition 1
Condition 2
Cell/tissue extracts
Inhibitor
+
+
Bead
Bait
Bead
Bait
1-wash
2-Digest Proteins
3- Lebel peptides
(light)
1-wash
2-Digest Proteins
3- Lebel peptides
(Heavy)
Combine
LC-MS/MS
m/z

Figure 15. Quantitative chemical proteomics strategy, that combines the pull-down from two differentially treated samples and isotopic labeling approach.
Before pull-down assays, one sample is treated with 'free' inhibitor. After pull-down, the beads are washed and the binding proteins are digested. The tryptic peptides from different conditions are differentially labeled and combined before MS/MS analysis. Equal ratios of the isotopic peptide pairs indicate nonspecific binding, whereas high isotopic ratios show specificity in protein binding.

III. Scope and outline of this thesis

The primary goal of the work described in this thesis is to profile the interaction of a variety of PDE5 inhibitors (i.e. the drugs well-known for treatment of erectile dysfunction in men) directly in mammalian tissue. The PDE5 inhibitors were synthesized using the basic chemical structures of sildenafil and vardenafil as template. To achieve this goal, in **chapter 2**, a chemical proteomics strategy was developed, optimized and applied to determine the interactome of these inhibitors in tissue. We initially investigated the PF4540124 (a chemically modified linkable PDE5 inhibitor) interactome. The affinity enrichment protocol was refined in order to diminish the disturbance of nonspecific interactors binding to the affinity beads. The distinction of the specific 'inhibitor interactome' from the nonspecific interactome was further achieved by using dimethyl stable isotope labeling at the peptide level. This enabled identification of several low abundant specific interactors in a complex tissue proteome, amongst them two isoforms of the expected PDE5 enzyme. In **chapter 3**, we further optimized the chemical proteomics approach and applied it to selectively enrich for the interactome of PF-3717842 (another linkable PDE5 inhibitor) now in testis tissue. The selected tissue is close to the site of the affected disease and could possibly provide more precise information about the inhibitor interactome involved in the therapeutic pathway. We largely focused on one novel specific interactor of PF-3717842, namely phosphatidyl ethanolamine binding protein-2 (PEBP-2). After recombinant protein expression, the PEBP-2-PF-3717842 interaction could be validated by complementary in-vitro assays. Furthermore we produced and purified the closely related homologues of PEBP-2; PEBP-1 and the human orthologue of this protein called the Raf Kinase Inhibitory Protein (RKIP) to investigate their potential interaction with PDE5 inhibitors. The specific interaction of RKIP with this PDE5 inhibitor in-vitro could be confirmed. As RKIP is an important protein in several signaling pathways, this finding is of great importance. In **Chapter 4** we explored initially a label-free mass spectrometric protein quantification method, to reveal the selectivity profile of four chemically closely related PDE5 inhibitors. The four analogous compounds, including the compounds used in **chapter 2** and **chapter 3**, were synthesized based on the core structures of vardenafil and sildenafil with different chemical modifications in the main predicted binding site. The label free quantification method, based on peptide counting, enabled the differential quantitative analysis of binding proteins to the four analogues, from which a selectivity profile could be established. For most of the selective binding proteins, a parallel approach based on stable isotope peptide labeling confirmed the determined selectivity profile of the inhibitors. In **Chapter 5** a summary of the work described in this thesis is given, with a short outlook on possible future investigations.

References:

1. J. A. Beavo and L. L. Brunton, **Nat Rev Mol Cell Biol**, *2002*, 3, 710-718.
2. L. M. Currie, S. A. Livesey, J. R. Harper and J. Connor, **Transfusion**, *1998*, 38, 160-167.
3. R. F. Furchgott and J. V. Zawadzki, **Nature**, *1980*, 288, 373-376.
4. L. J. Ignarro, G. M. Buga, K. S. Wood, R. E. Byrns and G. Chaudhuri, **Proc Natl Acad Sci USA**, *1987*, 84, 9265-9269.
5. R. M. Rapoport, S. A. Waldman, R. Ginsburg, C. R. Molina and F. Murad, J Cardiovasc **Pharmacol**, *1987*, 10, 82-89.
6. C. Lugnier, Pharmacol **Ther,** *2006*, 109, 366-398.
7. M. J. Lohse, U. Forstermann and H. H. Schmidt, Naunyn Schmiedebergs Arch Pharmacol, 1998, 358, 111-112.
8. C. Wahl-Schott and M. Biel, **Cell Mol Life Sci**, *2009*, 66, 470-494.
9. G. Borland, B. O. Smith and S. J. Yarwood, Br **J Pharmacol**, *2009*.
10. X. Cheng, Z. Ji, T. Tsalkova and F. Mei, **Acta Biochim Biophys Sin (Shanghai)**, *2008*, 40, 651-662.
11. A. P. Somlyo and A. V. Somlyo, **Physiol Rev,** *2003*, 83, 1325-1358.
12. L. Li, M. Eto, M. R. Lee, F. Morita, M. Yazawa and T. Kitazawa, J Physiol, *1998*, 508 (Pt 3), 871-881.
13. J. Yong, I. Tan, L. Lim and T. Leung, J Biol Chem, *2006*, 281, 31202-31211.
14. A. A. Wooldridge, J. A. MacDonald, F. Erdodi, C. Ma, M. A. Borman, D. J. Hartshorne and T. A. Haystead, **J Biol Chem**, *2004*, 279, 34496-34504.
15. K. M. Tang, G. R. Wang, P. Lu, R. H. Karas, M. Aronovitz, S. P. Heximer, K. M. Kaltenbronn, K. J. Blumer, D. P. Siderovski, Y. Zhu and M. E. Mendelsohn, **Nat Med**, *2003*, 9, 1506-1512.
16. A. T. Bender and J. A. Beavo, Pharmacol Rev, *2006*, 58, 488-520.
17. K. Omori and J. Kotera, **Circ Res**, *2007*, 100, 309-327.
18. J. A. Beavo, **Physiol Rev,** *1995*, 75, 725-748.
19. M. Conti, G. Nemoz, C. Sette and E. Vicini, Endocr Rev, 1995, 16, 370-389.
20. R. K. Sharma, S. B. Das, A. Lakshmikuttyamma, P. Selvakumar and A. Shrivastav, **Int J Mol Med**, *2006*, 18, 95-105
21. A. Simon, P. Barabas and J. Kardos, **Neurochem Int**, *2006*, 49, 215-222.
22. S. D. Rybalkin, I. G. Rybalkina, M. Shimizu-Albergine, X. B. Tang and J. A. Beavo, EMBO J, *2003*, 22, 469-478.
23. P. Deterre, C. Pfister, J. Bigay and M. Chabre, **Biochimie**, *1987*, 69, 365-370.
24. Y. H. Jeon, Y. S. Heo, C. M. Kim, Y. L. Hyun, T. G. Lee, S. Ro and J. M. Cho, **Cell Mol Life Sci,** *2005*, 62, 1198-1220.
25. J. F. Coquil, D. J. Franks, J. N. Wells, M. Dupuis and P. Hamet, Biochim Biophys Acta, *1980*, 631, 148-165.
26. P. Hamet and J. F. Coquil, **J Cyclic Nucleotide Res**, 1978, 4, 281-290.
27. S. H. Francis and J. D. Corbin, **Methods Enzymol**, *1988*, 159, 722-729.
28. S. H. Francis, T. M. Lincoln and J. D. Corbin, **J Biol Chem**, *1980,* 255, 620-626.
29. R. Zoraghi, E. P. Bessay, J. D. Corbin and S. H. Francis, **J Biol Chem**, *2005,* 280, 12051-12063.
30. S. H. Francis, E. P. Bessay, J. Kotera, K. A. Grimes, L. Liu, W. J. Thompson and J. D. Corbin, **J Biol Chem**, *2002*, 277, 47581-47587.
31. J. D. Corbin, I. V. Turko, A. Beasley and S. H. Francis, **Eur J Biochem,** *2000*, 267, 2760-2767.
32. M. K. Thomas, S. H. Francis and J. D. Corbin, **J Biol Chem**, *1990*, 265, 14964-14970.
33. F. Mullershausen, M. Russwurm, W. J. Thompson, L. Liu, D. Koesling and A. Friebe, **J Cell Biol,** *2001*, 155, 271-278.
34. L. M. McAllister-Lucas, T. L. Haik, J. L. Colbran, W. K. Sonnenburg, D. Seger, I. V. Turko, J. A. Beavo, S. H. Francis and J. D. Corbin, **J Biol Chem**, *1995*, 270, 30671-30679.
35. I. V. Turko, T. L. Haik, L. M. McAllister-Lucas, F. Burns, S. H. Francis and J. D. Corbin, **J Biol Chem**, *1996*, 271, 22240-22244.
36. R. Zoraghi, J. D. Corbin and S. H. Francis, **Mol Pharmacol**, *2004*, 65, 267-278.
37. S. Sopory, S. Balaji, N. Srinivasan and S. S. Visweswariah, **FEBS Lett**, *2003*, 539, 161-166.
38. C. C. Heikaus, J. R. Stout, M. R. Sekharan, C. M. Eakin, P. Rajagopal, P. S. Brzovic, J. A. Beavo and R. E. Klevit, **J Biol Chem**, *2008*, 283, 22749-22759.

39. M. A. Blount, R. Zoraghi, H. Ke, E. P. Bessay, J. D. Corbin and S. H. Francis, **Mol Pharmacol**, *2006*, 70, 1822-1831.
40. Y. S. Ho, L. M. Burden and J. H. Hurley, **EMBO J**, *2000*, 19, 5288-5299.
41. B. J. Sung, K. Y. Hwang, Y. H. Jeon, J. I. Lee, Y. S. Heo, J. H. Kim, J. Moon, J. M. Yoon, Y. L. Hyun, E. Kim, S. J. Eum, S. Y. Park, J. O. Lee, T. G. Lee, S. Ro and J. M. Cho, **Nature,** *2003*, 425, 98-102.
42. I. V. Turko, S. H. Francis and J. D. Corbin, **J Biol Chem**, *1998*, 273, 6460-6466.
43. K. Y. Zhang, G. L. Card, Y. Suzuki, D. R. Artis, D. Fong, S. Gillette, D. Hsieh, J. Neiman, B. L. West, C. Zhang, M. V. Milburn, S. H. Kim, J. Schlessinger and G. Bollag, **Mol Cell**, *2004*, 15, 279-286.
44. H. Wang, Y. Liu, Q. Huai, J. Cai, R. Zoraghi, S. H. Francis, J. D. Corbin, H. Robinson, Z. Xin, G. Lin and H. Ke, **J Biol Chem**, *2006*, 281, 21469-21479.
45. J. D. Corbin, M. A. Blount, J. L. Weeks, 2nd, A. Beasley, K. P. Kuhn, Y. S. Ho, L. F. Saidi, J. H. Hurley, J. Kotera and S. H. Francis, **Mol Pharmacol**, *2003*, 63, 1364-1372.
46. M. A. Blount, R. Zoraghi, E. P. Bessay, A. Beasley, S. H. Francis and J. D. Corbin, **J Pharmacol Exp Ther,** *2007*, 323, 730-737.
47. M. A. Blount, A. Beasley, R. Zoraghi, K. R. Sekhar, E. P. Bessay, S. H. Francis and J. D. Corbin, **Mol Pharmacol**, *2004*, 66, 144-152.
48. O. Pauvert, C. Lugnier, T. Keravis, R. Marthan, E. Rousseau and J. P. Savineau, Br **J Pharmacol**, *2003*, 139, 513-522.
49. K. A. Hanson, F. Burns, S. D. Rybalkin, J. W. Miller, J. Beavo and W. R. Clarke, **Am J Respir Crit Care Med**, 1998, 158, 279-288.
50. D. Giordano, M. E. De Stefano, G. Citro, A. Modica and M. Giorgi, **Biochim Biophys Acta**, *2001*, 1539, 16-27.
51. H. Senzaki, C. H. Chen, S. Masutani, M. Taketazu, J. Kobayashi, T. Kobayashi, N. Sasaki, H. Asano, S. Kyo and Y. Yokote, **J Thorac Cardiovasc Surg**, *2001*, 122, 535-547.
52. J. F. Kameni Tcheudji, L. Lebeau, N. Virmaux, C. G. Maftei, R. H. Cote, C. Lugnier and P. Schultz, **J Mol Biol,** *2001*, 310, 781-791.
53. M. Ito, M. Nishikawa, M. Fujioka, M. Miyahara, N. Isaka, H. Shiku and T. Nakano, **Cell Signal**, *1996*, 8, 575-581.
54. T. R. Dunkern and A. Hatzelmann, **Cell Signal**, *2005*, 17, 331-339.
55. J. Kotera, K. Fujishige, K. Yuasa and K. Omori, **Biochem Biophys Res Commun**, *1999*, 261, 551-557.
56. C. S. Lin, S. Chow, A. Lau, R. Tu and T. F. Lue, **Int J Impot Res**, *2002*, 14, 15-24.
57. J. Berthet, E. W. Sutherland and T. W. Rall, **J Biol Chem**, *1957*, 229, 351-361.
58. H. A. Ghofrani, I. H. Osterloh and F. Grimminger, **Nat Rev Drug Discov**, *2006*, 5, 689-702.
59. E. P. Bessay, R. Zoraghi, M. A. Blount, K. A. Grimes, A. Beasley, S. H. Francis and J. D. Corbin, **Front Biosci**, *2007*, 12, 1899-1910.
60. A. L. Burnett, **J Androl**, *2008*, 29, 3-14.
61. J. D. Corbin, **Int J Impot Res,** *2004*, 16 Suppl 1, S4-7.
62. J. Kotera, S. H. Francis, K. A. Grimes, A. Rouse, M. A. Blount and J. D. Corbin, **Front Biosci**, *2004*, 9, 378-386.
63. C. C. Carson, **Can J Urol**, *2006*, 13 Suppl 1, 34-39.
64. J. B. McKinlay, **Int J Impot Res**, *2000*, 12 Suppl 4, S6-S11.
65. N. Mehrotra, M. Gupta, A. Kovar and B. Meibohm, **Int J Impot Res**, *2007*, 19, 253-264.
66. J. Corbin, S. Francis and R. Zoraghi, **Int J Impot Res**, *2006*, 18, 251-257.
67. R. Zoraghi, J. D. Corbin and S. H. Francis, **J Biol Chem**, *2006*, 281, 5553-5558.
68. L. J. Ignarro, P. A. Bush, G. M. Buga, K. S. Wood, J. M. Fukuto and J. Rajfer, **Biochem Biophys Res Commun**, *1990*, 170, 843-850.
69. D. P. Rotella, **Nat Rev Drug Discov**, *2002*, 1, 674-682.
70. T. Lue, I. I. Goldstein and A. Traish, **Int J Impot Res**, *2000*, 12, S81-S88.
71. T. F. Lue, **N Engl J Med**, *2000*, 342, 1802-1813.
72. H. A. Flores Toque, F. B. Priviero, C. E. Teixeira, E. Perissutti, F. Fiorino, B. Severino, F. Frecentese, R. Lorenzetti, J. S. Baracat, V. Santagada, G. Caliendo, E. Antunes and G. De Nucci, **J Med Chem**, *2008*, 51, 2807-2815.
73. D. Lykouras, F. Sampsonas, A. Kaparianos, G. Efremidis, K. Karkoulias, G. Tsoukalas and K. Spiropoulos, **Inflamm Allergy Drug Targets**, *2008*, 7, 260-269.
74. A. Sebkhi, J. W. Strange, S. C. Phillips, J. Wharton and M. R. Wilkins, **Circulation**, *2003*, 107, 3230-3235.

75. L. Zhao, N. A. Mason, N. W. Morrell, B. Kojonazarov, A. Sadykov, A. Maripov, M. M. Mirrakhimov, A. Aldashev and M. R. Wilkins, **Circulation**, *2001*, 104, 424-428.
76. A. L. Trachte, E. B. Lobato, F. Urdaneta, P. J. Hess, C. T. Klodell, T. D. Martin, E. D. Staples and T. M. Beaver, **Ann Thorac Surg**, *2005*, 79, 194-197; discussion 194-197.
77. J. Wharton, J. W. Strange, G. M. Moller, E. J. Growcott, X. Ren, A. P. Franklyn, S. C. Phillips and M. R. Wilkins, **Am J Respir Crit Care Med,** *2005*, 172, 105-113.
78. E. Takimoto, H. C. Champion, M. Li, D. Belardi, S. Ren, E. R. Rodriguez, D. Bedja, K. L. Gabrielson, Y. Wang and D. A. Kass, **Nat Med,** *2005*, 11, 214-222.
79. A. Salonia, P. Rigatti and F. Montorsi, **Curr Med Res Opin**, *2003*, 19, 241-262.
80. S. A. Ballard, C. J. Gingell, K. Tang, L. A. Turner, M. E. Price and A. M. Naylor, **J Urol,** *1998*, 159, 2164-2171.
81. I. Goldstein, T. F. Lue, H. Padma-Nathan, R. C. Rosen, W. D. Steers and P. A. Wicker, **N Engl J Med,** *1998*, 338, 1397-1404.
82. W. J. Hellstrom, M. Gittelman, G. Karlin, T. Segerson, M. Thibonnier, T. Taylor and H. Padma-Nathan, **J Androl**, *2002*, 23, 763-771.
83. W. J. Hellstrom, M. Gittelman, G. Karlin, T. Segerson, M. Thibonnier, T. Taylor and H. Padma-Nathan, **Urology**, *2003*, 61, 8-14.
84. C. C. Carson, J. Rajfer, I. Eardley, S. Carrier, J. S. Denne, D. J. Walker, W. Shen and W. H. Cordell, **BJU Int**, *2004*, 93, 1276-1281.
85. F. Sommer and U. Engelmann, **Drugs Aging**, *2004*, 21, 555-564.
86. S. J. Choi, H. Y. Ji, H. Y. Lee, D. S. Kim, W. B. Kim and H. S. Lee, **Biomed Chromatogr**, *2002*, 16, 395-399.
87. S. J. Lee, S. K. Bae, J. W. Kwon, M. You, D. C. Lee and M. G. Lee, **J Pharm Pharmacol,** *2005*, 57, 1397-1405.
88. G. J. Christ, J. Rehman, N. Day, L. Salkoff, M. Valcic, A. Melman and J. Geliebter, **Am J Physiol**, *1998*, 275, H600-608.
89. S. K. Mencher and L. G. Wang, **BMC Clin Pharmacol**, *2005*, 5, 3.
90. P. Cohen, **Nat Rev Drug Discov,** *2002*, 1, 309-315.
91. Y. Liu and N. S. Gray, **Nat Chem Biol**, *2006*, 2, 358-364.
92. H. Daub, K. Specht and A. Ullrich, **Nat Rev Drug Discov,** *2004*, 3, 1001-1010.
93. C. D. Mol, D. Fabbro and D. J. Hosfield, **Curr Opin Drug Discov Devel,** *2004*, 7, 639-648.
94. D. Fabbro and C. Garcia-Echeverria, **Curr Opin Drug Discov Devel**, *2002*, 5, 701-712.
95. H. Daub, K. Godl, D. Brehmer, B. Klebl and G. Muller, **Assay Drug Dev Technol**, *2004*, 2, 215-224.
96. A. Cuenda, J. Rouse, Y. N. Doza, R. Meier, P. Cohen, T. F. Gallagher, P. R. Young and J. C. Lee, **FEBS Lett**, *1995*, 364, 229-233.
97. M. Vieth, R. E. Higgs, D. H. Robertson, M. Shapiro, E. A. Gragg and H. Hemmerle, **Biochim Biophys Acta**, *2004,* 1697, 243-257.
98. T. Sako, A. I. Tauber, A. Y. Jeng, S. H. Yuspa and P. M. Blumberg, **Cancer Res**, *1988*, 48, 4646-4650.
99. M. J. Morin, **Oncogene**, *2000*, 19, 6574-6583.
100. M. W. Karaman, S. Herrgard, D. K. Treiber, P. Gallant, C. E. Atteridge, B. T. Campbell, K. W. Chan, P. Ciceri, M. I. Davis, P. T. Edeen, R. Faraoni, M. Floyd, J. P. Hunt, D. J. Lockhart, Z. V. Milanov, M. J. Morrison, G. Pallares, H. K. Patel, S. Pritchard, L. M. Wodicka and P. P. Zarrinkar, **Nat Biotechnol**, *2008*, 26, 127-132.
101. M. J. Schofield, N. Sharma and H. Ge, **Drug discovery today**: targets, *2004*, 3, 246-252.
102. Y. Tang, W. Zhu, K. Chen and H. Jiang, **Drug discovery today:** technologies, *2006*, 3.
103. M. Inagaki, M. Watanabe and H. Hidaka, **J Biol Chem**, *1985*, 260, 2922-2925.
104. A. Kaiser, K. Nishi, F. A. Gorin, D. A. Walsh, E. M. Bradbury and J. B. Schnier, **Arch Biochem Biophys**, 2001, 386, 179-187.
105. J. B. Schnier, G. Kaur, A. Kaiser, S. F. Stinson, E. A. Sausville, J. Gardner, K. Nishi, E. M. Bradbury and A. M. Senderowicz, **FEBS Lett**, *1999*, 454, 100-104.
106. S. P. Davies, H. Reddy, M. Caivano and P. Cohen, **Biochem J**, *2000*, 351, 95-105.
107. K. Godl, J. Wissing, A. Kurtenbach, P. Habenberger, S. Blencke, H. Gutbrod, K. Salassidis, M. Stein-Gerlach, A. Missio, M. Cotten and H. Daub, **Proc Natl Acad Sci U S A,** *2003*, 100, 15434-15439.
108. M. Bantscheff, D. Eberhard, Y. Abraham, S. Bastuck, M. Boesche, S. Hobson, T. Mathieson, J. Perrin, M. Raida, C. Rau, V. Reader, G. Sweetman, A. Bauer, T. Bouwmeester, C. Hopf, U. Kruse, G. Neubauer, N. Ramsden, J. Rick, B. Kuster and G. Drewes, **Nat Biotechnol,**

2007, 25, 1035-1044.
109. P. Mohr and K. Prommerening, affinity chromatography, practical and theoretical aspects.
110. D. A. Jeffery and M. Bogyo, **Curr Opin Biotechnol**, *2003*, 14, 87-95.
111. A. Murza, R. Fernandez-Lafuente and J. M. Guisan, **J Chromatogr B Biomed Sci Appl**, *2000*, 740, 211-218.
112. T. Tamura, T. Terada and A. Tanaka, **Bioconjug Chem**, *2003*, 14, 1222-1230.
113. K. Yamamoto, A. Yamazaki, M. Takeuchi and A. Tanaka, **Anal Biochem**, *2006*, 352, 15-23.
114. D. Brehmer, K. Godl, B. Zech, J. Wissing and H. Daub, **Mol Cell Proteomics**, *2004*, 3, 490-500.
115. P. R. Graves, J. J. Kwiek, P. Fadden, R. Ray, K. Hardeman, A. M. Coley, M. Foley and T. A. Haystead, **Mol Pharmacol**, *2002*, 62, 1364-1372.
116. A. Scholten, M. K. Poh, T. A. van Veen, B. van Breukelen, M. A. Vos and A. J. Heck, J **Proteome Res**, *2006*, 5, 1435-1447.
117. M. von Rechenberg, B. K. Blake, Y. S. Ho, Y. Zhen, C. L. Chepanoske, B. E. Richardson, N. Xu and V. Kery, **Proteomics,** *2005*, 5, 1764-1773.
118. B. Blagoev, I. Kratchmarova, S. E. Ong, M. Nielsen, L. J. Foster and M. Mann, **Nat Biotechnol**, *2003*, 21, 315-318.
119. Y. Oda, K. Huang, F. R. Cross, D. Cowburn and B. T. Chait, Proc Natl Acad Sci U S A, 1999, 96, 6591-6596.
120. S. E. Ong, B. Blagoev, I. Kratchmarova, D. B. Kristensen, H. Steen, A. Pandey and M. Mann, **Mol Cell Proteomics,** *2002*, 1, 376-386.
121. W. X. Schulze and M. Mann, **J Biol Chem**, *2004*, 279, 10756-10764.
122. S. P. Gygi, B. Rist, T. J. Griffin, J. Eng and R. Aebersold, **J Proteome Res,** *2002*, 1, 47-54.
123. A. Schmidt, J. Kellermann and F. Lottspeich, **Proteomics**, *2005*, 5, 4-15.
124. A. M. Boehm, S. Putz, D. Altenhofer, A. Sickmann and M. Falk, **BMC Bioinformatics,** *2007*, 8, 214.
125. J. L. Hsu, S. Y. Huang, N. H. Chow and S. H. Chen, **Anal Chem**, *2003*, 75, 6843-6852.
126. J. L. Hsu, S. Y. Huang and S. H. Chen, **Electrophoresis**, *2006*, 27, 3652-3660.
127. T. T. Aye, S. Mohammed, H. W. Toorn, T. A. Veen, M. A. Heyden, A. Scholten and A. J. Heck, **Mol Cell Proteomics**, *2008*.
128. P. J. Boersema, T. T. Aye, T. A. van Veen, A. J. Heck and S. Mohammed, **Proteomics**, *2008*, 8, 4624-4632.
129. M. A. Fabian, W. H. Biggs, 3rd, D. K. Treiber, C. E. Atteridge, M. D. Azimioara, M. G. Benedetti, T. A. Carter, P. Ciceri, P. T. Edeen, M. Floyd, J. M. Ford, M. Galvin, J. L. Gerlach, R. M. Grotzfeld, S. Herrgard, D. E. Insko, M. A. Insko, A. G. Lai, J. M. Lelias, S. A. Mehta, Z. V. Milanov, A. M. Velasco, L. M. Wodicka, H. K. Patel, P. P. Zarrinkar and D. J. Lockhart, **Nat Biotechnol**, *2005*, 23, 329-336.
130. Z. A. Knight and K. M. Shokat, **Chem Biol**, *2005*, 12, 621-637.
131. F. Hofmann, **J Biol Chem**, *2005*, 280, 1-4.
132. F. Hofmann, A. Ammendola and J. Schlossmann, **J Cell Sci**, *2000,* 113 (Pt 10), 1671-1676.
133. T. M. Lincoln, N. Dey and H. Sellak, **J Appl Physiol**, *2001*, 91, 1421-1430.
134. T. Munzel, R. Feil, A. Mulsch, S. M. Lohmann, F. Hofmann and U. Walter, **Circulation,** *2003*, 108, 2172-2183.
135. J. Schlossmann and F. Hofmann, **Drug Discov Today**, *2005*, 10, 627-634.

Chapter 2

A chemical proteomics based enrichment technique targeting the interactome of the PDE5 inhibitor PF-4540124

Poupak Dadvar[a], Martina O'Flaherty[a], Arjen Scholten[a], Klaus Rumpel[b], and Albert J.R. Heck[a, *]

[a] Biomolecular Mass Spectrometry and Proteomics Group, Bijvoet Center for Biomolecular Research and Utrecht Institute for Pharmaceutical Sciences, Utrecht University, Sorbonnelaan 16, 3584 CA Utrecht, the Netherlands
[b] Pfizer Global Research and Development, Sandwich, United Kingdom

Based on: Molecular Biosystems, 2009; 5(5):472-82

Abstract

The starting point for the discovery and development of new drugs is the design of molecules that bind to their target proteins with high specificity. Here we describe a systematic chemical proteomics based approach, whereby we use a novel PDE5 inhibitor as bait in mouse lung tissue. The compound N-(6-aminohexyl)-3-(1-ethyl-3-methyl-7-oxo-6,7-dihydro-1H-pyrazolo[4,3-d]pyrimidin-5-yl)-4-propoxybenzenesulfonamide (or PF-4540124), which binds to phosphodiesterase-5 (PDE5) with high affinity, was therefore immobilized on an affinity support. Initial affinity enrichment revealed the binding of hundreds of proteins to this immobilized PDE5 inhibitor. Therefore, selective pre-clearing and elution protocols were designed and used in combination with differential stable-isotope labeling to discriminate between the specific binding of low abundant proteins and less specific binding of high abundant proteins. The optimized method allowed us to selectively analyze the “interactome” of the PDE5 inhibitor PF-4540124 and enabled us to identify different isoforms of PDE5 present in mouse lung. Additionally, we enriched for the prenyl binding protein PrBP, which is also known as PDE6δ. Further analysis, applying in-vitro binding assays allowed us to verify PrBP as a novel interactor of PF-4540124. The presented method provides a generic highly-specific chemical proteomics based enrichment technique for analyzing drug-protein interactions in mammalian tissue lysates.

Introduction

Identification and validation of the intracellular targets of bioactive molecules is an essential part of drug development. If the difference in therapeutic windows between compound pharmacology at the primary target and off-target pharmacologies is not sufficient this can lead to toxic or other adverse effects and will prevent compound progression. One of the most direct approaches to screen for drug-protein interactions, including potential off-target binders, is affinity-based enrichment in combination with mass spectrometry, sometimes called chemical proteomics, whereby potential interactions of the drug molecules with thousands of proteins present in a lysate can be investigated[1-5]. Affinity purification, based on a highly specific reversible interaction of proteins with a tagged or immobilized drug, aids extensively in decreasing the complexity of the “drug-interactome” prior to mass spectrometric analysis allowing the identification of low abundant proteins, which are generally missed in global proteome analyses. The efficiency of the pull-down assay is dependent on many factors, such as (i) the immobilization efficiency of the drug (ii) the concentration of the target protein (iii) the relative abundance of background proteins in the extract and (iv) the affinity /association-/dissociation-rates of the target proteins. Drug molecules are often quite small compared to the proteins they target, which makes the synthetic design of the drug-support linker moiety an essential part of chemical proteomics; modifications to the molecule should not hamper its bioactivity. To discriminate between specific binding of low abundant proteins and less specific binding of high abundant proteins several approaches have been introduced in chemical proteomics. A crucial part of any experiment is the design of the control. The application of an inactivated affinity matrix and/or the preparation of an immobilized inactive drug-derivative serve as an important factor in establishing whether proteins are non-specifically bound. Furthermore, competitive elution, pre-clearing of the beads with specific washing steps[5] and serial affinity chromatography[6] can be used to reduce the amount of non-specific protein binding to the beads. Finally, stable isotope labeling[7], either metabolic[4, 8] or chemical[9-11], can be combined with mass spectrometric analysis to distinguish specific from non-specific binding, allowing accurate quantification of affinity enriched proteins.

Here, we targeted a strong interactor of the cyclic guanosine monophosphate (cGMP) specific phosphodiesterase 5 (PDE5), an enzyme that degrades and thus regulates the intracellular levels of cGMP[12]. PDE5 is widely distributed in rat cerebellum; kidney; pancreas; aortic smooth-muscle cells; heart; placenta; skeletal muscle; and to a lesser extent, in other regions of the brain, liver, and lungs[13].

Several PDE5 inhibitors, like Sildenafil, Vardenafil and Tadalafil are commercially available and primarily used to treat male erectile dysfunction; in addition, sildenafil is used in the treatment of pulmonary arterial hypertension. Upon administration of the drug in the treatment of male erectile dysfunction sexual stimulation leads to an enhanced level of cGMP in the corpus cavernosum[14]. Increased cGMP levels in this tissue cause blood vessel relaxation and thereby increased blood flow, which then leads to improved erectile function[12,15]. PDE5 is also expressed in lung tissue and it has been reported that PDE5 is the only Sildenafil/Vardenafil/Tadalafil binding PDE in the lung[16]. PDE5 expression levels in lung are on the same order as in penile corpus cavernosum. In addition, PDE5 has been found to be expressed in a variety of other tissues[17]. Therefore, the lung tissue could act as an appropriate protein source for the pull-down assays. It has been suggested that the presence of PDE5 in lung vascular smooth muscle may provide a basis for PDE5 inhibitor treatment of pulmonary arterial hypertension (PAH)[18]. PDE5 is a member of a large family of PDEs, which degrade the cyclic nucleotides cAMP and cGMP. There are over a dozen different mammalian PDEs, some of them degrade both cAMP and cGMP, while others are more selective. PDE5 is selective for cGMP, as are PDE6 and PDE9. Next to PDE5, some other PDE's such as PDE1, PDE6 and PDE11 have significant affinity for used PDE5 inhibitors, like Sildenafil, Vardenafil and Tadalafil, although it requires higher doses of the inhibitors to inhibit these phosphodiesterases to a significant extent[19]. Here, we designed and optimized a chemical proteomics approach, amenable to tissue material, which can selectively enrich for proteins that specifically interact with the PDE5 inhibitor PF-4540124. The aim of this study was to investigate whether proteins other than the target protein PDE5 can be identified as potential novel binders.

Material and Methods

Chemicals and proteins

NHS-activated Affi-Gel 10 was purchased from Biorad (Veenendaal, The Netherlands). Protease inhibitor cocktail and trypsin (analytical grade) were purchased from Roche Diagnostics (Basel, Switzerland). Guanosine- 3´, 5´-cyclic monophosphate (cGMP), guanosine 5'-diphosphate (GDP) and adenosine diphosphate (ADP) were provided by Biolog (Bremen, Germany). HPLC- gradient grade acetonitrile was from Biosolve (Valkenswaard, The Netherlands). N,N'-Diisopropylethylamine, formaldehyde (37% solution in water), formaldehyde-D2 (20 % solution in D2O), sodium cyanoborohydride and hydroxylamine were purchased from Aldrich (Milwaukee, WI). Slide-A-Lyzer casettes were obtained from Pierce (Etten-Leur, The Netherlands). Recombinant prenyl binding protein (PrBP) was purchased from ProSci (Poway, CA, USA) and recombinant catalytic domain of PDE5 was kindly provided by Pfizer.

Synthesis, characterization and immobilization of the tagged PF-4540124 PDE5 inhibitor

PF-4540124 and the tagged PF-4540124 were synthesized as described previously[20,21]. IC50s against a panel of phosphodiesterases were determined using the phosphodiesterase [^{3}H] cGMP SPA enzyme assay from GE Healthcare following the manufacturer's instructions. In order to be able to immobilize the PF-4540124 to the amino reactive bead that contains an N-hydroxy succinimide ester on sepharose, the inhibitor was designed to contain an aminohexyl group[22]. In order to increase the solubility, the coupling reaction was performed in H2O/AcN (1:1, V/V) at room temperature. A mixture of PF-4540124 (10 mg, 20 µmol) and DIPEA (3.3 µL, 20 µmol) was stirred in 500 µL acetonitrile-water (1:1) at RT for 2 h and completion of the reaction was confirmed by TLC (Thin Layer Chromatography). 500 µL of NHS-activated sepharose affinity beads were washed with 10 volumes of cold HCl followed by 5 volumes of acetonitrile-water (1:1) and then resuspended in 2 mL acetonitrile-water (1:1), in which 10 mg of PF-4540124 (in the form of free amine) had been dissolved. The suspension was incubated overnight at room temperature with mild stirring. The residual reactive sites on the beads were inactivated by reaction with 2 M ethanolamine for 2 hours. The beads were subsequently washed with 2 volumes of Tris buffer (1M Tris, pH 7.4) followed by 2 volumes of phosphate buffer (0.1 M sodium phosphate buffer, pH 7.2) and stored in PBS at 4°C until use.

Mouse lung tissue

One month old BALB/c mice were sacrificed by exposure to carbon monoxide for 5 minutes. Subsequently, lungs were removed , frozen in liquid nitrogen and stored at 80 °C until further use. For preparation of the cell lysate, a mortar and pestle were pre-chilled with liquid nitrogen. Approximately 200 mg of lung tissue was pulverized to a fine powder, resuspended in 1 mL of ice-cold lysis buffer (150 mM sodium chloride, 12.5 mM sodium phosphate dibasic, pH 7.4, 12.5 mM sodium phosphate monobasic, 250 mM sucrose, 0.05% tween 20, protease inhibitor cocktail (1 tablet per 15 mL incubation buffer)) and incubated at RT for 5 min. The sample was subsequently incubated on ice for 15 min. In order to separate soluble from insoluble protein fraction, the sample was centrifuged at 20,200 ×g at 4°C for 10 min. The pellet was further washed with 1ml of lysis buffer and centrifuged. The supernatant was collected and added to the first obtained soluble fraction. The total protein concentration was determined using the Bradford assay. All mice experiments were in compliance with Dutch legislation and were approved by Utrecht University Committee for animal experimentation. Special care was taken to avoid any discomfort for the mice.

Affinity Pull-Down / Chemical Proteomics approach

Freshly prepared mouse lung tissue lysate (15 mg) was diluted with lysis buffer to a final concentration of 4 mg/mL. 1mM GDP and 1mM ADP were added to the lysate before incubation with the immobilized PF-4540124-beads. As a negative control for non-specific binding, the same amount of cell lysate was supplemented with 1mM GDP, 1mM ADP and 100 µM PF-4540124, and left on ice for 15 min at 4°C. The immobilized PF-4540124 -beads (50 µL) were separately incubated with the two different treated cell lysates at 4°C. After 2 h, the beads were precipitated by centrifugation in a bench top centrifuge at 1440 ×g for 1 min. The supernatant was discarded and the beads were transferred to a 15 mL tube and washed 7 times with a 100 volumes of washing buffer (150 mM sodium chloride, 12.5 mM sodium phosphate dibasic, pH 7.4, 12.5 mM sodium phosphate monobasic, 250 mM sucrose). Selective elution was achieved by placing the beads in an empty spin column (Mo Bi Tec Molecular Biotechnology, Göttingen, Germany), incubating with 50 µL of PF-4540124 (100 µM) dissolved in PBS (136 mM NaCl, 2.6 mM KCl, 9.8 mM Na2HPO4, 1.7 mM KH2PO4) for 5 minutes on ice. This process was repeated four times and the eluates were pooled. The beads were washed with 10 volumes of PBS buffer. Eluates from the lysates were concentrated by use of a 5 kDa cut-off spin-column (Millipore) and divided into two parts. Half of this was analyzed using a 12% SDS-PAGE 1D gel by adding SDS page loading buffer to the eluate. The other fraction was subjected to in-solution digestion. On-bead in-solution digestion was performed to detect the remaining proteins on the affinity bead after elution with PF-4540124.

Before in-solution digestion, to remove excess PF-4540124, which may hamper mass spectrometric analysis, dialysis was performed on the pooled eluate using the Slide-A-Lyzer (2 kDa cut-off). Following the selective elution steps, the eluates were dialyzed against PBS buffer for 2 hours, the dialysis buffer was then changed and the eluates were further dialyzed overnight at 4°C. Finally, these pulled down proteins were subjected to in-solution digestion followed by isotopic dimethyl labeling.

In-solution digestion of pulled down proteins prior to chemical labeling

The protein samples were resuspended in triethylammonium bicarbonate (100 mM, pH 8) containing 4 M urea. DTT (dissolved in 100 mM triethylammonium bicarbonate) was added to a final concentration of 2 mM into the solution, which was incubated for 15 min at 56°C. Iodoacetamide (dissolved in 100 mM triethylammonium bicarbonate) was added to a final concentration of 4 mM. To increase protein coverage two proteases were sequentially used to digest the samples. Endoproteinase-Lys C was used as the first protease and added at an enzyme/substrate ratio of 1:100 followed by gentle mixing. Digestion was carried out for 4 hours at 37°C. The urea concentration was reduced to 1 M by diluting the reaction mixture with triethylammonium bicarbonate (100 mM). The second protease, trypsin, was applied at an enzyme/substrate ratio of 1:50 for further digestion. The digestion was carried out overnight at 37°C. The sample was acidified by the addition of formic acid to a final concentration of 5% and then desalted using a preparative C18 StageTip and eluted in 80% acetonitrile/5% formic acid. The peptides were dried down and reconstituted in triethylammonium bicarbonate (100 mM, 100 µL) for subsequent chemical labeling.

Stable-isotope dimethyl labeling for quantitative proteomics

The peptides resulting from the in-solution digestion of normal and control eluates were labeled using reductive dimethylation with formaldehyde-D2 and formaldehyde-H2, respectively[10, 23, 24]. The peptide mixture was dissolved in triethylammonium bicarbonate (100mM, 100µL) and mixed with formaldehyde (4% in water, 4µL). The mixture was briefly vortexed and mixed with freshly prepared sodium cyanoborohydride (4 µL, 580mM), and vortexed for a further 10 min. To remove excess formaldehyde, hydroxylamine (1%) was added to the reaction mixture. The samples were then acidified with formic acid to a final concentration of 5%, and mixed at a 1:1 ratio. A tryptic digest of BSA (100 fmol) was added to all digested samples before labeling as an internal standard to check the chemical labeling efficiency and peptide recovery. The ‘heavy’ and ‘light’ labeled peptides were then mixed, concentrated and resuspended in 5% formic acid, in preparation for desalting on a preparative C18 column.

Mass spectrometric analysis, protein identification

To separate the complex peptide mixtures nanoscale liquid chromatography MS/MS was performed by coupling an Agilent 1100 Series LC system (Agilent, San Jose, CA) to a hybrid LTQ-FT-ICR mass spectrometer (Thermo, San Jose, CA). Peptide extracts were loaded onto a 20 mm C18 trap column (100 µm ID, 5 µm AQUA C18, Phenomenex, CA). Sequential elution of peptides was accomplished using a 90 min linear gradient from 0-40 % solution B (80%acetonitrile; 0.6% acetic acid) in solution A(0.6% acetic acid) over the precolumn in-line with a homemade 20-25 cm resolving column (50 μmID, 3 μm Resprosil C18-AQ, Dr Maisch, Germany) at a flow rate of 0.3 μl/min . The total run time was 120 min. The mass spectrometer was operated in positive ion mode using data dependent acquisition. The top most two intense ions were selected for MS/MS in the LTQ concurrent to the acquisition of a full survey scan (m/z 300-1500) in the FTICR with a resolution of 100,000 at 400 m/z. Peptide ions already selected for MS/MS were dynamically excluded for 30s. Proteins were identified using MASCOT v2.2 in the IPI_MOUSE database v3.36. Mascot data were analyzed using the Scaffold software (www.proteomesoftware.com) and re-searched against IPI_mouse v3.36 with the X-Tandem search algorithm which is part of the Scaffold software for confident protein identification.

Characterization of drug-protein interaction, protein quantification

Relative quantification ratios of the identified peptides were derived by an in-house modified version of MSQuant (http://msquant.spurceforge.net/). Briefly, peptide ratios between the monoisotopic peaks of “normal” and “heavy” forms of the peptide were calculated and averaged over consecutive MS cycles for the duration of their respective LC-MS peaks in the total ion chromatogram using the orbitrap FT-survey scans. Manual validation of peptide sequences was performed using the software packages MSQuant and Xcalibur (Thermo, San Jose, CA). If, after correction for the labeling efficiency, equal amounts of a protein were detected in both specific and control pull-down-samples it was considered to be a non-specific interactor. Specific PF-4540124 interactors were identified as proteins giving high (>2 fold) ratios. Identifications of specific interacting proteins could be confirmed in an independent cross-over experiment, in which the peptides generated from the control lysate were labeled with the heavy isotope and the digest from the normal pull-down were labeled with the light isotope (data not shown).

In vitro verification of the PrBP- PF-4540124 interaction

Recombinant full-length human PrBP (Accession number NP_002592, ProSci (Poway, CA, USA), 0.1 μM) was incubated with immobilized PF-4540124 -beads (40 μL) in PBS buffer for 2 h at 4 ºC followed by gentle mixing. Bound protein was eluted by addition of SDS-sample buffer to the beads. Samples were heated for 5 min at 95 ºC. As a negative control the same amount of PrBP was incubated with chemically inactivated NHS-sepharose beads. To confirm that PrBP interacts directly with PF-4540124 and not with PDE5, we performed these pull-downs also in the presence and absence of recombinant cdPDE5 (0.1 μM). Moreover, we tested whether PrBP incubated with PF-4540124-beads could be eluted using a100 μM PF-4540124 containing solution (in PBS buffer). The final eluates of all control experiments were concentrated by use of a 5 kDa cut-off spin-column. All samples were analyzed by SDS-PAGE (12 %), whereby the proteins were Coomassie stained. Fluorescence emission spectra were recorded on a Perkin-Elmer 3000 fluorescence spectrometer (Gouda, The Netherlands) in 1 cm ×1 cm

× 4 cm cuvettes at λexc = 295 nm, using a slid width of 5 nm. All experiments were performed at room temperature at a protein concentration of 400 nM.

Results

Design and optimization of the affinity pull-down assay

The high-resolution structures available of PDE5 in complex with inhibitors like Sildenafil and Vardenafil[25] indicate that the methyl piperazine group present in these molecules is accessible to solvent and thus does not interact with the hydrophobic binding pocket. A 6-carbon linker containing a free amine which replaces the methyl piperazine group was therefore designed into the inhibitor PF-4540124 to ensure that it could be attached to a solid support without compromising binding affinity towards PDE5 (Figure 1A and B). We determined that PF-4540124 had an inhibitory potency (IC50) for the PDE5 catalytic domain of 3.2 nM. We evaluated the IC50s (n=2) of PF-4540124 against a range of PDEs (Table 1). PF-4540124 seems to have a significant inhibitory potency towards both PDE5 and PDE6, but also somewhat weaker towards PDE1A and PDE1C (Table 1).

We immobilized PF-4540124 on N-hydroxy succinimide (NHS) ester-activated sepharose beads (Figure 1). The ability of the PF-4540124-immobilized beads to specifically bind PDE5 was first evaluated using the recombinant catalytic domain of PDE5, cdPDE5 (35 kDa). Pull-down experiments were performed with PF-4540124-immobilized beads and as control chemically inactivated NHS-

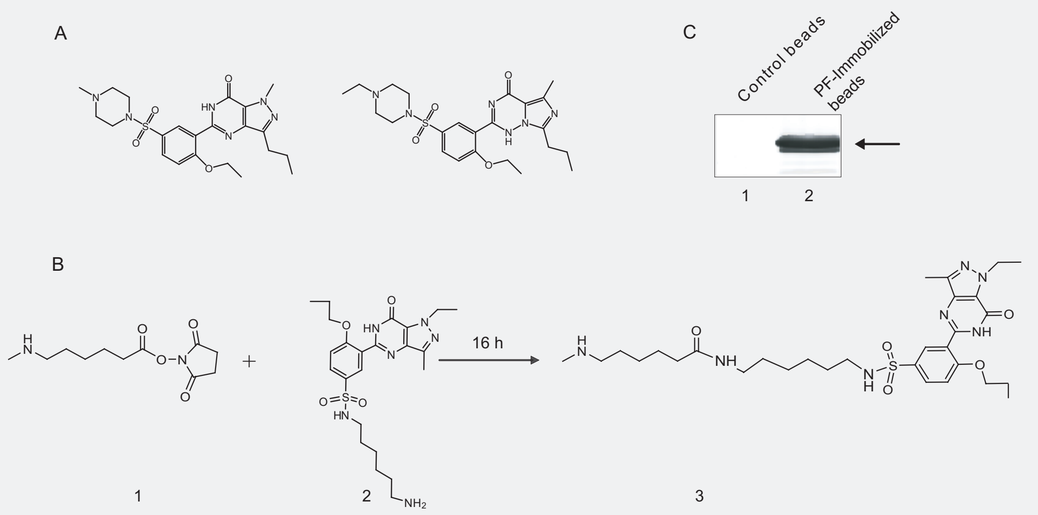

Figure 1. (A) Chemical structures of clinically used PDE5 inhibitors Sildenafil and Vardenafil. (B) Schematic of the immobilization of PF-4540124 on NHS-activated sepharose beads; (1) end-group of NHS-activated sepharose beads, (2) PF-4540124, (3) immobilized PF-4540124. (C) Coomassie stained SDS-PAGE gel of a pull-down of recombinant cdPDE5 added to the coupling buffer using PF-4540124 immobilized beads (total eluates were loaded) Lane 2 shows the detection of pulled down cdPDE5, whereas inactivated sepharose beads did not specifically pull-down cdPDE5 (lane 1).

sepharose, i.e. without immobilized PF-4540124. The selective pull-down is indicated by an intense distinct band at 35 kDa in Figure 1C.

Next, we performed a first affinity pull-down in mouse lung tissue lysate. In Figure 2 1D gel analysis of the pulled-down proteins using this simple straightforward protocol is displayed in lane 1, and for comparison in lane 4 the proteins present in the crude lysate prior to any enrichment. Although there are obvious differences between lane 1 and 4, evidencing that there is enrichment, lane 1 reveals the presence of a significant number of proteins in the pull-down. Proteomic analysis of all the proteins in lane 1 revealed a large number of pulled-down proteins. Top hits included hemoglobin, apolipoproteins, serum albumin, heat shock proteins, uteroglobin, keratin (cytoskeletal) and tubulin that are known to be highly abundant proteins likely interacting non-specifically with the beads. This analysis reveals a general phenomenon in chemical proteomics, i.e. the masking effect caused by highly abundant proteins, even if they have lower affinity to the beads.

Therefore, we opted for a much more targeted selective enrichment. We noted amongst the proteins retrieved in the initial pull-down (Figure 2, lane 1) many nucleotide (e.g. ADP/ATP/GDP/GTP) binding proteins. Therefore, in a first optimization step we suppressed binding of these proteins by adding a relatively high concentration of ADP and GDP to the lysate, which decreased the amount of binding proteins significantly (data not shown). Next, the affinity pull-down assay was further optimized as illustrated in Figure 3. The lung lysate was divided into two parts, termed for further use in this manuscript the “normal” and “control” lysates. PF-4540124 was added at a final concentration of 100 µM to the control lysate, aiming to block all potential high-affinity sites of PF-4540124 binding proteins. The appropriate concentration of PF-4540124 was determined by titration assays, i.e., a concentration of 100 µM resulted in

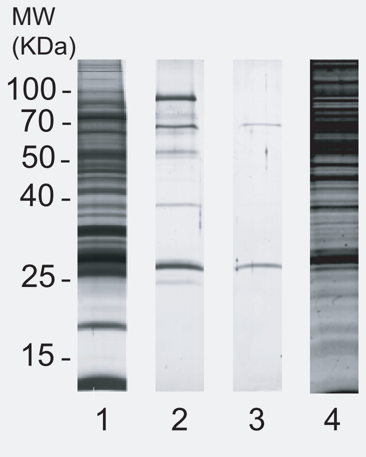

Figure 2. Silver stained SDS-PAGE gel lanes from mouse lung tissue cell lysates. Lane 1 shows the results of the initial pull-down, whereby lysates were incubated with PF-4540124 -immobilized beads, and bound proteins eluted with SDS sample buffer. Although the observed bands on the gel are distinct from the gel obtained for the crude lysate (lane 4), analysis of gel lane 1 resulted in the identification of numerous less-specific binding proteins. Lane 2 and 3 show the gel lanes obtained following the optimized protocol shown in Figure 3. Lane 2 represents the “normal” sample, whereas lane 3 shows the corresponding results from the “control” lysate where binding to the beads was competed with free PF-4540124.

maximal suppression of specific binding of PDE5 (data not shown). Moreover, to selectively retrieve the PF-4540124 binding proteins from the beads we eluted the proteins using a buffer solution containing 100 µM PF-4540124. In Figure 2, lane 2, the proteins pulled-down by this optimized procedure are visualized on a 1D gel, whereas in Figure 2 lane 3, the corresponding results for the control lysate are shown. This highly targeted, optimized method resulted in a dramatic decrease in the amount of affinity enriched proteins. The results displayed in Figure 2 clearly show that, using the optimized protocol, including competitive blocking and elution by PF-4540124, enabled us to isolate highly specific protein populations from the lysate. The control pull-down, shown in lane 3, resulted in the identification of false positive PF-4540124-interactors. Two non-specifically PF-4540124-interacting proteins visible in lanes 2 and 3 as 30 kDa and 70 kDa bands could be identified as ribosyldihydronicotinamide dehydrogenase and serum albumin. Interestingly, the most striking difference between lane 2 and lane 3 is the band at 100 kDa, which mass spectrometric interrogation revealed to represent full-length PDE5, thereby validating our approach.

Identification of proteins in 1D gel bands

The samples used for the 1D SDS-PAGE gel analysis shown in Figure 2 were also subjected to in-solution digestion and LC/MS/MS analysis using a hybrid LTQ-FT-ICR mass spectrometer. The initial lysate was analyzed to obtain a global overview of the most abundant proteins in the lung lysate, which can be used to verify whether we were specifically enriching for lower abundant proteins

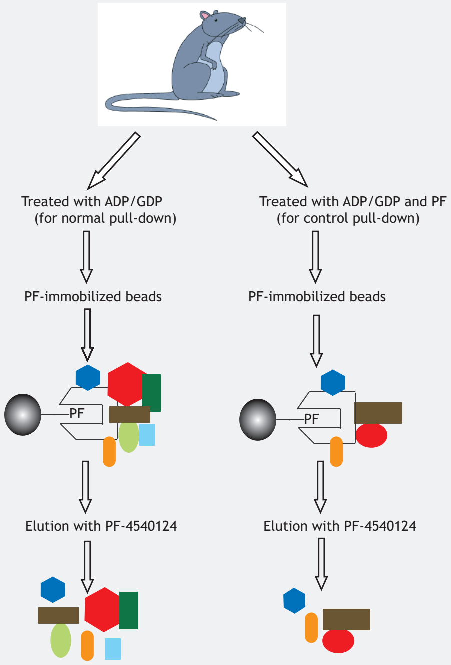

Figure 3. Schematic representation of the optimized protocol for selective enrichment of the PF-4540124 "interactome". The mouse lung tissue lysate was first divided into two equal parts. Both lysates were first pre-cleared with ADP/GDP to block binding of nucleotide binding proteins to the PF-4540124-beads. The "control" sample was also pre-cleared with PF-4540124, so that also binding of PF-4540124 binding proteins to the beads would be blocked. After incubation with the beads, proteins were eluted with a buffer containing PF-4540124.

Table 1. Overview of IC50s (n=2) of PF-4540124 against several phosphodiesterases

	1A	1B	1C	2	3A	3B	4A	4B	4C	4D	5	6	7A	7B	8A	8B	9	10	11
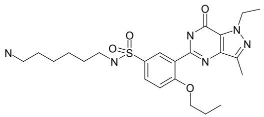	5.1 µM n=2	>10 µM	2.4 µM n=2	>10 µM	6.4 µM	>10 µM	>10 µM	>10 µM	>10 µM	>10 µM	3.2 nM n=2	7.4 nM n=2	>10 µM	>10 µM	>10 µM	>10 µM	>10 µM	6.1 µM	4.5 µM

Table 2. Selectively enriched proteins in the PF-4540124 -pull downs as determined by differential stable isotope labeling. # provides the number of quantifiable peptide pairs per protein. The average ratio determined from these peak pairs is given together with the standard deviation. In parenthesis the ratios are given that were obtained in a repeat experiment in which the isotope labels were swapped. The first three proteins are specific PF-4540124 binders including the PrBP protein, whereas the others are known to be NADP/NADPH binding proteins.

Protein	IPI Mouse	MW	#	Ratio[b]	st.dev
	accession no.	(kDa)			
PDE5 A	IPI00229355	100	12	20 (20) a	-
PDE6 subunit delta (PrBP/delta)	IPI00115190	18	2	20 (20) a	-
Pde5a 13 days embryo male testis cDNA	IPI00465762	32	1	20 (20)	-
NADPH-dependent retinol reductase	IPI00318750	31	2	8.9 (5.2)	4.3
Delta(3,5)-Delta(2,4)-dienoyl-CoA	IPI00130804	37	3	7.0 (2.2)	16
Lactoylglutathione lyase	IPI00321734	21	1	9.4 (1.6)	-
Liver carboxylesterase	IPI00138342	62	10	2.0 (2.6)	1.1
Serum albumin	IPI00131695	71	6	1 (1) b	1.3

a: When only peptide ion signals were found in the specific pull-down an arbitrary ratio of 20 was chosen.
b: Serum albumin was used for normalization of the data
Note: Apo-lipoproteins, hemoglobins, immunoglobulins and common heat shock proteins, which showed high query numbers also in the analysis of the full lysates were excluded from this table, but are described in Supplementary Table 1.

in the pull-down. An overview of the detected proteins in each of these three mentioned samples is given in the Supplementary Table 1. For unambiguous protein identifications a minimum of three unique peptides per protein was used with a MASCOT score cut-off of 20 per individual peptide. Applying such a stringent threshold reduced the number of identified proteins in the specific pull-down to 32 (Suppl. Table 1). With the same threshold the number of identified proteins in the control pull-down was 22 (Suppl. Table 1) and the number of proteins identified in the lysate 116. It should be noted that the latter analysis on the lysate, was less in-depth as just a single LC-MS run was used as the objective was to define just the most abundant background proteins in the lysate, that potentially obscure the pull-down. Amongst the 32 identified proteins in the specific pull-down were still some high abundant background proteins such as hemoglobin, several apolipoproteins, serum albumin, heat shock proteins, and uteroglobin. Those proteins were also detected in the full lysate with quite a few unique peptides (see Suppl. Table 1) and therefore disregarded in the further analysis. Several proteins identified in the specific pull-down were also identified in the control pull-down, i.e. wherein PF-4540124 was added to the lysate prior to the pull-down, but not detected (with 3 unique peptides) in the lysate. Those include Liver carboxylesterase, Ribosyldihydronicotinamide dehydrogenase, Pyridoxal kinase, Lactoylglutathione lyase, Serum amyloid A-4 protein, Synaptic vesicle membrane protein VAT-1 homolog, glycosylphosphatidylinositol specific phospholipase D1 and the Sulfated glycoprotein. Their IPI accession numbers are also given in Suppl. Table 1. Of most interest to our study, were the proteins exclusively identified in the specific pull-down with more than three peptides, namely two different isoform of PDE5, Delta(3,5)-Delta(2,4)-dienoyl-CoA isomerase, PDE6 δ-subunit (or PrBP), afamin, a selenium binding protein, and Glutathione S-transferase Mu 2 (see Suppl. Table 1).

Assessment of specific PF-4540124 interactors by stable-isotope labeling

The results presented in Supplementary Table S1 were promising, but we sought to use a more selective and rigorous approach for effective discrimination between specific and non-specific interactors[26] and therefore adapted a differential stable isotope labeling approach using reductive amination with sodium cyanonborohydride and either normal or deuterated formaldehyde[10,23,24]. Therefore, the tryptic peptides originating from the proteins out of the 'normal' pull-down were labeled with CD2O (heavy), while peptides originating from the control pull-down were labeled with CH2O (light) (Figure 4). Highly specific PF-4540124 interactors, such as PDE5, would then show up as single peptides, whereas non-specific binders such as apolipoproteins A would show up as equally intense stable isotope peptide pairs (Figure 4). Using the stable isotope labeling technique in combination with the affinity pull-down enabled us to enrich for proteins with a still sufficient number of (unique) peptides

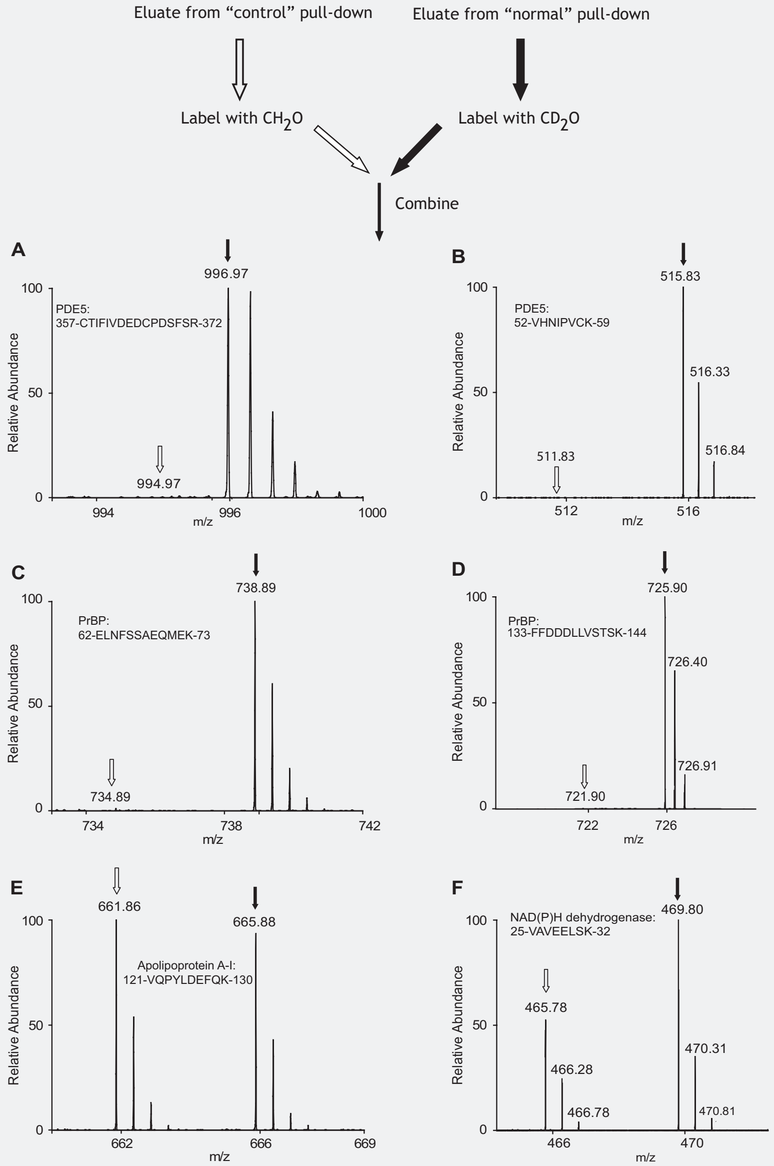

Figure 4. Typical mass spectra of peptide pairs generated by differential stable isotope dimethyl-labeling of peptides from proteins retrieved from the specific and control pull down. (A, B) Mass spectra of peptides of PDE5 revealing the high specificity towards PF-4540124. (C, D) Mass spectra of peptides of the prenyl binding protein (PrBP) revealing the specific interaction with PF-4540124. (E) Mass spectrum of peptides of apo-lipoprotein, a background protein equally present in the specific and control pull-downs. (F) Mass spectrum of a peptide pair originating from NAD(P)H dehydrogenase classified as a less specific PF-4540124 binding protein.

PrBP (0.4 µM) in the absence and presence of increasing amounts of PF-4540124 (Figure 5C). PF-4540124 by itself did not reveal any significant fluorescence intensity in this wavelength range. PrBP, which contains 4 Trp residues showed a reasonably intense fluorescence spectrum. Addition of increasing amounts and/or peptide pairs to allow confident identification and quantification. Table 2 lists the selectively enriched and identified proteins and their quantitative binding ratio between the selective and control pull-down. If there were only peptides detected from the selective pull-down we artificially set the ratio at an arbitrary value of 20. As a control serum albumin is also listed in Table 2, for which the measured ratio was 1, showing a high isotopic labeling efficiency. From our isotope labeling experiments it is evident that only three proteins are uniquely detected in the selective pull down, namely two PDE5 isoforms, and the PDE6δ. It should be noted that the name PDE6δ is misleading, as this protein is not a phosphodiesterase. This protein has been shown to interact with a number of proteins, among which the catalytic subunits of PDE6[27]. Therefore, we choose to use the more appropriate alternative name of this protein, i.e. Prenyl Binding Protein (PrBP), in the remainder of this work. To a lesser extent NADPH-dependent retinol reductase, Delta(3,5)-Delta(2,4)-dienoyl-CoA and Lactoylglutathione lyase are potential specific interactors of PF-4540124. We also performed a duplicate experiment in which we “swapped” the heavy and light label, to use for the normal and control pull-down, which confirmed our findings (data not shown). Globally, the more selective and rigorous approach for effective discrimination between specific and non-specific interactors using stable isotope labeling (Table 2) confirmed the data already obtained by the label-free analysis of the in-solution digests (Suppl. Table 1).

Of the few proteins revealed to be potentially specific PF-4540124 interactors, we evidently expected PDE5. More surprisingly we found also the relatively small PrBP protein to be a specific competitive interactor, and therefore we decided to follow up this finding in more detail.

Prenyl binding protein interacts specifically with PF-4540124

The specific interaction of PrBP with PF-4540124 was further investigated using recombinant (human) PrBP. In Figure 5A lane 1 shows the recombinant PrBP used for these experiments as a 17 kDa protein. To verify direct or indirect interaction of PrBP with PF-4540124, a pull-down experiment was performed with the immobilized-PF-4540124 beads using either recombinant PrBP or a mixture of recombinant PrBP and the recombinant catalytic domain of cdPDE5. The resulting data are shown in Figure 5A, lane 2 and 3, and indicate that the affinity enrichment of PrBP by the immobilized-PF-4540124 beads is independent from the presence of cdPDE5, revealing that PrBP is a direct interactor of PF-4540124. Beads without immobilized PF-4540124 were unable to enrich for PrBP, (Figure 5A, lane 4). Next, we attempted to specifically elute PrBP from the immobilized PF-4540124 beads with a solution containing PF-4540124. We did observe specific elution of PrBP at concentration of about 100 µM PF-4540124 further confirming specific interaction of PrBP with immobilized PF-4540124 (Figure 5B). To authenticate the binding of PrBP with PF-4540124 further we recorded tryptophan fluorescence emission spectra (300-450 nm) of this 32 kDa putative N-terminal end of a PDE5 isoform into the Swissprot rat database. The Swissprot entry O54735 (termed PDE5A) matched extremely well with our second isoform, sharing 89% sequence identity in the 32 kDa N-terminal

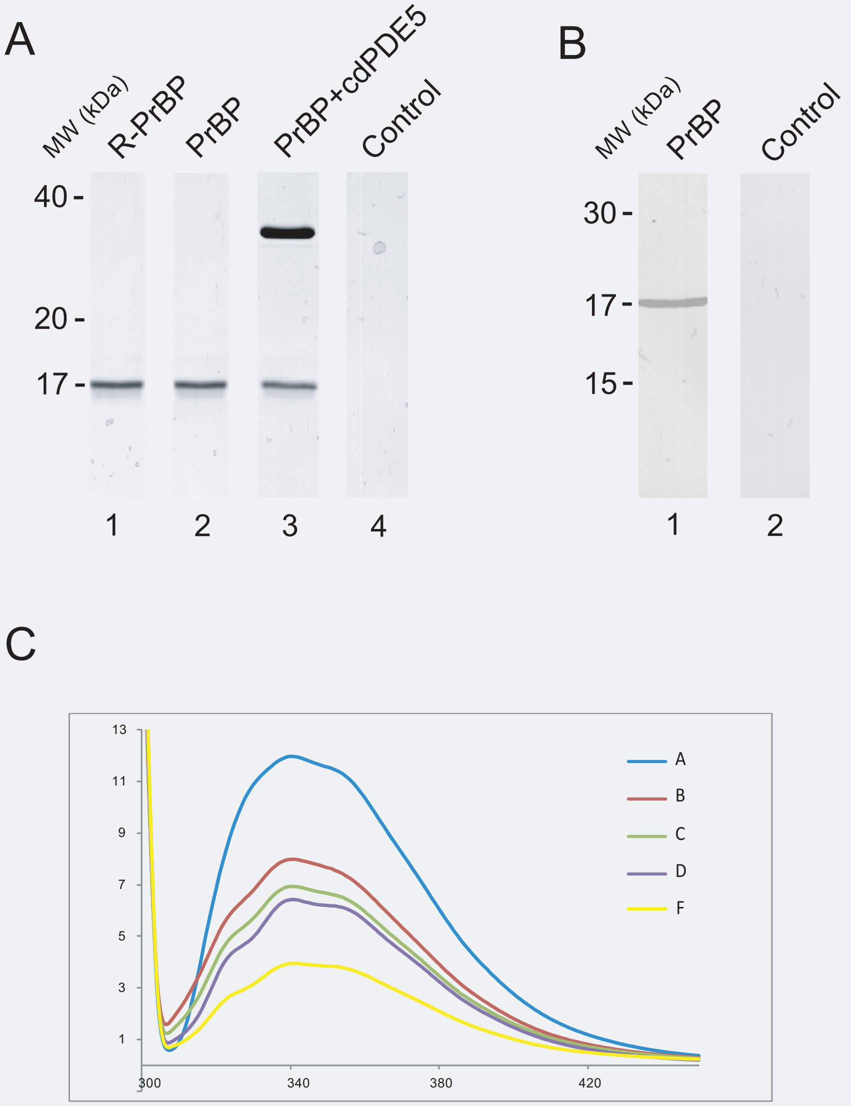

Figure 5. Overview of pull-down assays to validate specific interaction of PrBP with PF-4540124. (A) Lane 1 of the 1D gel shows the recombinant PrBP at the expected position of a 17 kDa protein (1/3 of input). In lane 2 PrBP is clearly visible, now retrieved after incubation of the PF-4540124 beads in a solution containing PrBP, eluting with a SDS buffer (total eluate (50 µL loaded). A similar pull-down assay in a solution containing both PrBP and recombinant cdPDE5, resulted in the retrieval of the two bands presented in lane 3 (total eluate (50 µL loaded). The 35 kDa en 17 kDa signals are cdPDE5 and PrBP, respectively. In lane 4 no band is observed, as here inactivated sepharose beads were used (total eluate (50 µL loaded). (B) Following incubation of the PF-4540124 beads with a solution containing PrBP, the proteins were specifically eluted with a solution containing PF-4540124. The data show that PrBP elution is achieved using the buffer containing 100 µM PF-4540124 (lane1), whereas PrBP is not eluted using the buffer alone. (C) Fluorescence emission spectra of PrBP (400 nM) in the absence and presence of increasing amounts of PF-4540124. The static quenching observed is attributed to the formation of a complex between PF-4540124 and PrBP. The blue line shows the PrBP emission spectrum in the absence of PF-4540124. (red, green, gray and yellow) PrBP fluorescence emission spectra in the presence of 200 nM , 400 nM, 2 µM and 4 µM PF-4540124, respectively.

of PF-4540124, led to quenching of the tryptophan fluorescence, which we attribute to static quenching involving the formation of a complex between the PF-4540124 quencher and PrBP. Based on the Stern-Volmer equation, on the assumption of a linear relationship between the concentration of PF-4540124 and its fluorescence, the quenching constant K_{SV} was estimated to be 2 µM. We therefore take it that under these in vitro conditions the affinity constant between PrBP and PF-4540124 lies in the 1-10 micro molar range, a factor 1000 lower than the affinity for PDE5.

Discussion

Targets of PF-4540124 in mouse lung tissue lysate

We developed an enrichment protocol for proteins having affinity towards the PDE5 inhibitor PF-4540124. Using a combination of pre-clearing and competitive blocking of proteins from binding to the beads, in conjunction with differential stable isotope labeling we were able to establish a stringent method, allowing the very selective enrichment of only a limited number of proteins. In our quest to identify specific PF-4540124 interacting proteins using a chemical proteomics approach, primarily three distinct protein categories were identified that will be further discussed in more detail below, namely: two PDE5 isoforms, NADP(H) binding proteins and PDE6δ or Prenyl-binding Protein (PrBP).

PDE5

The affinity of PF-4540124 was measured against a panel of 19 different PDEs. It was found that the inhibitor had the highest affinity against PDE5 but also showed significant affinity against PDE6. Our very selective pull-down method resulted in the enrichment of PDE5, as evidenced by the detectable strong band at about 100 kDa on the 1D gel (Figure 2, lane 2). Combining the data of three experiments using peptide LC MS/MS approximately 60 % sequence coverage was achieved for PDE5, identifying 55 unique queries (see also Suppl. Table 1 and Supplementary Figure 1A). Such a high sequence coverage allows the proteome mapping of potential PDE5 isoforms. In our analysis one other isoform of PDE5 was identified with at least 3 confident unique peptides (Supplementary Figure 1B) besides the main mouse PDE5 isoform (IPI00229355, named Pde5a cGMP-specific 3’,-5’-cyclic phosphodiesterase, 100 kDa); a unique feature of this other isoform was an N-terminally acetylated peptide. The annotation of this gene in the used IPI Mouse database is IPI00465762 and has been named “Pde5a 13 days embryo male testis cDNA”. In Supplementary Figure 1A and 1B, for each isoform the identified peptides which were unique are highlighted in red, the ones they have in common in yellow. Remarkably, as can be seen in Supplementary Figure 1B, in the used MOUSE IPI database (version IPI_Mouse v3.36, 51326 sequence entries) the “Pde5a 13 days embryo male testis cDNA” gene lacks a large part of the C-terminus, including the PDE5 catalytic domain, which is expected to be essential for PF-4540124 binding. Therefore, we blasted part, including the specific N-terminus. Interestingly, the rat Swissprot entry O54735, represents a full length PDE5 (100 kDa), thus including the catalytic domain. Therefore, we hypothesize that in mouse a similar gene exists, not properly annotated yet in the used Mouse IPI database. Our proteomics data reveal unambiguously the presence of at least two PDE5 isoforms in mouse lung tissue. The genomic annotation of the second isoform is currently in mouse imperfect, and therefore it is not surprising that no specific functions have so far been assigned to this isoform.

Detection of NADP(H) binding proteins

Several dehydrogenases/reductases, including NADPH-dependent retinol dehydrogenase/reductase, lung carbonyl reductase and L-xylulose reductase were pulled-down in our chemical proteomics experiments. Although, generally with less selectivity, they may still present potential competitive targets of PF-4540124 at high doses, as they may be quite more abundant than PDE5. Interestingly, these proteins all seem to share an affinity for NADP(H). Alignment of the sequences of these NADP(H) binding proteins with the catalytic, Sildenafil/Vardenafil/Tadalafil binding domain of PDE5 revealed that all of them shared several of the primary binding amino acids involved in inhibitor binding to PDE5, which may rationalize the identification of NADP(H) interacting proteins in our PF-4540124 pull-downs.

Prenyl-binding Protein (PrBP)

Besides the highly specific enrichment of PDE5, we retrieved a small protein named PDE6δ as a rather specific PF-4540124 -interactor. We could confidently identify 6 unique peptides of this small protein and obtained in this way 54% sequence coverage (Supplementary Figure 1C). This small protein was originally co-purified with the cone photoreceptor phosphodiesterase (PDE6)[28], and therefore named PDE6δ. Later this protein has been renamed and functionally annotated as a 17 kDa prenyl binding protein (PrBP), which can interact with prenylated proteins at their farnesylated or geranylgeranylated C-termini[29]. However, it has also been shown to interact with non-prenylated proteins[29]. Reported interaction partners of PrBP include; the PDE6α and PDE6ß-catalytic domains, Rab13, Ras, Rap, Rho6, Arl2-GTP, retinitis pigmentosa GTPase regulator (RPGR), farnesylated rhodopsin kinase (GRK1) and its homolog GRK7[27,29-31]. In spite of the alternative name of the protein, PDE6δ, PrBP is not a phosphodiesterase and has no phosphodiesterase activity. Therefore, we were somewhat puzzled by the presence of this protein in our pull-downs. We hypothesize that there may be two reasons; PrBP has high affinity for PF-4540124 or it binds specifically to PDE5. When considering the latter option, on the basis of electron microscopic images, it is interesting to note that the global structure of PDE5 is quite similar to PDE6α or PDE6ß[32]. The catalytic domains of PDE5 and PDE6 also display a high degree of homology (approximately 45%)[33-35]. However, PDE6α and PDE6ß can be farnesylated or geranylgeranylated at the cysteine of the CaaX motif[27]

(PrBP binding domain), whereas no similar CaaX motif is present in PDE5. Therefore it is unlikely that PrBP binds to PDE5 via a prenylated residue. Further examination of PrBP- PF-4540124 interaction using a pull-down assay confirmed our hypothesis indicating direct interaction of PrBP with PF-4540124 under our in-vitro conditions. Our data using recombinant PrBP clearly demonstrated that PrBP is a direct interactor of PF-4540124. Both pull-down with recombinant PrBP and tryptophan-fluorescence spectroscopy indicated that PrBP binds in vitro to PF-4540124 with an affinity constant that is in the micromolar range. This is much weaker than the binding of PDE5 to PF-4540124, which is in the nanomolar range. Therefore, a possible competitive binding of PF-4540124 to PrBP, is likely of little relevance in the present pharmacological use of PDE5 inhibitors as a treatment for erectile dysfunction and pulmonary arterial hypertension, which use much lower concentrations.

Conclusion

We have developed and optimized a multi-step chemical proteomics approach to enrich for off-target binders of the drug PF-4540124. Although it is known that this molecule has very high (nanomolar) affinity towards its target protein PDE5 and also significant affinity towards PDE6, the initial uncomplicated pull-down revealed that hundreds of proteins have some affinity for the PF-4540124-immobilized beads. We were able to optimize our protocol by pre-clearing the lysate with nucleotides (ADP and GDP) which reduced the binding of nucleotide binding proteins to the beads. We used PF-4540124 complemented lysates as a control, which, in combination with chemical stable isotope labeling, resulted in the highly selective detection of PF-4540124 binding proteins in mouse lung tissue. Using the optimized protocol, we were able to specifically enrich for PDE5, obtaining high sequence coverage by peptide LC MS/MS, enabling the identification of at least two PDE5 isoforms.

More interestingly, we also enriched for the small prenyl binding protein PrBP, and showed it to be a direct PF-4540124 interactor. While the possible promiscuous nature of PF-4540124 is revealed in this report we also demonstrated the high specificity of the PF-4540124 interaction with PDE5 over PrBP and over other proteins. For this reason the results obtained here have likely no direct pharmacological relevance as the concentration of PDE5 inhibitors used in the treatment of erectile dysfunction and pulmonary arterial hypertension is much lower. The methodology presented here is generally applicable to any compound, if it can be tagged in a way that does not interfere with the binding to its target; it may thus provide a simple and convenient tool for identification of novel targets of known drugs.

Possibly PF-4540124-based derivatives could be designed that have higher and more selective affinity for PrBP over PDE5. Such experiments would reveal whether there is chemical space to isolate PrBP affinity over PDE5 affinity. If this is the case, with minimal effort, a whole new target class, and thereby possibly a new disease area, can be targeted without the need to go through large screens to identify new leads.

Acknowledgements

We like to thank Dr. Esmaeil Mortaz for providing the mice lung samples. We acknowledge Dr. Martijn Pinkse for support with the chemical proteomics optimization procedures, Dr. Shabaz Mohammed with support in the LC MS/MS analyses, Dr. Joost Gouw for assistance with MSQuant analyses, and Dr. Jos Boekhorst and Dr. Bas van Breukelen for support in bioinformatics. We thank Dr. Andrew Bell and Keith Reeves for design and synthesis of modified PF-4540124. Darren Baldock and Lindsey Weiser are gratefully acknowledged for preparation of PDE5 catalytic domain and IC50 related experiments. The Netherlands Proteomics Centre (www.netherlandsproteomicscentre.nl) and Pfizer financially supported this research.

References

1. Y. Oda, T. Owa, T. Sato, B. Boucher, S. Daniels, H. Yamanaka, Y. Shinohara, A. Yokoi, J. Kuromitsu and T. Nagasu, **Anal Chem,** *2003*, 75, 2159-2165.
2. H. Daub, K. Godl, D. Brehmer, B. Klebl and G. Muller, **Assay Drug Dev Technol**, *2004*, 2, 215-224.
3. M. Bantscheff, D. Eberhard, Y. Abraham, S. Bastuck, M. Boesche, S. Hobson, T. Mathieson, J. Perrin, M. Raida, C. Rau, V. Reader, G. Sweetman, A. Bauer, T. Bouwmeester, C. Hopf, U. Kruse, G. Neubauer, N. Ramsden, J. Rick, B. Kuster and G. Drewes, **Nat Biotechnol**, *2007*, 25, 1035-1044.
4. W. X. Schulze and M. Mann, **J Biol Chem**, *2004*, 279, 10756-10764.
5. A. Scholten, M. K. Poh, T. A. van Veen, B. van Breukelen, M. A. Vos and A. J. Heck, **J Proteome Res**, *2006*, 5, 1435-1447.
6. K. Yamamoto, A. Yamazaki, M. Takeuchi and A. Tanaka, **Anal Biochem**, *2006*, 352, 15-23.
7. A. J. Heck and J. Krijgsveld, **Expert Rev Proteomics,** *2004*, 1, 317-326.
8. B. Blagoev, I. Kratchmarova, S. E. Ong, M. Nielsen, L. J. Foster and M. Mann, **Nat Biotechnol,** *2003*, 21, 315-318.
9. S. Julka and F. Regnier, **J Proteome Res,** *2004*, 3, 350-363.
10. J. L. Hsu, S. Y. Huang, N. H. Chow and S. H. Chen, **Anal Chem**, *2003*, 75, 6843-6852.
11. J. A. Ranish, E. C. Yi, D. M. Leslie, S. O. Purvine, D. R. Goodlett, J. Eng and R. Aebersold, **Nat Genet**, *2003*, 33, 349-355.
12. J. D. Corbin and S. H. Francis, **J Biol Chem**, *1999*, 274, 13729-13732.
13. S. K. Kulkarni and C. S. Patil, **Methods Find Exp Clin Pharmacol**, *2004*, 26, 789-799.
14. J. D. Corbin, **Int J Impot Res**, *2004*, 16 Suppl 1, S4-7.
15. S. A. Ballard, C. J. Gingell, K. Tang, L. A. Turner, M. E. Price and A. M. Naylor, **J Urol,** *1998*, 159, 2164-2171.
16. J. D. Corbin, M. A. Blount, J. L. Weeks, 2nd, A. Beasley, K. P. Kuhn, Y. S. Ho, L. F. Saidi, J. H. Hurley, J. Kotera and S. H. Francis, **Mol Pharmacol**, *2003*, 63, 1364-1372.
17. H. A. Ghofrani, I. H. Osterloh and F. Grimminger, **Nat Rev Drug Discov**, *2006*, 5, 689-702.
18. J. D. Corbin, A. Beasley, M. A. Blount and S. H. Francis, **Biochem Biophys Res Commun,** *2005*, 334, 930-938.
19. E. Bischoff, **Int J Impot Res**, *2004*, 16 Suppl 1, S11-14.
20. A. S. Bell, D. Brown and N. K. Terrett, *1992*.
21. N. K. Terrett, A. S. Bell, D. Brown and P. Ellis, **Bioorganic & Medicinal Chemistry Letters,** *1996*, 6, 1819-1824.
22. G. B. Fields, **Curr Protoc Mol Biol**, *2002*, Chapter 11, Unit 11 15.
23. R. Raijmakers, C. R. Berkers, A. de Jong, H. Ovaa, A. J. Heck and S. Mohammed, **Mol Cell**

Proteomics, *2008*.
24. S. Lemeer, C. Jopling, J. W. Gouw, S. Mohammed, A. J. Heck, M. Slijper and J. den Hertog, **Mol Cell Proteomics**, *2008*.
25. K. Y. Zhang, G. L. Card, Y. Suzuki, D. R. Artis, D. Fong, S. Gillette, D. Hsieh, J. Neiman, B. L. West, C. Zhang, M. V. Milburn, S. H. Kim, J. Schlessinger and G. Bollag, **Mol Cell,** *2004*, 15, 279-286.
26. M. Mann, **Nat Rev Mol Cell Biol,** *2006*, 7, 952-958.
27. T. A. Cook, F. Ghomashchi, M. H. Gelb, S. K. Florio and J. A. Beavo, **Biochemistry**, *2000*, 39, 13516-13523.
28. P. G. Gillespie and J. A. Beavo, **J Biol Chem**, *1988*, 263, 8133-8141.
29. H. Zhang, S. Hosier, J. M. Terew, K. Zhang, R. H. Cote and W. Baehr, **Methods Enzymol,** *2005*, 403, 42-56.
30. M. Hanzal-Bayer, L. Renault, P. Roversi, A. Wittinghofer and R. C. Hillig, **Embo J**, *2002*, 21, 2095-2106.
31. H. Zhang, X. H. Liu, K. Zhang, C. K. Chen, J. M. Frederick, G. D. Prestwich and W. Baehr, **J Biol Chem**, *2004*, 279, 407-413.
32. J. F. Kameni Tcheudji, L. Lebeau, N. Virmaux, C. G. Maftei, R. H. Cote, C. Lugnier and P. Schultz, **J Mol Biol**, *2001*, 310, 781-791.
33. L. M. McAllister-Lucas, W. K. Sonnenburg, A. Kadlecek, D. Seger, H. L. Trong, J. L. Colbran, M. K. Thomas, K. A. Walsh, S. H. Francis, J. D. Corbin and et al., **J Biol Chem**, *1993*, 268, 22863-22873.
34. P. G. Gillespie and J. A. Beavo, **Mol Pharmacol,** *1989*, 36, 773-781.
35. I. V. Turko, S. A. Ballard, S. H. Francis and J. D. Corbin, **Mol Pharmacol**, *1999*, 56, 124-130.

Supplementary figure

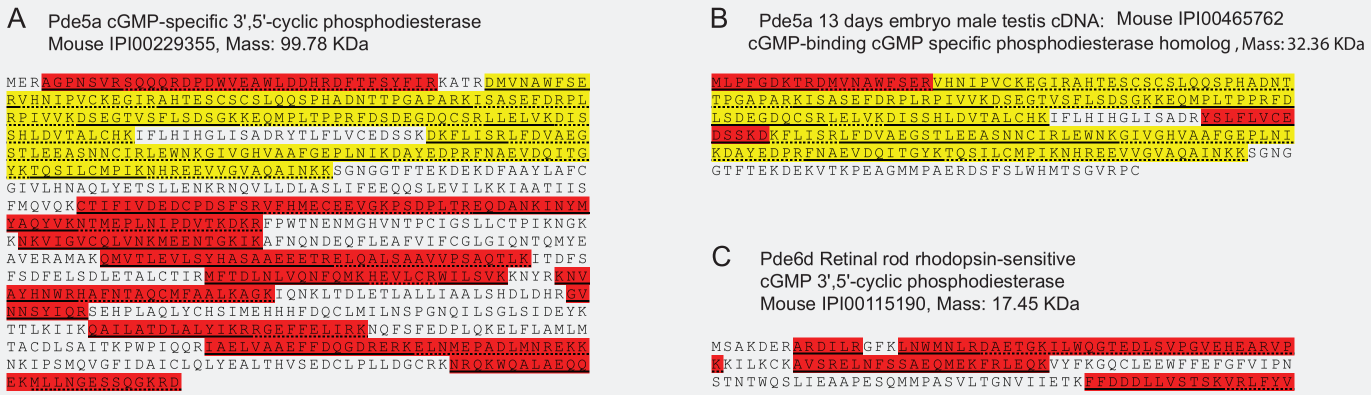

A Pde5a cGMP-specific 3',5'-cyclic phosphodiesterase
Mouse IPI00229355, Mass: 99.78 KDa

```
MERAGPNSVRSQQQRDPDWVEAWLDDHRDFTFSYFIRKATRDMVNAWFSE
RVHNIPVCKEGIRAHTESCSCSLQQSPHADNTTPGAPARKISASEFDRPL
RPIVVKDSEGTVSFLSDSGKKEQMPLTPPRFDSDEGDQCSRLLELVKDIS
SHLDVTALCHKIFLHIHGLISADRYTLFLVCEDSSKDKFLISRLFDVAEG
STLEEASNNCIRLEWNKGIVGHVAAFGEPLNIKDAYEDPRFNAEVDQITG
YKTQSILCMPIKNHREEVVGVAQAINKKSGNGGTFTEKDEKDFAAYLAFC
GIVLHNAQLYETSLLENKRNQVLLDLASLIFEEQQSLEVILKKIAATIIS
FMQVQKCTIFIVDEDCPDSFSRVFHMECEEVGKPSDPLTREQDANKINYM
YAQYVKNTMEPLNIPDVTKDKRFPWTNENMGHVNTPCIGSLLCTPIKNGK
KNKVIGVCQLVNKMEENTGKIKAFNQNDEQFLEAFVIFCGLGIQNTQMYE
AVERAMAKQMVTLEVLSYHASAAEEETRELQALSAAVVPSAQTLKITDFS
FSDFELSDLETALCTIRMFTDLNLVQNFQMKHEVLCRWILSVKKNYRKNV
AYHNWRHAFNTAQCMFAALKAGKIQNKLTDLETLALLIAALSHDLDHRGV
NNSYIQRSEHPLAQLYCHSIMEHHHFDQCLMILNSPGNQILSGLSIDEYK
TTLKIIKQAILATDLALYIKRRGEFFELIRKNQFSFEDPLQKELFLAMLM
TACDLSAITKPWPIQQRIAELVAAEFFDQGDRERKELNMEPADLMNREKK
NKIPSMQVGFIDAICLQLYEALTHVSEDCLPLLDGCRKNRQKWQALAEQQ
EKMLLNGESSQGKRD
```

B Pde5a 13 days embryo male testis cDNA: Mouse IPI00465762
cGMP-binding cGMP specific phosphodiesterase homolog , Mass: 32.36 KDa

```
MLPFGDKTRDMVNAWFSERVHNIPVCKEGIRAHTESCSCSLQQSPHADNT
TPGAPARKISASEFDRPLRPIVVKDSEGTVSFLSDSGKKEQMPLTPPRFD
LSDEGDQCSRLELVKDISSHLDVTALCHKIFLHIHGLISADRYSLFLVCE
DSSKDKFLISRLFDVAEGSTLEEASNNCIRLEWNKGIVGHVAAFGEPLNI
KDAYEDPRFNAEVDQITGYKTQSILCMPIKNHREEVVGVAQAINKKSGNG
GTFTEKDEKVTKPEAGMMPAERDSFSLWHMTSGVRPC
```

C Pde6d Retinal rod rhodopsin-sensitive
cGMP 3',5'-cyclic phosphodiesterase
Mouse IPI00115190, Mass: 17.45 KDa

```
MSAKDERARDILRGFKLNWMNLRDAETGKILWQGTEDLSVPGVEHEARVP
KKILKCKAVSRELNFSSAEQMEKFRLEQKVYFKGQCLEEWFFEFGFVIPN
STNTWQSLIEAAPESQMMPASVLTGNVIIETKFFDDDLLVSTSKVRLFYV
```

Supplementary Figure 1. Obtained sequence coverage of the three most abundant specific PF-4540124 interactors. (A) PDE5A, IPI00229355, 60% sequence coverage. (B) PDE5a 13 days embryo male testis cDNA, IPI00465762, 81 % sequence coverage. (C) PrBP, IPI00115190, 54% sequence coverage. The red boxes indicate unique peptides found solely for this protein. The yellow boxes represent peptides identified, but shared in between the two PDE5 isoforms.

Chapter 3

Phosphatidylethanolamine binding proteins, including RKIP, exhibit affinity for phosphodiesterase-5 inhibitors

Poupak Dadvar[†,^], Donna Kovanich[†,^], Gert E Folkers[‡], Klaus Rumpel[#], Reinout Raijmakers[†,^], and Albert J.R. Heck†[^,*]

[†] Biomolecular Mass Spectrometry and Proteomics Group, Bijvoet Center for Biomolecular Research and Utrecht Institute for Pharmaceutical Sciences, Utrecht University,
Padualaan 8, 3584 CH Utrecht, the Netherlands,
[^] Netherlands Proteomics Centre, Padualaan 8, 3584 CH Utrecht, the Netherlands,
[‡] Department of NMR Spectroscopy, Bijvoet Center for Biomolecular Research, Utrecht University, The Netherlands, [#] Pfizer Global Research and Development, Sandwich, United Kingdom

Accepted in the ChemBioChem Journal

Abstract

Identifying protein interactors of drugs is of great importance to understand their mode of action and possible cross-reactivity to off-target protein binders. In this study, we profile proteins that bind to PF-3717842, a high-affinity phosphodiesterase-5 (PDE5) inhibitor, using a refined affinity pull-down approach with PF-3717842 immobilized beads. By performing these pull-downs in rat testis tissue lysate, we enriched strongly and specifically for PDE5 and a few other phosphodiesterases. Besides these expected affinity enriched proteins we also detect the rodent specific phosphatidylethanolamine binding protein 2 (PEBP2), as a putative binder to the used PDE5 inhibitor. Using recombinant forms of the related murine mPEBP2, mPEBP1 and human hPEPB1 (also known as Raf kinase inhibitor protein or RKIP) we confirm that they all can bind strongly to immobilized as well as soluble PF-3717842. As the phosphatidylethanolamine binding proteins are involved in various important signal transduction pathways, the synthetic PDE5 inhibitor used here may form a platform to synthesize enhanced binders/inhibitors of the family of PEBP proteins. Our approach shows how chemical proteomics may be used to profile the biochemical space (interactome) of small molecule inhibitors.

Introduction

Phosphodiesterase-5 (PDE5) belongs to a family of enzymes that hydrolyze cyclic nucleotides, whereby PDE5 is more specifically targeting cGMP. PDE5 is an interesting pharmaceutical target as its inhibition enhances the activity of the nitric oxide–cGMP pathway that is involved in penile erection[1]. Several very potent PDE5 inhibitors, such as Sildenafil, Vardenafil and Tadalafil are now used widely for the treatment of erectile dysfunction, but also for pulmonary arterial hypertension (PAH)[2, 3]. The first commercial PDE5 inhibitor Sildenafil (UK-92,480, trade name Viagra) was originally developed to treat hypertension and angina pectoris. Phase I clinical trials indicated that Sildenafil had limited therapeutic potential effect for angina[2], but was shown to restore erectile function in men with erectile dysfunction (ED) and became the first approved oral therapy for ED in 1998[4]. More recently sildenafil became also approved for the treatment of pulmonary arterial hypertension (PAH)[3].

The therapeutically used PDE5 inhibitors have by now a track-record of being well tolerated, with nearly negligible side-effects. Some side effects have been reported though, including visual disturbance[5] headaches[6,7] and mild systemic vasodilatory effects[8]. Side effects might potentially be caused by binding of a drug to undesirable off-target interactors, and therefore it is important to have tools to better characterize the “interactome” of a drug. On the other hand, identification of new interactors of an established drug could also lead to new applications for the drug, or closely related optimized derivatives, in other human diseases.

Until recently the more global identification of drug interactors was rather difficult. An interesting development in this area enabling a rather unbiased approach is by using an affinity based pull-down assay in cellular or tissue lysates in combination with mass spectrometric identification of pulled down proteins[9-11]. This procedure typically involves the immobilization of a (chemically modified) drug to a solid state support (e.g. beads), either directly or by using a flexible linker. These functionalized beads are then incubated with a tissue extract or a cell lysate to allow proteins to bind to the drug[12]. Finally, interacting proteins are eluted under either native or denaturing conditions, digested and analyzed by MS. A main bottleneck for the identification of specifically interacting, often low abundant proteins are the nonspecific interactions of the drug with much more abundant "housekeeping" proteins[13, 14]. We therefore recently developed an optimized affinity pull-down proteomics approach to identify the interactome of the PDE5 inhibitor PF-4540124[15], that we tested on a lung tissue lysate. Here, we have extended these studies, now using a structurally related PDE5 inhibitor; PF-3717842, targeting its interactome in rat testis. While PF-3717842 also belongs to the class of pyrazolopyrimidines it is structurally distinct from the commercially used PDE5 inhibitors Sildenafil, Vardenafil and Tadalafil. Its structure is displayed in Figure 1. As phosphodiesterases (PDE's) have an important role in the process of spermatogenesis and are known to be highly expressed in testis tissue, we selected this tissue to profile the interactome of our PDE5 inhibitor. The available Sildenafil-PDE5 crystal structure[16] suggested that the methyl-piperazine group in the related PF-3717842 compound could be modified to an amino-linker without interfering with its specific interaction with PDE5. This linker was used to couple PF-3717842 to a sepharose matrix essentially as described previously[15]. The immobilized PF-3717842 beads were then used to pull-down potential protein interactors of PF-3717842 in rat testis lysate. As anticipated we enriched strongly and specifically for PDE5 and a few other phosphodiesterases. Besides these expected affinity enriched proteins we also detected phosphatidylethanolamine binding protein 2 (PEBP2), as a putative binder to the inhibitor. Using recombinant forms of the related murine mPEBP2, mPEBP1 and human hPEBP1 proteins we could confirm that they all can bind strongly to immobilized as well as soluble PF-3717842. These interactions could be verified using fluorescence and NMR spectroscopy assays. The human protein hPEBP1 (also known as the RAF kinase inhibitor protein; RKIP) plays a pivotal modulator role in several protein kinase signalling pathways[17-19]. Therefore, we propose that the synthetic PDE5 inhibitor used here may form a platform to synthesize enhanced inhibitors of the family of PEBP proteins.

Material and methods

Materials

Protease inhibitor cocktail, trypsin (analytical grade) and Lys-C were purchased from Roche Diagnostics. Guanosine- 3´, 5´- cyclic monophosphate (cGMP), guanosine 5'-diphosphate (GDP) and adenosine diphosphate (ADP) were from

Biolog. NAD was purchased from Sigma-Aldrich. HPLC-grade acetonitrile was from Biosolve. Slide-A-Lyzer casettes were obtained from Pierce. The rabbit antibody against mouse and human PEBP1 was obtained from Cell Signaling Technology.

Synthesis and characterization of PF-3717842

PF-3717842 was synthesized as described previously[15] . IC50s against a panel of phosphodiesterases were determined using the phosphodiesterase [^{3}H] cGMP SPA enzyme assay from GE Healthcare following the manufacturer's instructions.

Rat testis tissue cell lysate

Testis tissue of six months old Wistar rats was frozen in liquid nitrogen and stored at -80 ºC until use. Whole testis tissue was pulverized in a custom made mortar which was pre-cooled with liquid nitrogen. Powdered tissue was resuspended in 1 ml lysis buffer (25 mM sodium phosphate buffer containing 150 mM NaCl, 5 mM MgCl2, 1 mM EDTA, 300 mM Sucrose, protease inhibitor cocktail) and left at RT for 5 minutes. Subsequently, the sample was incubated on ice for 10 minutes and centrifuged at 20,000 ×g. The supernatant was collected and the pellet was washed with 1 ml lysis buffer and centrifuged. The supernatant was added to the first fraction. Protein concentration in the lysate was quantified using a bicinchoninic acid (BCA) protein assay. The obtained lysate was aliquoted and stored at -80°C until use. All rat experiments were in compliance with Dutch legislation and were approved by Utrecht University Committee for animal experimentation.

Recombinant PEBP proteins

The proteins mPEBP1 and mPEBP2 with an N-terminal 6x histidine tag were expressed from plasmids pOXP1 and pOXP2, respectively. The full length cDNA (1-187) encoding hPEBP1 was obtained by PCR amplification from a cDNA library obtained from a mixture of RNA from various cell lines and tissues as described before [20], using an enzyme free cloning procedure (1F: tgatgccggtggacctcagcaag, 1 FL: gccgcgcggcagcctgatgccggtggacctcagcaag 187rv: tcacttcccagacagctgctcgt 187 RL: caagaagaacccctcacttcccagacagctgctcgt) into the expression vector LICHIS[21]. Recombinant proteins were expressed and affinity purified largely as described previously[22]. Briefly, each plasmid was transformed to Escherichia coli BL21 by heat-shock transformation. After transformation, 75 µl of fresh Luria broth (LB) was added. The mixtures were incubated at 37°C for 45 min and plated on LB-agar with 100 µg/mL ampicillin. After overnight incubation, a single colony was used to inoculate 2 mL of LB medium with 100 µg/mL ampicillin. Cells were grown to an optical density of ~0.6 and the culture was used to inoculate (1% v/v) 500 mL of LB medium with 100 µg/mL ampicillin. The protein was overexpressed using autoinduction medium[23]. The culture was incubated overnight at 37°C with shaking and grown until an optical density of ~0.6. cells were harvested by centrifugation and resuspended in 10 mL lysis buffer (50mM phosphate buffer pH 8, 500mM NaCl, 20mM imidazole, 0.2mM phenyl-methyl-sulfonyl fluoride (PMSF), 10mM ß-mercaptoethanol (BME), protease inhibitors (10µl/10ml buffer), and lysozyme (1mg/500ml culture)). Cells were stored at -80 ºC until required. Protein purification was performed as described before[20] using metal affinity chromatography followed by size exclusion chromatography. Protein was purified to near homogeneity (>99% pure), as judged by SDS-PAGE. Purified proteins were dialysed against 50 mM Tris, pH 6.5, 150 mM NaCl.

Affinity pull-down protocol for testis tissue lysates

Testis tissue cell lysate was used for affinity pull-downs with PF-3717842 immobilized beads. The PF-3717842 was immobilized as described before[15]. As previous experiments showed non-specific enrichment/pull-down of NAD (nicotinamide adenine dinucleotide) binding proteins and ADP/GDP interactors, NAD, ADP and GDP (5 mM) were added to the lysate to block binding of these classes of proteins, before incubation with PF-3717842 immobilized beads. Competitive elution (with 100 µM PF-3717842) was used for the specific elution of binding proteins. Excess PF-3717842 was removed by dialysis using a Slide-A-Lyzer (2 kDa cut-off). The eluate was dialysed against PBS buffer overnight at 4 °C. The eluted sample was concentrated using 5 kDa cut-off spin columns (Millipore) and subjected to in-solution digestion before mass spectrometric analysis. The proteins retained on the beads were treated by on-bead in solution digestion for MS identification.

Affinity pull-down protocol for HeLa cells

HeLa S3 cells were cultured as described before[24]. To prepare the lysate of HeLa cells, lysis buffer (25 mM sodium phosphate buffer containing 150 mM NaCl, 5 mM MgCl2, 1 mM EDTA, 300 mM Sucrose, protease inhibitor cocktail, 0.1 % tween-20) was added to the cell pellet. HeLa cells were disrupted using a dounce homogenizer. Cells were incubated on ice for 15 min, centrifuged (13000 ×g, 15 min, 4 ºC), and the soluble fraction was collected. The remaining pellet was washed with 0.5 mL lysis buffer and the supernatant was pooled with the first fraction.

Affinity pull-down protocol for recombinant PEBP proteins

Recombinant proteins were incubated with immobilized PF-3717842-beads (50 µL) in PBS buffer for 2 h at 4 ºC with gentle mixing. Bound proteins were eluted by the addition of PF-3717842 (100 µM) or nonspecifically by the addition of SDS-sample buffer (4× conc. 0.5 M Tris-HCL pH 6.8, 20% SDS, 18.5 % glycerol, 100 mM DDT and a trace amount of bromophenol blue) to the beads. Samples were heated for 5 min at 95 ºC. Unconjugated beads were used as a negative control. All eluted proteins were visualized by SDS-PAGE (12 %) followed by Coomassie blue staining.

Immunoblotting

PF-3717842 interacting proteins were pulled down from HeLa cell lysate, analyzed by SDS-PAGE (15%) and transferred to a PVDF membrane (Bio-rad), by electroblotting for 2 hours at 40 mA. After transfer of the proteins, the membrane was blocked overnight with 5 % BSA (Bovine Serum Albumin, Fraction V, Calbiochem). The membrane was incubated with anti-PEBP1 rabbit antibody at 1:1000 dilution, followed by incubation with goat-anti-rabbit HRP-conjugated secondary antibody. Finally, proteins were visualized by enhanced chemiluminescence.

In solution digestion

Concentrated protein samples were dissolved in 100 µL 8 M urea / 50 mM ammonium bicarbonate and incubated for 15 min at RT. After addition of DTT to a concentration of 2 mM and incubation for 15 min at 56°C, iodoacetamide was added to a concentration of 4 mM. After incubation in the dark for 30 minutes, endoproteinase-Lys C was added at an enzyme/substrate ratio of 1:100 and the sample was incubated at 37 °C for 4 hours. Next, the urea concentration was lowered to 2 M by the addition of 50 mM ammonium bicarbonate. Trypsin was added at an enzyme/substrate ratio of 1:50 for overnight digestion at 37°C. The sample was acidified by the addition of formic acid to a final concentration of 1% and then desalted using a preparative C18 StageTip and eluted in 80% acetonitrile / 0.1% formic acid. The peptides were dried down and reconstituted in 5% formic acid for reversed phase LC-MS/MS analysis.

LC-MS/MS analysis

The peptide mixtures obtained after in-solution digestion were loaded onto a 20 mm C18 trap column (100 µm ID, 5 µm AQUA C18, Phenomenex, CA). The peptides were eluted using a 90 min linear gradient from 0-40 % solution B (80% acetonitrile; 0.6% acetic acid) in solution A (0.6% acetic acid) over the precolumn in-line with a homemade 20-25 cm resolving column (50 µm ID, 3 µm Resprosil C18-AQ, Dr Maisch) at a flow rate of 100 nl/min with a total analysis time of 120 min directly coupled to a FT-ICR mass spectrometer (Thermo Fisher Scientific). Each MS scan was followed by two subsequent MS/MS scans of the two most abundant ions, with a 30 second dynamic exclusion. Proteins were identified using MASCOT (Matrix Science) and MS/MS data were search against the IPI-rat database version 3.36 and IPI-human database version 3.36. Trypsin was chosen as the enzyme, allowing 2 missed cleavages. Precursor and fragment mass tolerances were set at 10 ppm and 0.9 Da, respectively. Carbamidomethylation (Cys) was selected as a fixed modification and acetylation (K, N-terminus) and oxidation (M) were set as variable modifications. Proteins were identified with a at least two peptides with a Mascot ion score of >20. Mascot data were analyzed using the Scaffold software (Proteome Software) and re-searched against related database with the X-Tandem search algorithm as a part of the Scaffold software for confident protein identification.

Fluorescence measurements and UV-Vis difference spectroscopy

Fluorescence emission spectra were recorded on a Perkin-Elmer 3000 fluorescence spectrometer at the excitation wavelength for tryptophan (295 nm), using emission and excitation slits of 5 nm and 1×1×4 cm cuvettes. All experiments were performed in triplicate at room temperature at a protein concentration of 400 nM. Absorbance spectra were obtained at room temperature with a Shimadzu UV-2450 spectrometer using 1-cm path length cuvettes. A measurement without protein was used as a negative control to correct the base line absorption of the buffer used.

NMR measurements

All ^{15}N HSQC spectra were recorded at 298K on a Bruker Avance 500 MHz spectrometer, processed using XWINNMR (Bruker), and analyzed using Sparky. For the non-overlapping peaks, the chemical shifts in the ^{1}H and ^{15}N were combined to a weighted composite chemical shift perturbation by taking $\sqrt{(5*\delta H)^2+(\delta N)^2}$. Apparent dissociation constants were estimated using $K_d=[\text{mPEBP1}]_{free}*[\text{PF-3717842}]_{free}/[\text{mPEBP1-PF-3717842}]_{complex}$. Therefore the maximal chemical shift for each peak is determined and the relative chemical shift change for each titration point is calculated relative to this maximum. The average is calculated at each ligand concentration, for all the peaks that show similar chemical shift perturbation patterns (23 and 15 peaks respectively for group A and B). The average fraction bound is used to estimate liganded $[\text{mPEBP1-PF-3717842}]_{complex}$ (fraction bound*[mPEBP1]) and thus $[\text{PF-3717842}]_{free}$ and $[\text{mPEBP1}]_{free}$ can be determined. The average and standard deviation from the calculated K_d for the two sets of peaks is calculated from the various titration points to estimate the apparent dissociation constants.

Results

Identification of PEBP2 as a PF-3717842 interacting protein in rat testis tissue lysate

In order to profile the interactome of the PDE5 inhibitor PF-3717842, we used the soluble cytosolic protein fraction of testis tissue lysate and PF-3717842 immobilized beads. Rat testis tissue was chosen because of the expected relative high abundance of PDE5, and other members of the PDE superfamily in this tissue, and also because of its important role in the reproductive system. To minimize nonspecific interactions of “housekeeping” proteins with PF-3717842, we extended our recently described pull-down affinity approach[15], which is schematically depicted in Figure 1. In this approach, the protein extract from the rat testis tissue lysate is first incubated with optimized concentrations of ADP, GDP and NAD to circumvent the pull-down of more aspecific high abundant nucleotide binding proteins. After incubation of this lysate with the PF-3717842-beads and extensive washing, the specifically bound proteins were eluted from the beads using a high concentration of PF-3717842. The protein fraction obtained by specific elution, as well as the proteins still retained on the beads were digested and analyzed by LC mass spectrometry. We also analysed the "proteome" of whole testis lysate (Supplementary Table 1), to construct a reference list of probable high abundant non-specific binding proteins that may be pulled-down as putative false positive interactors. In total, only 41 proteins were identified in the specific eluate (Supplementary Table 1), with a threshold of at least 3 unique peptides per protein, illustrating our targeted approach. Some of these proteins were dismissed as highly abundant non-specific binders as they were also detected in the whole testis lysate, but quite a few were less abundant proteins in the cell lysate and exclusively present in the specific elution. Table 1 shows a selection of highly specific eluted proteins which are potential PF-3717842 interactors. These include the anticipated phosphodiesterase PDE5, pyridoxal kinase (PLK), phosphatidylethanolamine binding protein 2 and prenyl binding protein (PrBP). Pyridoxal kinase is a known ATP binding protein, which probably has a weak affinity for PF-3717842 as well. The prenyl binding protein PrBP was previously identified as a specific interactor of the chemically closely related PDE5 inhibitor PF-4540124 in lung tissue[15]. Due to the chemical similarity between PF-4540124 and PF-3717842 we interpret these results as a confirmation of the pyrazolopyrimidinone interaction between these PDE5 inhibitors and PrBP. In addition to PDE5, one other member of the PDE superfamily, PDE1A, was detected in our pull-downs. PDE1A is known to bind PF-3717842, but with a approximately 50 fold lower dose-related inhibitory potency than PDE5 (IC50 data not shown).

Our attention was mostly drawn to the PEBP2 protein, a relative small protein (21 kDa) for which we detected 10 unique peptides in the sample obtained after the specific elution. Comparative genome analysis showed that the sequence is annotated in the rat genome, but the mouse gene is better described. In the mouse, mPEBP2 is described as a testis-specific member of the phosphatidylethanolamine binding protein family. Proteins in this family are

Table 1. Specific PF-3717842 binding proteins enriched from rat testis tissue

Protein	Name	Accession number (rat)	MW (kDa)	specific elution*	nonspecific elution*	Whole lysate*
PDE5	cGMP-specific phosphodiesterase 5	IPI00328073	98	27	0	0
PLK	Pyridoxal kinase	IPI00208348	35	13	0	0
PEBP2	Phosphatidylethanlomine	IPI00558041	21	10	2	0
PDE1A	Phosphodiesterase 1A	IPI00189442	62	6	3	0
PrBP	PDE6 delta-subunit or Prenyl binding protein	IPI00367117	17	5	3	0

* Number of detected unique peptides

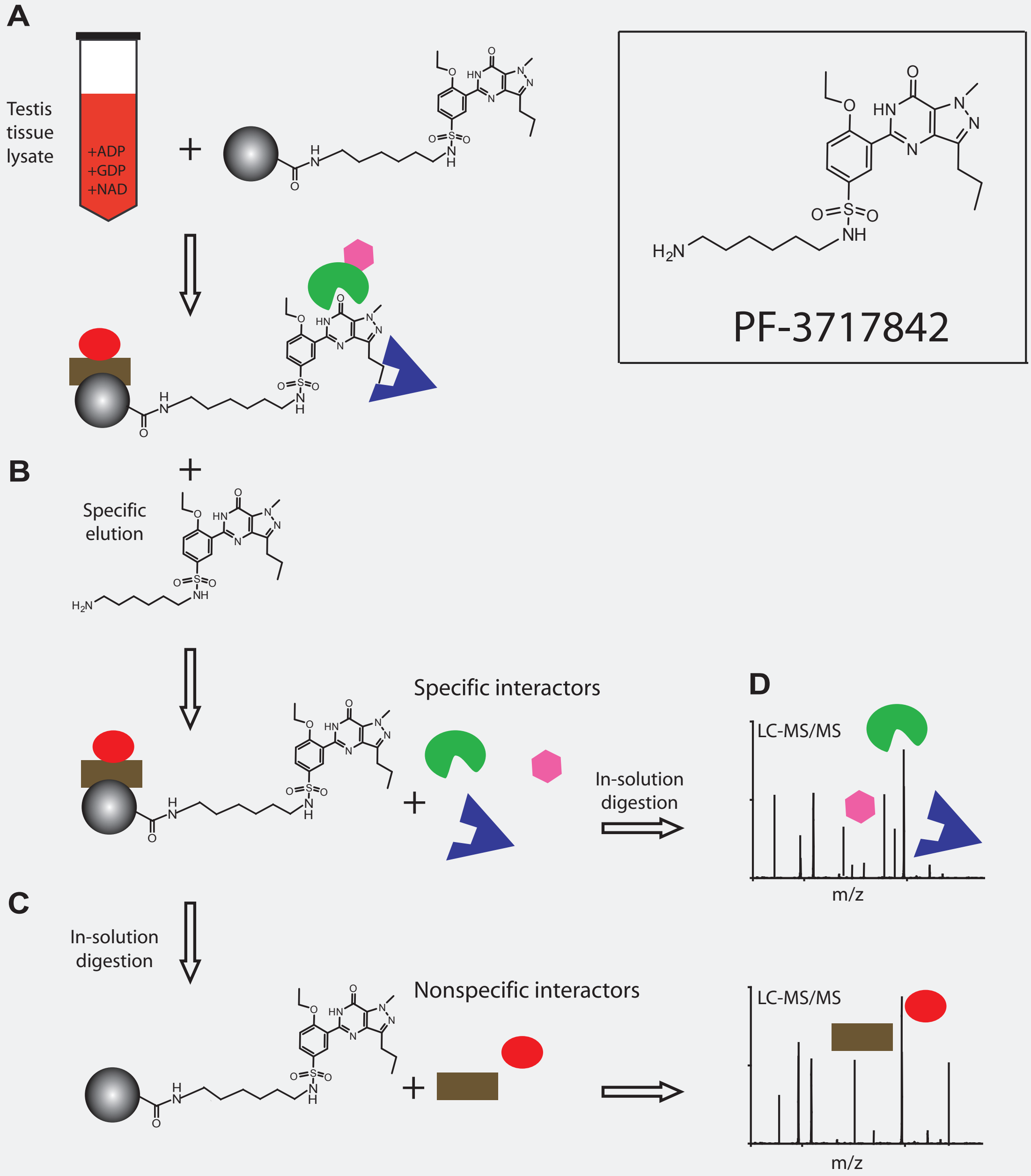
A
Testis tissue lysate
+ADP
+GDP
+NAD
PF-3717842
B
Specific elution
Specific interactors
In-solution digestion
D
LC-MS/MS
m/z
C
In-solution digestion
Nonspecific interactors
LC-MS/MS
m/z

Figure 1. Schematic overview of the chemical proteomics approach used to characterize the interactome of the PDE5 inhibitor PF-3717842. (A) Total rat testis lysate, supplemented with ADP, GDP and NAD, was incubated with PF-3717842 immobilized affinity beads. (B) All specifically interacting proteins were competitively eluted using a buffer with a high concentration of the soluble PDE5 inhibitor. (C) The remaining nonspecifically bound proteins were identified following in solution digestion. (D) All proteins were digested and identified by LC-MS/MS.

known to have a binding site for phospholipids, like phosphatidylethanolamine (PE)[22]. Even though the murine mPEBP1 has 80% sequence identity with its homolog mPEBP2; no unique peptides for mPEBP1 were detected in our analysis, likely because it is less abundant in rat testis tissue (see Supplementary Table 1).

Affinity pull-down assay using recombinant PEBPs

To further investigate and confirm the interaction of PEBP2 with the PDE5 inhibitor PF-3717842, we generated mouse recombinant mPEBP2, and its close homologues mPEBP1 and human hPEBP1. First, we tested whether the recombinant mPEBP2 could be pulled down by the PF-3717842-immobilized beads, from a solution containing either mPEBP2 alone or mPEBP2 and the recombinant catalytic domain of PDE5 (cd-PDE5). The rationale for this last experiment being that theoretically mPEBP2 could also be a secondary binder to the primary target of PF-3717842; PDE5. As can be seen in Figure 2, mPEBP2 bound selectively to the PF-3717842-beads both in the absence and presence of PDE5, revealing it to be a primary interactor of PF-3717842. A control experiment using non-functionalized beads, showed no binding of the mPEBP2 protein. Considering the high sequence homology of the mouse proteins mPEBP2 and mPEBP1 and the human hPEBP1 protein (see the alignment in Figure 3A and 3B), we used the same assay to investigate the ability of the PF-3717842-beads to interact with these homologous proteins as well. Equal amounts of all three recombinant PEBP proteins were incubated with the PF-3717842-beads. Following specific elution using soluble PF-3717842, the eluates were loaded on a 1D SDS-PAGE gel (Figure 3C). All three proteins could be enriched using the PF-3717842-beads, whereas no significant protein could be detected in the corresponding negative controls using inactivated beads (Figure 3C). The amount of mPEBP2 observed after the pull-down seemed to be higher than that of the mPEBP1 and hPEBP1 proteins indicating possibly a more efficient in vitro binding of PF-3717842 to

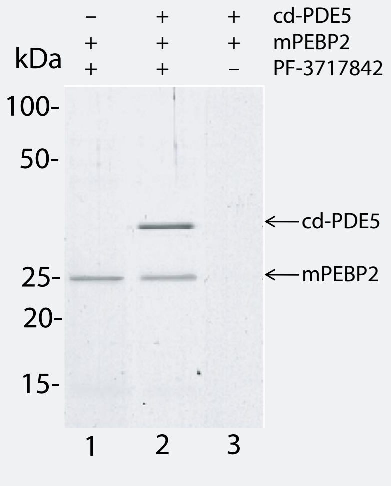

Figure 2. Recombinant mPEBP2 binds to immobilized PF-3717842. Coommassie stained SDS-PAGE gel of PF-3717842 affinity pull-downs with either only mPEBP2 (lane 1) or mPEBP2 in the presence of the recombinant catalytic domain of PDE5 (cd-PDE5) (lane 2). A pull-down using control beads (i.e. without immobilized PF-3717842) with both proteins was included as a negative control (lane 3).

mPEBP2. As the recombinant proteins were all expressed with a his-tag, we used a his-tagged protein (SUMO protein) as negative control, which showed no binding to the PF-3717842-beads (Figure 3C).

Pull-down of hPEBP1 by PF-3717842-beads in HeLa cells

Next we investigated whether endogenous hPEBP1 could also be enriched by immobilized PF-3717842, choosing HeLa cells for our pull down experiments, as they show a significant expression of hPEBP1[25]. A cytosolic protein extract of the HeLa cells was incubated with either the PF-3717842-beads or inactivated control beads, followed by specific elution using soluble PF-3717842, similar to the protocols used above. We used an anti-hPEBP1 antibody for immunoblotting of the eluted fractions, which revealed clear enrichment of hPEBP1 on the PF-371784 2-beads but not on the inactivated control beads (Supplementary Figure 1). We also identified by LC MS/MS all proteins eluted from the PF-3717842-

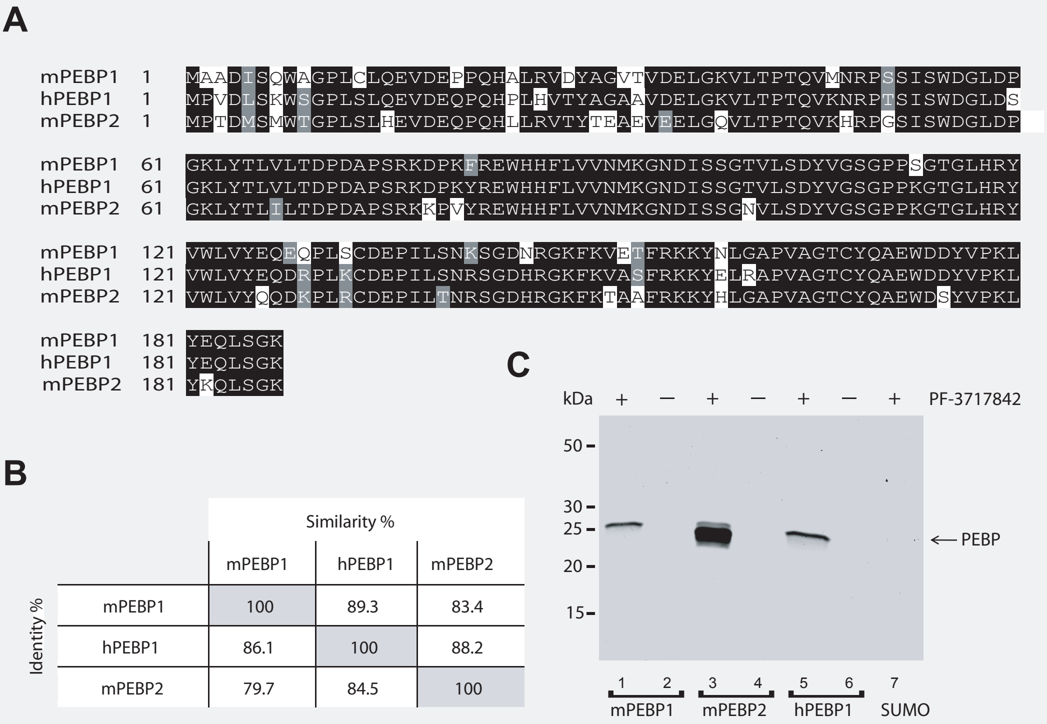

```
mPEBP1   1   MAADISQWAGPLCLQEVDEPPQHALRVDYAGVTVDELGKVLTPTQVMNRPSSISWDGLDP
hPEBP1   1   MPVDLSKWSGPLSLQEVDEQPQHPLHVTYAGAAVDELGKVLTPTQVKNRPTSISWDGLDS
mPEBP2   1   MPTDMSMWTGPLSLHEVDEQPQHLLRVTYTEAEVEELGQVLTPTQVKHRPGSISWDGLDP

mPEBP1   61  GKLYTLVLTDPDAPSRKDPKFREWHHFLVVNMKGNDISSGTVLSDYVGSGPPSGTGLHRY
hPEBP1   61  GKLYTLVLTDPDAPSRKDPKYREWHHFLVVNMKGNDISSGTVLSDYVGSGPPKGTGLHRY
mPEBP2   61  GKLYTLILTDPDAPSRKKPVYREWHHFLVVNMKGNDISSGNVLSDYVGSGPPKGTGLHRY

mPEBP1   121 VWLVYEQEQPLSCDEPILSNKSGDNRGKFKVETFRKKYNLGAPVAGTCYQAEWDDYVPKL
hPEBP1   121 VWLVYEQDRPLKCDEPILSNRSGDHRGKFKVASFRKKYELRAPVAGTCYQAEWDDYVPKL
mPEBP2   121 VWLVYQQDKPLRCDEPILTNRSGDHRGKFKTAAFRKKYHLGAPVAGTCYQAEWDSYVPKL

mPEBP1   181 YEQLSGK
hPEBP1   181 YEQLSGK
mPEBP2   181 YKQLSGK
```

		Similarity %		
		mPEBP1	hPEBP1	mPEBP2
Identity %	mPEBP1	100	89.3	83.4
	hPEBP1	86.1	100	88.2
	mPEBP2	79.7	84.5	100

Figure 3. Comparison of PEBP family members. (**A**) Multiple sequence alignment of mouse PEBP1 (mPEBP1, accession number P70296), mouse PEBP2 (mPEBP2, accession number Q8VIN1) and human PEBP1 (hPEBP1, accession number P30086). The alignment was generated using ClustalW (http://www.ebi.ac.uk/Tools/clustalw2/). Residues are colored black when identical between all proteins and gray when similar between at least two sequences (similarity groups used are FYW, LVIM, RK, DE, GA,TS and NQ). (**B**) Sequence similarity and identity between all three proteins included in the multiple alignment. (C) Coomassie stained gel of affinity pull-downs with recombinant mPEBP1 (lanes 1 and 2), mPEBP2 (lanes 3 and 4) and hPEBP1 (lanes 5 and 6) using either PF-3717842 immobilized beads (lanes 1, 3 and 5) or control beads (i.e. without immobilized PF-3717842) (lanes 2, 4 and 6). All three PEBP proteins could be specifically eluted using 100 μM of soluble PF-3717842 and no protein was detected when using control beads. A control recombinant protein (SUMO) showed no binding to the beads (lane 7).

beads by specific elution using soluble PF-3717842, and compared that to a proteome analysis performed on the whole cell lysate. Supplementary Table 2 provides a list of PF-3717842 interacting proteins detected following the specific elution, ranked on the detected number of unique peptides. For comparison, this table also lists the number of unique peptides detected for these proteins in the analysis of the full HeLa cell lysate. As expected, hPEBP1 was found to be significantly enriched in the PF-3717842 eluted fraction. Besides the hPEBP1 protein, several PDE member proteins were identified to be highly enriched in the PF-3717842 pull down (e.g. PDE4D and PDE3A), as well as previous mentioned PrBP. These results indicate that the pull-down with PF-3717842-beads in the cytosolic protein extract of the HeLa cells was working well, and thus confirm that endogenous hPEBP1, also known as the Raf kinase inhibitory protein (RKIP), has some affinity for the PDE5 inhibitor PF-3717842.

Binding assays to validate the interaction between the human and mouse PEBPs and PF-3717842

We next determined whether the PEBP proteins could also bind to unmodified PF-3717842, by analyzing the interaction of mixed protein and the inhibitor by 1) UV-VIS absorption spectroscopy, 2) fluorescence emission spectroscopy and, 3) ^{15}N NMR spectroscopy. UV-VIS absorption spectra (200-400 nm) of mPEBP2 (6 μM) were measured with and without the addition of the PF-3717842 inhibitor. As can be seen in Figure 4A the absorption of the protein in the presence of PF-3717842 increased markedly compared to the theoretical sum of the absorption of the individual components, suggesting an interaction of mPEBP2 with PF-3717842 at this concentration. Measurements performed with hPEBP1 (6 μM) revealed a similar behaviour (Supplementary Figure 2A).

Next, fluorescence emission spectra (λmax= 295 nM) of the mPEBP2 protein (400 nM) were measured in the absence and presence of PF-3717842. Addition of PF-3717842 to mPEBP2 increased the fluorescence intensity, even at equimolar (400 nM) concentration. At similar concentrations, the interaction of PF-3717842 with hPEBP1, led to fluorescence quenching (Supplementary Figure 2B). Although the of inhibitor binding to mPEBP2 and hPEBP1 had quite different effects, both effects can be indicative of a modulation of the environment around the tryptophan residues in mPEBP2 and hPEBP1, confirming a direct interaction of PF-3717842 with these proteins at nM concentrations.

Subsequently we studied the interaction of the PF-3717842 inhibitor with mPEBP1 and mPEBP2 by NMR, first expressing fully ^{15}N labeled versions of these recombinant proteins. ^{15}N HSQC spectra at 100 μM mPEBP2 protein concentration were recorded in absence and presence of an 1-3 fold access of the inhibitor PF-3717842. Figure 4C and 4D present an overlay of these spectra and confirm indeed that PF-3717842 can bind to mPEBP2, as revealed by several significant chemical shift changes. We estimated a binding constant for mPEBP2 in the submicromolar range. We performed similar experiment with the mPEBP1 recombinant protein, and these results are summarized in Supplementary

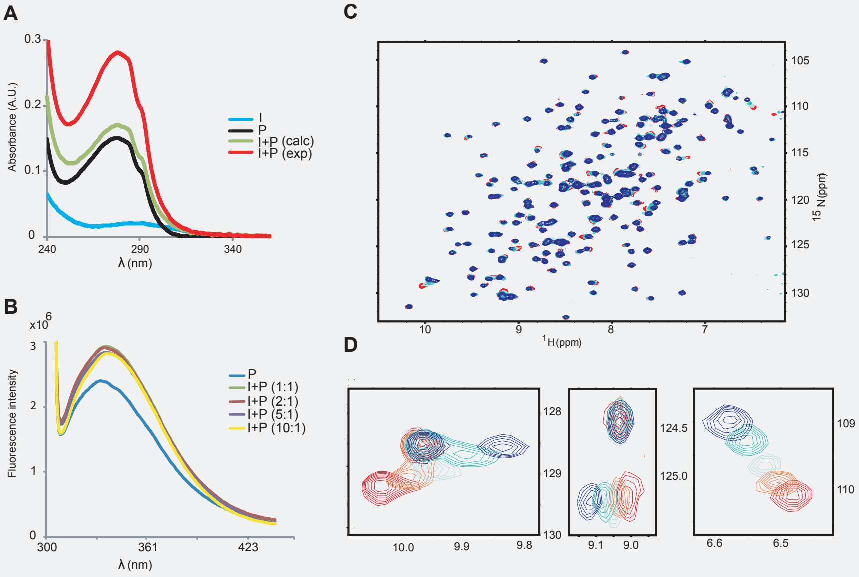

Figure 4. Interaction of mPEBP2 with soluble PF-3717842. (**A**) UV-VIS spectra of PF-3717842 (blue line), mPEBP2 alone (3.3 μM) (black line) the constructed sum of the latter two spectra (green line) and the experimental spectrum of mPEBP2 in the presence of PF-3717842 (at 1:1 ratio) (red line). (**B**) Fluorescence emission spectra recorded for mPEBP2 in the absence and the presence of PF-3717842. The blue line represents mPEBP2 (500 nM) alone, while the lines colored green, red, purple, yellow are emission spectra of mPEBP2 in the presence of increasing amounts of PF-3717842 (inhibitor:protein, 1:1, 2:1, 5:1, 10:1). (**C**) ^{15}N HSQC NMR spectrum of mPEBP2 (100 μM) in the absence (red) or presence of PF-3717842 (light blue: 25 μM, cyan: 50 μM and blue: 100 μM). (**D**) Close-ups of a few selected NMR resonances from 15N HSQC NMR spectra of 100 μM mPEBP2 in the absence (red) or presence of PF-3717842 (orange: 25 μM, light blue 50 μM, cyan: 100 μM and blue: 200 μM).

Figure 3. For mPEBP1 we found, by plotting the chemical shift as a function of the added ligand concentration, evidence for the presence of at least two protein populations. The first population reached the maximal chemical shift by the addition of a 1.5 to 2 fold excess of the PF-3717842 inhibitor, while the other subset of populated states was affected only marginally by the addition of ligand and saturation was probably not obtained even at a 4 fold molar excess of PF-3717842. Due to this biphasic behavior of many peaks, and the inability to reach binding saturation, we could only roughly estimate the apparent binding constants between mPEBP1 and the PF-3717842 ligand for the two different populations, revealing an apparent Kd of respectively 50 and 500 μM.

Discussion

Here we show by combining affinity based enrichment and mass spectrometry, nowadays often termed chemical proteomics[9,11], that members of the phosphatidylethanolamine binding protein family can interact directly with the high-affinity phosphodiesterase PDE5 inhibitor PF-3717842. We identified the rodent specific mPEBP2 as an endogenous PF-3717842 binder in rat testis lysate.

Next we showed that PF-3717842 can bind not only to recombinant mPEBP2, but also to the related protein mPEBP1 and its human homologue hPEBP1, also known as the Raf kinase inhibitory protein RKIP. The latter interaction between endogenous hPEBP1 and PF-3717842 could be confirmed by performing a pull-down in HeLa cells.

The interaction between the mPEBP2, mPEBP1 and hPEBP1 and underivatised PF-3717842 was confirmed by solution based assays using absorbance, fluorescence and NMR spectroscopy. Already at equal amounts of PEBP and PF-3717842 at sub µM concentrations prominent effects on UV absorption, fluorescence and NMR could be observed, suggesting that the binding of PF-3717842 to these proteins induces significant structural alterations. Remarkably, a prominent fluorescence quenching effect is observed for hPEBP1 upon addition of increasing amount of the inhibitor, whereas addition of PF-3717842 to mouse mPEBP2 increased the fluorescence intensity. This different behavior of the ligand binding was observed despite the high sequence homology and similarity of tertiary protein structure in mPEBP2 and human PEBP1 (see Figure 3). Although our data do not provide much structural insights into the nature of the inhibitor binding it is worth to note that a putative nucleotide binding site (residues 112-125) has been described in bovine PEBP1[27], which is also conserved in human hPEBP1. This nucleotide binding site might contribute to the binding of PF-3717842 to these proteins. Interestingly, there are crystal structures already for several of the PEBP proteins, which have revealed that there is also an extensive level of fold conservation between mPEBP2 and hPEBP1[27]. It will be worthwhile to see whether crystallography or NMR spectroscopy could further aid in elucidating the structural changes induced by binding of PF-3717842 to the PEBP proteins.

The rodent specific mPEBP2 was originally identified during a screen of rodent testis cDNA libraries. This novel cDNA had a high sequence homology with mPEBP1, and was found to be a new 21 kDa PEBP family member named mPEBP2, consisting of 187 amino acids[28]. In different species (e.g. human, rat) there are significant differences in the number of members of the PEBP family. The gene encoding the PEBP2 protein seems to be exclusively present in the genome of rodents (mouse and rat). Even though the relative genomic organization of the genes surrounding the mPEBP2 gene in the rodent genomes is quite similar in humans and rats as illustrated in Figure 5, a mPEBP2 encoding gene is not present in the human genome, nor is it present in any of the non-rodent mammalian genomes available. This absence is confirmed by the lack of EST sequences encoding a human orthologue of mPEBP2 (data not shown). Together with the high homology between mPEBP1 and mPEBP2 and with the fact that mPEBP2 is encoded by an intronless gene (as determined by a search of the mouse EST database), this suggests that mPEBP2 is likely a recently evolved paralogue of PEBP1 in rodents.

Human hPEBP1 and mouse mPEBP1 are also known as Raf kinase inhibitory protein (RKIP). It is an evolutionarily highly conserved protein, which plays an important role in mitogen-activated protein (MAP) kinase pathway regulation[22]. The protein can bind to Raf-1, thereby participating in the MAP kinase signaling pathway as a negative regulator[19]. hPEBP1/RKIP has been shown to be phosphorylated by PKC, resulting in a release from Raf-1 and binding to G-protein-coupled receptor kinase 2[29]. In response to stimulation with tumor necrosis factor alpha (TNF-alpha) or interleukin 1 beta, RKIP antagonizes the signal transduction pathways that mediate the activation of the transcription factor nuclear factor kappa B (NF-kappaB)[30]. The generic regulatory role of RKIP in cell signaling is reflected in its important role in physiology and pathophysiology. Human RKIP has been shown to play a role in neural development[31], cardiac physiology[31], Alzheimer's disease and diabetic nephropathy[32,33]. It is also involved in the organization of sperm membrane during spermatogenesis[34] and has an anti-metastatic role in prostate cancer[35]. Since the inhibitor concentrations that were used in this study are several orders of magnitude higher than the concentrations that are used in the treatment of erectile dysfunction and pulmonary arterial hypertension no conclusions can be drawn from the data on any potential pharmacological or clinical relevance. Due to the high importance of RKIP in several biological processes, a next important step is to investigate whether the binding of PF-3717842, or a further chemically optimized derivative of PF-3717842, with even higher affinity for RKIP, has a functional effect on RKIP and the signaling pathways it is involved in.

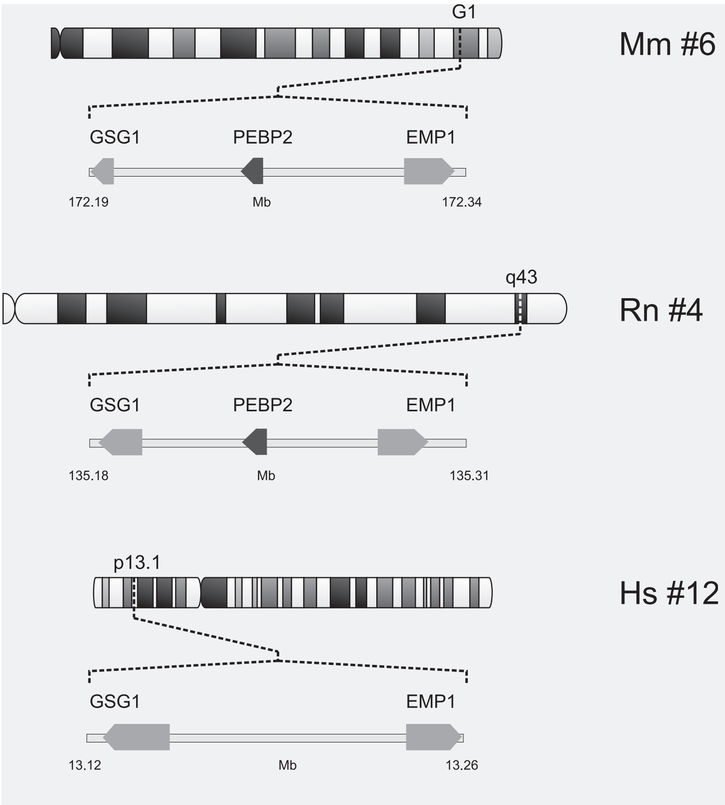

Figure 5. Shown are chromosomal locations of the gene encoding PEBP2. Shown are ideograms of mouse (Mus musculus, Mm) chromosome 6, rat (Rattus norvegicus, Rn) chromosome 4 and human (Homo sapiens, Hs) chromosome 12. The enlarged areas of the mouse and rat chromosomes contain the mPEBP2 gene and rPEBP2 gene, respectively, both flanked by GSG1 and EMP1 genes, which are on the same and opposite strand, respectively. The bottom panel shows the same area of human chromosome 12, with both a GSG1 and EMP1 gene present, but lacking a homologous gene for hPEBP1

Conclusion

Here, we have shown by using a chemical proteomics approach that several members of the phosphatidyl ethanolamine binding protein family have affinity for the PDE5 inhibitor PF-3717842. We used an immobilized PF-3717842 to selectively pull-down and identify PEBP2 in rat testis tissue and showed that the related hPEBP1 and mPEBP1 proteins can also interact with PF-3717842. As PEBP1 is known to be a RAF kinase inhibitor, which influences the MAP kinase pathway in many different tissues and cell types, this information might lead to potential new applications for PF-3717842, or a further chemically optimized derivative of PF-3717842, with even higher affinity for RKIP. In general, our chemical proteomics approach reveals its potential to screen, even in tissue lysates, for cross-reactivity of inhibitors with unexplored protein targets.

Acknowledgements

We would like to thank Stephanie Smith, Gerard Gibbs and Moira O'Bryan (Department of Biochemistry and Molecular Biology, Monash University, Melbourne, Australia) for supplying expression constructs for the mPEBP2 protein. We gratefully thank Toon van Veen for the preparation of the rat testis cell lysate. We thank Dr. Andrew Bell and Keith Reeves for design and synthesis of PF-3717842. Darren Baldock and Lindsey Weiser are gratefully acknowledged for preparation of PDE5 catalytic domain and IC50 related experiments.This work was supported by Pfizer, Sandwich, United Kingdom. Support of the Netherlands Proteomics Centre is greatly appreciated.

References

1. K. Purvis, G. J. Muirhead and J. A. Harness, Br **J Clin Pharmacol**, *2002*, 53 Suppl 1, 53S-60S.
2. S. Uthayathas, S. S. Karuppagounder, B. M. Thrash, K. Parameshwaran, V. Suppiramaniam and M. Dhanasekaran, **Pharmacol Rep**, *2007*, 59, 150-163.
3. K. F. Croom, M. P. Curran, S. H. Abman, R. N. Channick, G. A. Heresi, L. J. Rubin and A. Torbicki, **Drugs**, *2008*, 68, 383-397.
4. G. Jackson, H. Gillies and I. Osterloh, **Int J Clin Pract**, *2005*, 59, 680-691.
5. C. Foresta, N. Caretta, D. Zuccarello, A. Poletti, A. Biagioli, L. Caretti and A. Galan, **Eye,** *2008*, 22, 144-149.
6. A. R. McCullough, **Rev Urol**, *2002*, 4 Suppl 3, S26-38.
7. G. Wagner, F. Montorsi, S. Auerbach and M. Collins, **J Gerontol A Biol Sci Med Sci**, *2001*, 56, M113-119.
8. L. Ghiadoni, D. Versari and S. Taddei, **Curr Hypertens Rep**, *2008*, 10, 52-57.
9. M. Bantscheff, D. Eberhard, Y. Abraham, S. Bastuck, M. Boesche, S. Hobson, T. Mathieson, J. Perrin, M. Raida, C. Rau, V. Reader, G. Sweetman, A. Bauer, T. Bouwmeester, C. Hopf, U. Kruse, G. Neubauer, N. Ramsden, J. Rick, B. Kuster and G. Drewes, **Nat Biotechnol,** *2007*, 25, 1035-1044.
10. T. Kocher and G. Superti-Furga, **Nat Methods**, *2007*, 4, 807-815.
11. M. Bantscheff, A. Scholten and A. J. R. Heck, **Drug Discovery Today**, *2009*.
12. G. Lolli, F. Thaler, B. Valsasina, F. Roletto, S. Knapp, M. Uggeri, A. Bachi, V. Matafora, P. Storici, A. Stewart, H. M. Kalisz and A. Isacchi, **Proteomics**, *2003*, 3, 1287-1298.
13. W. X. Schulze and M. Mann, **J Biol Chem**, *2004*, 279, 10756-10764.
14. Y. Oda, T. Owa, T. Sato, B. Boucher, S. Daniels, H. Yamanaka, Y. Shinohara, A. Yokoi, J.

Kuromitsu and T. Nagasu, **Anal Chem**, *2003*, 75, 2159-2165.

15. P. Dadvar, M. O'Flaherty, A. Scholten, K. Rumpel and A. J. R. Heck, **Mol BioSystems**, *2009*.
16. B. J. Sung, K. Y. Hwang, Y. H. Jeon, J. I. Lee, Y. S. Heo, J. H. Kim, J. Moon, J. M. Yoon, Y. L. Hyun, E. Kim, S. J. Eum, S. Y. Park, J. O. Lee, T. G. Lee, S. Ro and J. M. Cho, **Nature**, *2003*, 425, 98-102.
17. S. Hagan, R. Garcia, A. Dhillon and W. Kolch, **Methods Enzymol**, *2006*, 407, 248-259.
18. K. Yeung, P. Janosch, B. McFerran, D. W. Rose, H. Mischak, J. M. Sedivy and W. Kolch, **Mol Cell Biol**, *2000*, 20, 3079-3085.
19. K. Yeung, T. Seitz, S. Li, P. Janosch, B. McFerran, C. Kaiser, F. Fee, K. D. Katsanakis, D. W. Rose, H. Mischak, J. M. Sedivy and W. Kolch, **Nature**, *1999*, 401, 173-177.
20. G. E. Folkers, B. N. van Buuren and R. Kaptein, **J Struct Funct Genomics**, *2004*, 5, 119-131.
21. R. N. de Jong, M. A. Daniels, R. Kaptein and G. E. Folkers, **J Struct Funct Genomics**, *2006*, 7, 109-118.
22. D. M. Hickox, G. Gibbs, J. R. Morrison, K. Sebire, K. Edgar, H. H. Keah, K. Alter, K. L. Loveland, M. T. Hearn, D. M. de Kretser and M. K. O'Bryan, **Biol Reprod,** *2002*, 67, 917-927.
23. F. W. Studier, **Protein Expr Purif,** *2005*, 41, 207-234.
24. F. Mousson, A. Kolkman, W. W. Pijnappel, H. T. Timmers and A. J. Heck, **Mol Cell Proteomics**, *2008*, 7, 845-852.
25. E. M. Eves, P. Shapiro, K. Naik, U. R. Klein, N. Trakul and M. R. Rosner, **Mol Cell**, *2006*, 23, 561-574.
26. F. Schoentgen, N. Seddiqi, S. Bucquoy, P. Jolles, L. Lemesle-Varloot, K. Provost and J. P. Mornon, **Protein Eng**, *1992*, 5, 295-303.
27. P. C. Simister, M. J. Banfield and R. L. Brady, **Acta Crystallogr D Biol Crystallogr,** *2002*, 58, 1077-1080.
28. F. Schoentgen, F. Saccoccio, J. Jolles, I. Bernier and P. Jolles, **Eur J Biochem**, *1987*, 166, 333-338.
29. T. Kroslak, T. Koch, E. Kahl and V. Hollt, **J Biol Chem,** *2001*, 276, 39772-39778.
30. K. C. Yeung, D. W. Rose, A. S. Dhillon, D. Yaros, M. Gustafsson, D. Chatterjee, B. McFerran, J. Wyche, W. Kolch and J. M. Sedivy, **Mol Cell Biol**, *2001*, 21, 7207-7217.
31. C. Moore, A. C. Perry, S. Love and L. Hall, **Brain Res Mol Brain Res,** *1996*, 37, 74-78.
32. R. Kikkawa, D. Koya and M. Haneda, **Am J Kidney Dis**, *2003*, 41, S19-21.
33. K. R. Tuttle and P. W. Anderson, **Am J Kidney Dis**, *2003*, 42, 456-465.
34. J. Frayne, A. McMillen, S. Love and L. Hall, **Mol Reprod Dev**, *1998*, 49, 454-460.
35. Z. Fu, P. C. Smith, L. Zhang, M. A. Rubin, R. L. Dunn, Z. Yao and E. T. Keller, **J Natl Cancer Inst,** *2003*, 95, 878-889.

Supplementary figures

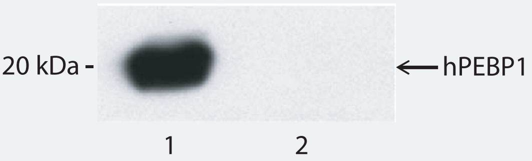

Supplementary Figure 1. Endogenous hPEBP1 binds to PF-3717842. Analysis of hPEBP1 in pull-downs from human HeLa cell lysate. Following nonspecific elution, SDS-PAGE and immunoblotting using an anti-hPEBP1 antibody, the hPEBP1 protein was detected in a pull-down with PF-3717842 functionalized beads (lane 1), but was absent when control beads were used (lane 2)

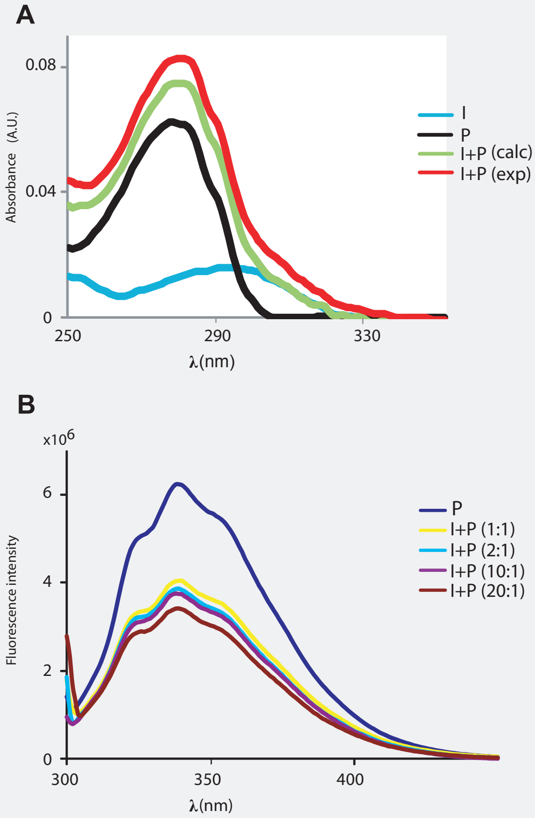

Supplementary Figure 2. hPEBP1 binds directly to PF-3717842. Panel **A** shows the superposition of the UV-VIS spectra recorded for PF-3717842 alone (I, blue line), hPEBP1 alone (2μM) (P, black line), the sum of the spectra A and B (I+P(calc), green line) and hPEBP1 in the presence of PF-3717842 (at 1:1 ratio) (I+P(exp), red line). Panel **B** shows the superposition of the fluorescence emission spectra recorded for h PEBP1 in the absence and the presence of PF-3717842. Line P represents human PEBP1 (400 nM) alone, while lines colored yellow, blue, purple and brown are emission spectra of hPEBP1 in the presence of increasing concentrations of PF-3717842, inhibitor: protein, (1:1), (2:1), (10:1), (20:1).

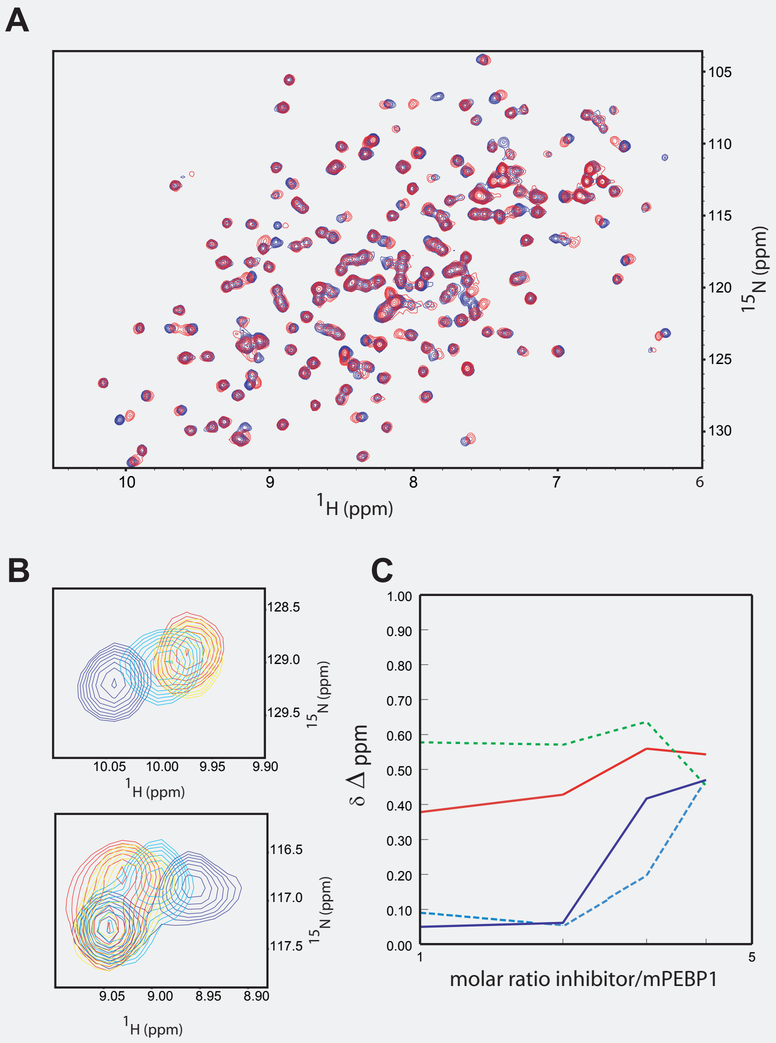

Supplementary Figure 3. mPEBP1 binds directly to PF-3717842. Panel **A** displays a ^{15}N HSQC NMR spectrum of 150 μM mPEBP1 in the absence (blue) or presence of PF-3717842(450 μM)(red). In panel **B**, close-ups of two affected resonances in mPEBP1 are shown. The spectra are shown for mPEBP1 alone (blue) and in the presence of 150 μM (yellow), 300 μM (orange) and 450 μM PF-3717842 (red). Indicated numbers are arbitrary. The maximum chemical shift was determined for all affected resonances and the relative chemical shift perturbation for each PF-3717842 titration point was calculated to this maximum and plotted as a function of the [PF-3717842] (μM) in panel **C**. At least two clusters were obtained with a distinct apparent dissociation constants, average fraction bound was determined separately for these clusters. Indicted K_d+/-standard deviation is calculated as described in material and methods section.

Chapter 4

Target profiling of a small library of PDE5 inhibitor derivatives using chemical proteomics

Poupak Dadvar[1,2], Reinout Raijmakers[1,2], Joost Gouw[1,2], Klaus Rumpel[3], Albert J.R. Heck[1,2,4]

[1] Biomolecular Mass Spectrometry and Proteomics Group, Bijvoet Center for Biomolecular Research and Utrecht Institute for Pharmaceutical Sciences, Utrecht University, Padualaan 8, 3584 CH Utrecht, the Netherlands
[2] Netherlands Proteomics Centre, Padualaan 8, 3584 CH Utrecht, the Netherlands
[3] Pfizer Global Research and Development, Sandwich, United Kingdom
[4] Centre for Biomedical Genetics, Padualaan 8, 3584 CH Utrecht, the Netherlands

Based on: Submitted manuscript

Abstract

Inhibitors of phosphodiesterase 5 (PDE5) are widely used for the treatment of erectile dysfunction and pulmonary hypertension. The commercially available inhibitors are effective drugs with limited side effects, but differ in their phosphodiesterase specificity. To explore the specificity of PDE5 inhibitors, a small library of four inhibitors was synthesized using the structure of known PDE5 inhibitors as a scaffold. The inhibitory potency of the inhibitors towards PDE5 was tested and they were immobilized on a matrix to perform affinity pull-downs followed by mass spectrometric analysis. We quantified the relative binding of a large set of proteins to these inhibitors by using the unique peptide counts of identified proteins in the MS analysis. This approach, the results of which were verified using quantitative isotopic dimethyl labelling and immunoblotting, allowed the confident determination of drug selectivity profiles of the inhibitors in vitro. We demonstrate that the combination of chemical proteomics and unique peptide counting allows for the confident and easy analysis of the differential interactome of bioactive small molecules. For the PDE5 inhibitors, we show that even slight chemical modifications could bias their selectivity towards other interacting proteins, opening up the potential of these compounds to be used as scaffolds for the development of inhibitors for new protein targets.

Introduction

Cyclic nucleotide phosphodiesterases (PDEs) are a superfamily of enzymes that catalyze the hydrolysis of the second messenger nucleotides, cAMP and cGMP, to their respective 5′-nucleotides monophosphate, AMP and GMP, to regulate the cellular levels of these ubiquitous nucleotides. There are at least 11 different PDEs, each with their specific structural and biochemical properties. Based on their enzymatic activity, they are classified as either class I or class II enzymes. Class I enzymes selectively catalyze the hydrolysis of the 3′ cyclic phosphate bonds, whereas class II enzymes will also catalyze the hydrolysis of the phosphodiesterase bond[1-3].

One of the members of the PDE superfamily is PDE5, which regulates vascular smooth muscle contraction[1] and is expressed in a wide variety of tissues such as lung, heart, brain, kidney and prostate[4]. PDE5 is a homodimer, containing two highly homologous regulatory GAF domains (GAF-A and GAF-B) and one catalytic domain near the carboxyl terminus. The GAF-A domain contains the high affinity cGMP binding site (Kd is about 40 nM)[5] and has a dominant role in the enzyme's activity[6]. The GAF-B domain is important in dimerization of the protein, and can inhibit cGMP binding to GAF-A[7]. Because of the role PDE5 plays in the NO/cGMP signaling pathway it is at present the main therapeutic target to treat erectile dysfunction (ED). After sexual stimulation, which triggers release and diffusion of NO into cells, soluble guanylate cyclase will be activated, which produces cGMP from GTP. The enhanced level of cGMP stimulates PKG, thereby activating a protein phosphorylation cascade. This causes the intracellular levels of calcium to decrease, leading to dilation of particular arteries in pennis followed by erection[8,9]. Because PDE5 normally hydrolyses cGMP, inhibiting PDE5 prevents degradation of cGMP and enhances the erectile response to sexual stimulation[10].

The most commonly used PDE5 inhibitors include sildenafil (Viagra), vardenafil (Lavitra) and tadalafil (Cialis). Tadalafil and vardenafil are slightly more potent inhibitors of PDE5 than sildenafil, with vardenafil showing the highest inhibitory potency even though sildenafil and vardenafil have high structural similarity[11]. The difference in inhibitory effect is caused by differences in the double cyclic part of their structure, as a conserved amino acid in the PDE5 catalytic site (Tyr612) interacts with the pyrazole ring in vardenafil and sildenafil. Due to the hydrogen bonds and hydrophobic interaction of this residue with the pyrazole ring of the inhibitors, vardenafil binds stronger to PDE5 than sildenafil[12]. The use of the chemically quite different inhibitor tadalafil has been reported to give the longest duration of PDE5 inhibition among these three PDE5 inhibitors[13].

All three commonly used inhibitors have much higher affinity for PDE5 in comparison with other PDEs. The crystal structure of PDE5A in complex with the inhibitor sildenafil and vardenafil indicates that several different chemical groups of the inhibitor interact with a specific area of the catalytic domain[14, 15]. Differences in specificity of different inhibitors of the PDE family arise from relative specific sequences in their catalytic domain[16, 17]. Although tadalafil is very selective for PDE5, it can also potently inhibit PDE11. Additionally, all aforementioned inhibitors are capable to inhibit PDE1 and PDE6, which might contribute to observed side effects like vasodilation / tachycardia and transiently disturbed vision, respectively[18].

We previously have described the target selectivity of the PDE5 inhibitors PF-4540124 and PF-3717842, structurally related to sildenafil and vardenafil, using chemical proteomics and showed that they can interact selectively with a few other proteins besides the members of the PDE superfamily, albeit with somewhat lower affinity compared to PDE5[19, 20].

Such information is important to better understand the full biological effects of a drug. Therefore, methods to determine protein interactors of drugs are of great importance for both research and drug development[21]. Target selectivity and specificity are common issues in the identification and development of candidate inhibitor based drugs, and selectivity profiling is a major part of drug discovery and development. Chemical proteomics is a relatively new approach to directly determine the inhibitor's selectivity from biologically relevant systems[21-23]. A typical chemical proteomics approach to determine a drug protein interactome involves the immobilization of the drug to an affinity support. Using this immobilized drug as bait, proteins interacting with the drug can be "pulled-down" from any relevant protein source of interest (e.g. a specific tissue) and characterized by proteomics methods like 2D-SDS PAGE and mass spectrometry[24, 25]. Mass spectrometry will allow the identification of all proteins interacting with the drug, but comparison of the affinity that proteins have for different drugs is difficult. However, quantitative mass spectrometric analysis of the interactome can supply such information and allows characterization of the selectivity profile of drugs. There are several approaches for quantitative mass spectrometric analysis of protein samples. One approach for protein quantification is the incorporation of differential stable isotopes in the samples by metabolic or chemical means[26-28], but there are also "label free" solutions such as unique peptide count, spectral counting[29-32] and peptide chromatographic peak intensity measurements[29, 30, 33-36].

Here, we use an affinity enrichment strategy as described above in combination with quantitative mass spectrometry to compare the protein binding profiles of four chemical derivatives of a compound structurally related to the PDE5 inhibitors sildenafil and vardenafil (see Figure 1 and 2). We essentially use a previously described, optimized chemical proteomics approach. In this approach we use pre-clearing of the tissue lysates with competitive binders to reduce the binding of non-specific high abundant proteins, which significantly improves the coverage and reliability of the bonafide inhibitor's interactome [19]. To quantitatively compare the selectivity profiles of the four inhibitors, we first used a label free approach, called emPAI (exponentially modified protein abundance index) that is based on the normalized number of unique peptides per proteins identified in the analysis[32] (Figure 1A). This semi-quantitative approach revealed already a few significant differences in the selectivity profiles of these structurally alike inhibitors. For some of the most significant protein binders we confirmed the selective binding by using stable isotope labeling based quantitative mass spectrometry (Figure 1B) and western blotting.

Material and methods

Materials

Affigel-10 pre-activated beads were purchased from Bio-Rad. Guanosine 3´,5´-cyclic monophosphate (cGMP), guanosine 5'-diphosphate (GDP) and adenosine diphosphate (ADP) were obtained from Biolog. NAD was purchased from Sigma-Aldrich. Trypsin (analytical grade), Lys-C and Protease inhibitor cocktail, were purchased from Roche Diagnostics. HPLC-gradient grade acetonitrile was from Biosolve. To detect PEBP-2 by immunoblotting, we used a rabbit polyclonal antibody towards PEBP-1 (cell signalling) which also recognizes PEBP-2. The goat polyclonal antibody directed against PrBP and the anti-PDE5 rabbit polyclonal antibody were purchased from Santa Cruz Biotechnology.

Preparation of rat testis tissue cell lysate

The testis lysate was essentially prepared as described before[20]. Briefly, testis tissue of six month old Wistar rats was pulverized in a pre-cooled custom made mortar with liquid nitrogen. The resulting powder was resuspended in 1 ml cold lysis buffer (25 mM sodium phosphate buffer containing 150 mM NaCl, 5 mM

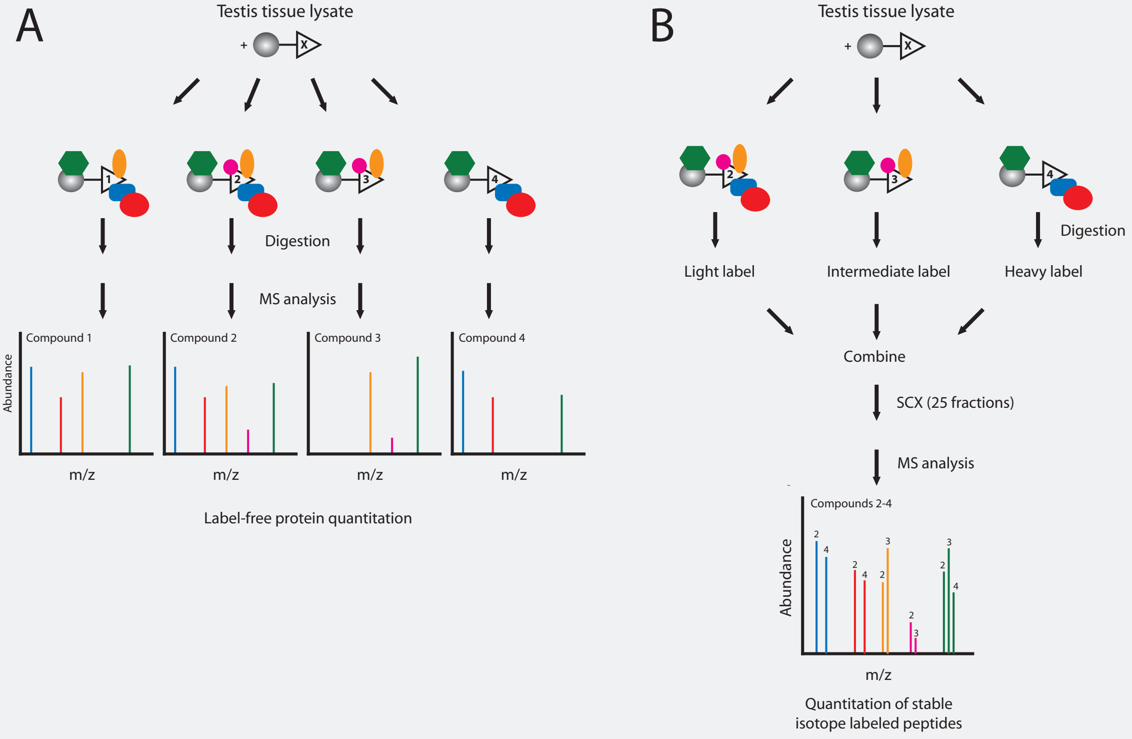
A
Testis tissue lysate
+
X
1
2
3
4
Digestion
MS analysis
Compound 1
Compound 2
Compound 3
Compound 4
Abundance
m/z
Label-free protein quantitation
B
Testis tissue lysate
+
X
2
3
4
Digestion
Light label
Intermediate label
Heavy label
Combine
SCX (25 fractions)
MS analysis
Compounds 2-4
Abundance
m/z
Quantitation of stable
isotope labeled peptides

Figure 1. Schematic overview of the quantitative LC-MS/MS analyses of the interactome of the four used PDE5 inhibitors. A) For the label free quantitation, all proteins pulled down from the rat testis tissue lysate are analyzed separately by LC-MS/MS for all four compounds, after which unique peptide counting allows relative semi-quantitation of the different interacting proteins. B) In the isotope labeling approach, peptides proteolytically derived from the enriched proteins pulled down with compounds 2, 3 and 4 are isotope labeled and mixed. After SCX separation, the resulting fractions are analyzed by LC-MS/MS and the relative intensities of the differentially labeled peptides quantified.

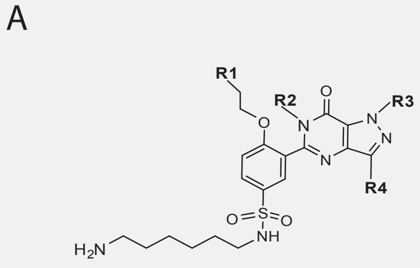
A
R1
R2
R3
R4
O
N
N
N
N
O
O=S=O
NH
H2N

Compound 1: R1= H, R2 = H, R3 = CH_3, R4 = $CH_2CH_2CH_3$
Compound 2: R1= CH_3, R2 = H, R3 = CH_2CH_3, R4 = CH_3
Compound 3: R1= H, R2 = H, R3 = CH_3, R4 = CH_3
Compound 4: R1= H, R2 = CH_3, R3 = CH_3, R4 = $CH_2CH_2CH_3$

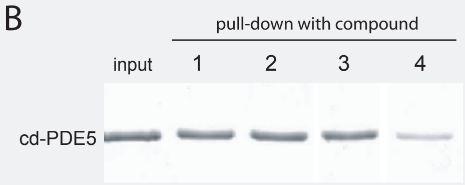
B
pull-down with compound
input
1
2
3
4
cd-PDE5

Figure 2. Structure and cd-PDE5 binding of the inhibitors. A) Core structure of the four different PDE5 inhibitors, with the positions varying between the inhibitors indicated in bold (R1-R4). The chemical groups present at each of these positions in the four inhibitors are listed below the structure. B) Coomassie staining of gel after a pull-down of a recombinant catalytic domain of PDE5 (cd-PDE5) with the four immobilized inhibitors (1-4). The input of the pull-down is shown in the leftmost lane.

$MgCl_2$, 1 mM EDTA, 300 mM sucrose, protease inhibitor cocktail) and incubated at RT for 5 minutes to solubilize all proteins. After centrifugation at 13.000 rpm for 10 minutes, the supernatant was collected and stored at -80 °C until further use. All rat experiments were in compliance with Dutch legislation and were approved by Utrecht University Committee for animal experimentation.

Synthesis and immobilization of inhibitors

The compounds 1, 2, 3 and 4 (Figure 2A) were synthesized as described previously[19, 37]. To obtain inhibitors suitable for immobilization to NHS-activated sepharose beads, all compounds were synthesized from a benzene sulfonyl chloride pyrazolopyrimidinon derivatives, functionalized with 1,6-diaminohexane and reacted with diisopropylethylamine to obtain the free amine functionalized compound. For immobilization, NHS-activated sepharose affinity beads (500 µL) were washed with 10 volumes of cold HCl (1 mM) followed by 5 volumes of acetonitrile/water (1:1). The hydrochloric acid salts of compound 1, 2, 3 and 4 (20 µM) were separately dissolved in 500 µL acetonitrile/water (1:1) containing diisopropylethylamine (DIPEA) and stirred overnight at room temperature (RT). The resulting free amine functionalized inhibitors were added individually to 500 µL beads and incubated for 4 hours at room temperature with mild stirring. The beads were collected and incubated with ethanolamine (2 M) for 2 hours (RT) to inactivate the residual reactive sites on the beads. The beads were subsequently washed with 2 volumes of phosphate buffer (0.1 M sodium phosphate buffer, pH 7.2) and stored in the same buffer containing 0.1% sodium azide at 4 ºC.

Affinity enrichment and digestion

Cell lysate of rat testis tissue was pre-incubated for 1 hour with nucleotides ADP, GDP and NAD (5 mM final concentration each) to decrease the binding of nonspecific proteins as described before[38].The cell lysate was incubated with 200 µL ethanolamine inactivated sepharose beads for 30 min to remove hydrophobic sepharose interactors[39]. The beads were removed and the remaining testis cell lysate was incubated individually with compound 1, 2, 3 and 4 functionalized beads for 2 hours followed by 6 times mild washing with 3 mL lysis buffer. The remaining bound proteins were either digested on the beads for mass spectrometric analysis or eluted with SDS sample buffer and analysed by SDS-PAGE. For on bead digestion, the beads were resuspended in 8 M urea (in 50 mM ammonium bicarbonate solution), Lys-C enzyme was added (1:50 ratio) and incubated overnight. Samples were reduced with DTT (final concentration 2 mM) at 56ºC, then alkylated with iodoacetamide (final concentration 4 mM) at RT. The eluate was diluted to 2M urea (in 50 mM ammonium bicarbonate solution) and subjected to trypsin enzyme digestion (1:100 ratio) twice for 4 hours at 37ºC. Digested samples were separated from the beads and peptides were desalted with C18 material (3M Empore C18 extraction disk) packed into GELloader Tips as previously described[40.] The samples were dried down and reconstituted in 5% formic acid.

Triple stable isotope dimethyl labelling

The digested eluates of the pull-downs with compound 2, 3 and 4 were also subjected to isotopic dimethyl labelling[41,42]. All peptides were desalted, dried in-vacuo and re-suspended in 100 μL of triethylammonium bicarbonate (100 mM). To estimate the labelling efficiency and peptide recovery, 100 fmol of tryptically digested BSA was added to each sample. To obtain "light" labelling of the peptides obtained with compound 2, formaldehyde (4 μL, 4% v/v in water) and freshly prepared sodium cyanoborohydride (4 μL, 600 mM) were added to the mixture followed by incubation for 120 min at 37 ºC with. The reaction was stopped by the addition of 16 μL 1% ammonium hydroxide. Peptides obtained with the compounds 3 and 4 were labelled with essentially the same method but now using D-formaldehyde- (4% v/v in water) to obtain "intermediate" labelling for compound 3 and using ^{13}C-D-formaldehyde (4% v/v in water) and cyanoborodeuteride for "heavy" labelling of the compound 4 peptides. The "light", "intermediate" and "heavy" dimethyl labelled samples were mixed in a 1:1:1 volume ratio and desalted. The sample was dried down and reconstituted in 20% acetonitrile, 0.05% formic acid and fractionated using cation exchange (SCX) chromatography to decrease the complexity of the sample. SCX separation was performed using a Zorbax BioSCX-series II columns (Agilent Technologies, ID: 0.8 mm x 1:50 mm, particle size 3.5 μm), a Famos autosampler (LC packings, Amsterdam, The Netherlands), a Shimadzu LC-9A binary pump and a SPD-6A UV-detector (Shimadzu, Tokyo, Japan). After 10 minutes of isocratic flow of 100% solvent A (0.05% formic acid in 8:2 (v/v) water acetonitrile, pH 3), a linear gradient was started of 1.3% solvent B per minute (500 mM NaCl in 0.05% formic acid in 8:2 (v/v) water acetonitrile, pH 3) for 60 minutes. In total 25 fractions were collected and dried by vacuum centrifugation. After re-constitution in 5% formic acid, all fractions were analyzed by LC-MS/MS.

NanoLC-MS/MS

Nanoscale liquid chromatography tandem mass spectrometry (nano-HPLC-MS/MS) was performed on an Agilent 1200 HPLC system directly connected to LTQ-Orbitrap mass spectrometer (Thermo Fisher Scientific, Bremen, Germany). The LC system was equipped with a 20 mm Aqua C18 (Phenomenex, Torrance, CA) trapping column (packed in-house, i.d., 100 μm; resin, 5 μm) and a 400 mm ReproSil-Pur C18-AQ (Dr. Maisch GmbH, Ammerbuch, Germany) analytical column (packed in-house, i.d., 50 μm; resin, 3 μm). Trapping was performed at 5 μL/min for 10 min, and elution was achieved with a gradient of 10 to 28% B (0.1 M acetic acid 80% acetonitrile and 20% water) in 70 min, 28 to 60% B in 10 min, 60 to 100% B in 7 min and 100% B for 2.5 min. The flow rate was passively split from 0.45 mL/min to 100 nL/min as described previously[43]. The mass spectrometer was operated in data dependent mode to automatically switch between MS and MS/MS. Survey full scan MS spectra were acquired from m/z 350 to 1500 and the two most intense ions were selected for fragmentation. The target ion setting was 5e^5 for the Orbitrap, with a maximum fill time of 250 ms. Fragment ion spectra were acquired by collisionally induced dissociation in the LTQ with a target ion setting of $3e^4$ and a maximum fill time of 500 ms. Dynamic exclusion for selected precursor ions was set at 30 seconds.

Data processing and analysis

All MS2 spectra were converted into peak lists using Bioworks version 3.3.1 SP1 (Thermo Fisher Scientific) and searched using an in-house licensed Mascot search engine (version 2.2.04; Matrix science, London, UK) against all rodent proteins of the NCBI non redundant database (version 20082710). Carbamidomethylation of cysteine was included as a fixed modification, and protein N-acetylation and oxidation of methionine as variable modifications. Trypsin was chosen as the proteolytic enzyme and two missed cleavages were allowed. The mass tolerance of the precursor ion and the fragments ions were set to 10 ppm and 0.9 Da respectively. To estimate the false discovery rate (FDR)[44] of our dataset, a search was performed against a decoy database based on the same NCBI database, in which the protein sequences were reversed[45]. At a peptide ion score cut-off of 20 with a protein threshold of 40 and a minimum of 2 identified peptides per protein, the estimated FDR was calculated to be 1%. To determine the relative protein abundance, we calculated, using Mascot, the emPAI values (defined as 10^{PAI}-1, in which PAI is the number of observed peptides divided by the total number of theoretically observable peptides) for all identified proteins. We extended this calculation by normalizing the emPAI values for each protein over the four different experiments. In the case of stable isotope labelling, dimethylation (K, N-term), dimethylation: $^2H(4)$ (K, N-term) and dimethylation: $^2H(6)^{13}C(2)$ (K, N-term) were included as additional variable modifications. Quantitation of peptides was performed using MSQuant (v 1.4.2a13). All quantified peptide triplets were manually inspected to exclude quantified peptides with poor MS/MS spectra or a high signal to noise ratio. We combined the XIC (extracted ion chromatogram) intensity values of all peptides from a protein to calculate the relative ratio of abundance of proteins in the different samples.

Immunoblotting

For immunoblot analysis, the proteins bound after pull-down with the immobilized inhibitors were recovered by the addition of SDS-sample buffer to the beads. After heat denaturation, the proteins were separated by 15% SDS-PAGE and electrotransferred to a PVDF membrane. The membrane was blocked by incubation with 5% BSA in Tris-buffered saline/Tween 20 (TBST) and incubated with either anti-PDE5 (1/500), anti-PEBP-2 (1/1000) or anti-PrBP (1/1000) antibodies for one hour. Next, the membranes were incubated with appropriate HRP labelled secondary antibodies and analyzed by enhanced chemiluminescence (Amersham Bioscience). Image analysis, quantitation and background correction were performed using the Quantity One software.

Results

Synthesis of PDE5 inhibitory compounds

Related to the structures of the PDE5 inhibitors sildenafil and vardenafil, four potential PDE5 inhibitor derivatives were synthesized (Figure 2A, compounds 1-4)[19, 37]. The core structure of all compounds is the same, with small variations introduced at four positions (R1-R4) in the phenyl and heterocyclic rings. In compound 2, the ethoxy phenyl group present in most compounds is changed to a propoxy phenyl and the methyl group on position (1)N is replaced by an ethyl group (R3). The hydrogen at the (6)N position is substituted by an extra methyl group in compound 4 (R2). At (3)C, compounds 1 and 4 contain a propyl group, whereas compounds 2 and 3 have a methyl group at that position (R4). Compounds 1 and 2 correspond to the previously described inhibitors PF-3717842 and PF-4540124, respectively[19 , 20].

Inhibition of PDE family proteins

To evaluate the inhibitory potency of the different compounds, we measured their IC50 against eleven members of the phosphodiesterase family using a phosphodiesterase [^{3}H] cGMP scintillation proximity assay (Table 1). Considerable differences in the IC50 values were observed between the various compounds, with most inhibitors showing affinity for PDE1 (subtypes A and C), PDE5 and PDE6. The presence of the extra methyl group at position (6)N (R2) in compound 4 strongly reduced the inhibition of all PDE family members, whereas the effects of the other modifications were more subtle. The propyl to methyl substitution at (3)C (R4) of the pyrazol group in compound 3 reduced the inhibition of the PDE1, PDE5 and PDE6 proteins slightly compared to compound 1. The additional modifications in compound 2 (at positions R1 and R3) increased its inhibition of PDE5 and PDE6 relative to compound 3, making this compound the most specific for PDE5 and PDE6 compared to the other PDE family members, including PDE1.

Functionality of inhibitor-immobilized sepharose beads

Having established the inhibitory potential of all four compounds for the PDE family members, we coupled the four inhibitors to NHS-activated sepharose beads to be able to pull-down interacting proteins. To assess the functionality of the functionalized beads following immobilization of the inhibitors, a pull-down assay with the recombinant catalytic domain of PDE5 (cd-PDE5) was performed. All four immobilized inhibitors were incubated with cd-PDE5, washed thoroughly and the remaining protein was eluted using SDS sample buffer. A Coomassie stained SDS-PAGE analysis (Figure 2B) of the eluted protein showed binding of cd-PDE5 to all four immobilized inhibitors. However, less cd-PDE5 was retrieved from the beads functionalized with compound 4. This suggests a lower affinity of compound 4 for cd-PDE5 compared to the other compounds, which conforms with the lower IC50 value determined for the inhibition of PDE5 by compound 4.

Table 1. IC50 values of the four compounds across different PDEs.

	PDE																		
Compound	**1A**	**1B**	**1C**	**2**	**3A**	**3B**	**4A**	**4B**	**4C**	**4D**	**5**	**6**	**7A**	**7B**	**8A**	**8B**	**9**	**10**	**11**
1	113 nM	>10 µM	43 nM	>10 µM	>10 µM	>10 µM	>10 µM	>10 µM	>10 µM	>10 µM	2.4 nM	6.2 nM	>10 µM	>10 µM	>10 µM	>10 µM	>10 µM	7.4 µM	3.7 µM
2	5.1 µM	>10 µM	2.4 µM	>10 µM	6.4 µM	>10 µM	>10 µM	>10 µM	>10 µM	>10 µM	3.2 nM	7.4 nM	>10 µM	>10 µM	>10 µM	>10 µM	>10 µM	6.1 µM	4.5 µM
3	4.8 µM	>10 µM	1.1 µM	>10 µM	>10 µM	>10 µM	>10 µM	>10 µM	>10 µM	>10 µM	34 nM	105 nM	>10 µM	>10 µM	>10 µM	8 µM	>10 µM	>10 µM	>10 µM
4	>10 µM	>10 µM	>10 µM	>10 µM	>10 µM	3.1 µM	>10 µM	>10 µM	>10 µM	>10 µM	1.1 µM	>10 µM	>10 µM	>10 µM	>10 µM	>10 µM	>10 µM	>10 µM	>10 µM

Identification of interacting proteins

Using the four immobilized compounds, we performed individual pull-down assays from rat testis tissue lysate. To reduce non-specific binding of generic nucleotide interacting proteins, the lysate was pre-incubated with nucleotides (NAD, ADP and GDP), aiming to reduce binding of abundant proteins having higher affinity for these compounds than for the PDE5 inhibitory compounds[19]. After incubating the beads with the lysate and extensive washing, the interacting proteins were eluted by on-bead digestion using endoproteinase Lys-C and trypsin. After desalting, the resulting peptides were analyzed by LC-MS/MS on an LTQ-Orbitrap mass spectrometer and searched against all rodent proteins in the NCBI database using the Mascot search engine. All proteins were identified with a minimum protein score of 40 and at least 2 unique peptides. Based on these criteria, 299 proteins were identified in the interactome of compound 1, 253 for compound 2, 105 proteins for compound 3 and 356 proteins for compound 4. Forty-five proteins were identified in the interactome of all four inhibitors and are considered to be the common interacting proteins. These include well-known nonspecific interactors such as hemoglobin, tubulin and oxidase/dehydrogenase enzymes, but also NAD and ATP binding proteins like peroxisomal multifunctional enzyme type 2 and glutamine synthetase. Among the proteins identified in the interactome of multiple compounds were also several previously identified targets such as PDE5 itself, but also the prenyl binding protein (PrBP, also known as PDE6D) and phosphatidylethanolamine binding protein-2 (PEBP-2). Four different members of the phosphodiesterase family (PDE5, PDE1, PDE10 and PDE 4) were identified in at least one interactome of the four compounds. Remarkably, not a single member of the PDE family was identified amongst the 356 proteins detected as the interactome of compound 4, although 4 was able to retrieve PEBP-2. It should be noted that the PEBP-2 protein identified in the NCBI database was actually the mouse PEBP-2 protein (mPEBP-2), even though we used rat testis tissue for the pull-down experiments. After close inspection, it became clear that the rat PEBP-2 protein (rPEBP-2) was not present in the used recent version of the NCBI database. However, mPEBP-2 shares 89% sequence identity with rPEBP-2 and all of the peptides assigned to PEBP-2 were present in both rPEBP-2 and mPEBP-2.

Selectivity profile generation by label free quantitation

To evaluate the relative binding efficiency of the compounds 1 to 4 to the identified proteins, we used a label-free approach to quantitatively compare the different interactomes. We performed quantification based on the number of unique peptides per protein (more specifically the emPAI approach[32]). The abundance of a given protein in a certain sample relative to all four pull-downs was then calculated as the ratio of its emPAI value in that sample over the sum of the emPAI values for that protein in all four samples. These ratios where then plotted in a heat map to compare the relative abundance of all interacting proteins for the four compounds (Supplementary Figure 1). A selected heat map, including data for some proteins known to interact with PDE5 inhibitors reveals for a few proteins clear specificity (Figure 3). The data presented in Figure 3 clearly reveal that PDE5 was most efficiently pulled-down by using compound 1, when compared to compound 2 and 3, while no PDE5 was retrieved using compound 4. Of the other identified phosphodiesterases, PDE10 could be pulled-down using each of the four immobilized inhibitors, but PDE1A and PDE4A were retrieved only by using compound 1. The protein PrBP was identified in all pull-downs except the one with compound 4, but most abundant in the pull-down using compound 3. Interestingly, the protein PEBP-2 bound most strongly to compound 4, but did not interact with compound 2, suggesting a different mode of binding of PEBP compared to PDE5 and PrBP. Most of the commonly identified (background) proteins showed very similar ratios in all the pull-downs (Figure 3 and Supplementary Figure 1), suggesting they bind either to a common constant region in the four used inhibitors or a-specifically to the affinity matrix or the linker.

Validation of the selectivity profiles

To validate the selectivity profiles obtained using the label free chemical proteomics approach, we also performed some quantitative differential isotope labelling using triplex stable isotope dimethyl labelling[41, 42]. We performed pull-downs with compound 2, 3 and 4 functionalized beads. In this approach, the proteolytic peptides resulting from the pulled-down proteins were chemically labelled using different isotopomers of formaldehyde and cyanoborohydride to be able to distinguish and quantify the different interactomes in the mass spectrometer after mixing the samples (Figure 1B). As the triple labelling and mixing causes a threefold increase in complexity of the sample, which can be

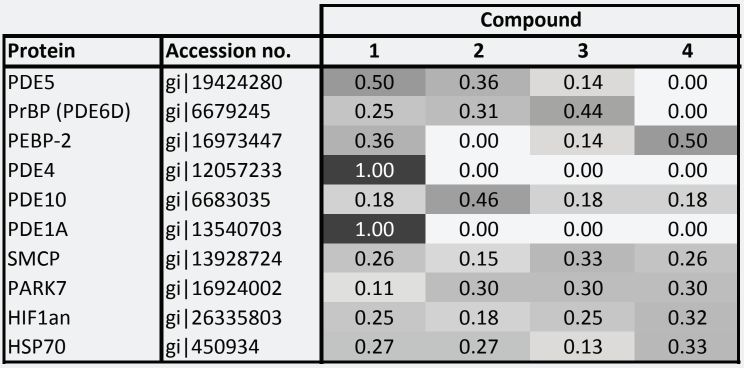

		Compound			
Protein	**Accession no.**	**1**	**2**	**3**	**4**
PDE5	gi|19424280	0.50	0.36	0.14	0.00
PrBP (PDE6D)	gi|6679245	0.25	0.31	0.44	0.00
PEBP-2	gi|16973447	0.36	0.00	0.14	0.50
PDE4	gi|12057233	1.00	0.00	0.00	0.00
PDE10	gi|6683035	0.18	0.46	0.18	0.18
PDE1A	gi|13540703	1.00	0.00	0.00	0.00
SMCP	gi|13928724	0.26	0.15	0.33	0.26
PARK7	gi|16924002	0.11	0.30	0.30	0.30
HIF1an	gi|26335803	0.25	0.18	0.25	0.32
HSP70	gi|450934	0.27	0.27	0.13	0.33

Figure 3. Relative abundance of selected proteins after rat testis tissue pull-down. After isolation of the proteins interacting with the four inhibitors by a pull-down assay from rat testis tissue and label free quantitation, the relative abundances of all proteins in the four pulldowns were calculated. The resulting abundances are indicated and colored according to their intensity (dark grey for high abundance, light grey for low abundance). Shown are the abundances obtained for selected specifically interacting proteins (PDE5, PEBP-2, PrBP, PDE4, PDE10 and PDE1A) and some nonspecific interactors (SMCP, PARK7, HIF1an and HSP70). The original NCBI accession numbers of the proteins are listed. A full heatmap containing all identified proteins, sorted by accession number, is shown in the supplementary figure 1.

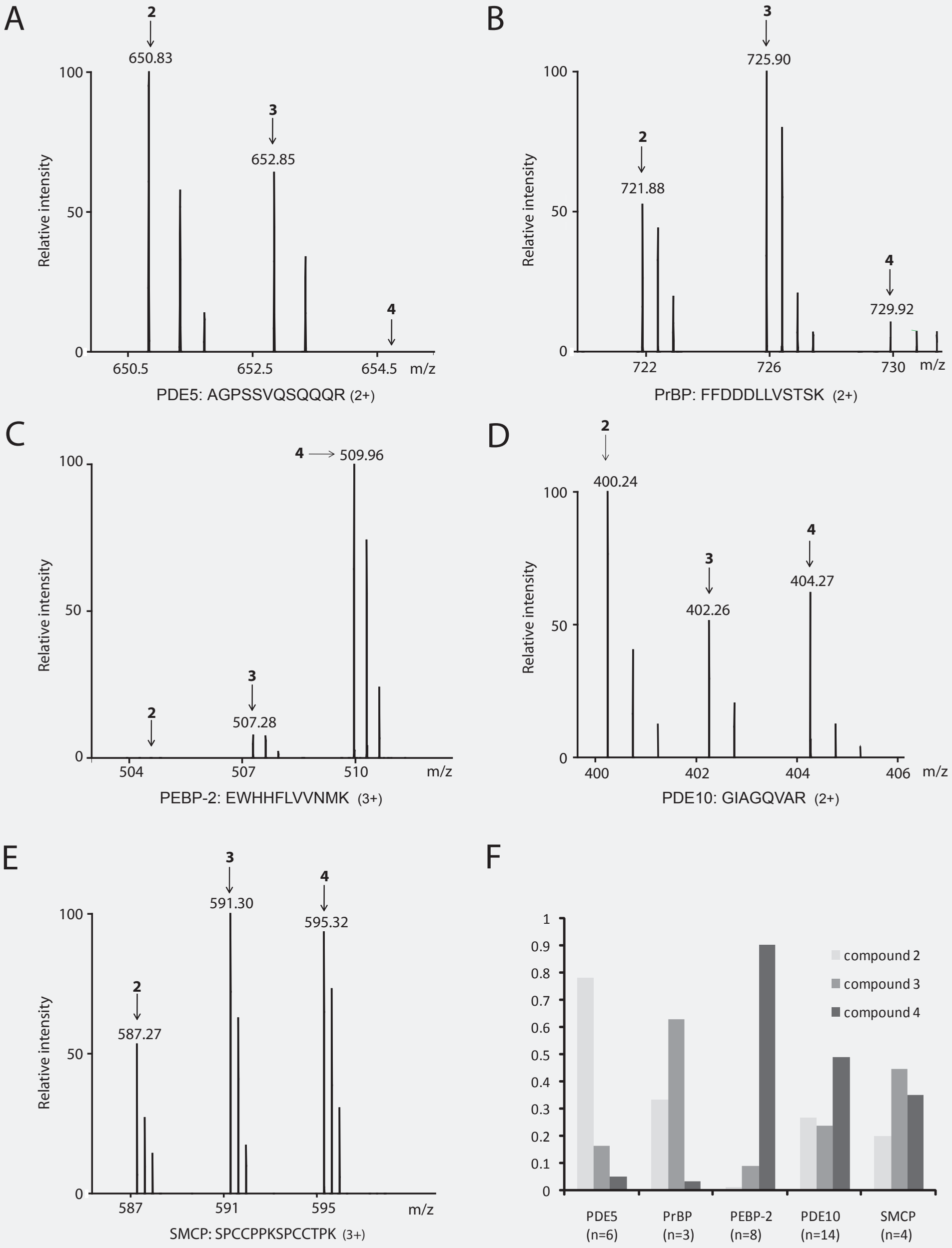

Figure 4. Stable isotope labeling based quantification of selected proteins. Typical mass spectra of peptide triplets derived from selected proteins after stable isotope labeling of proteins pull-down with compounds 2 (light label), 3 (intermediate label) and 4 (heavy label). The spectra shown are derived from the proteins PDE5 (**A**), PrBP (**B**), PEBP-2 (**C**), PDE10 (**D**) and SMCP (**E**). Mass ranges, peptide sequences and peptide charge state are indicated below the mass spectra. **F**) Graph showing per compound the summed intensities of all identified and quantified peptides for the analyzed proteins (compounds 2, 3 and 4 in light grey, grey and dark grey, respectively). The number of peptide used for the quantitation of each protein is indicated below the graph.

a barrier for protein identification in complex proteomes[46], we reduced the complexity of the sample by strong cation exchange chromatography (SCX) prior to LC-MS/MS analysis. The resulting fractions were then analysed by standard LC-MS/MS on an LTQ-Orbitrap mass spectrometer and searched against the NCBI database using Mascot. We quantified the abundances of labelled peptide triplets corresponding to selected proteins (PDE5, PrBP, PEBP-2, and SMCP) by calculating the extracted ion chromatogram intensity of each individual peptide isotopomer. The peptide intensities observed in the mass spectra for the three different isotopomers displayed a pattern very similar to the relative binding efficiencies obtained in the label-free approach. For PDE5 derived peptides, the light labelled isotopomer (corresponding to compound 2) was the most intense, followed by the intermediate isotopomer (compound 3), while the heavy isotopomer was either very low or not detected (Figure 4A). In the case of PrBP (Figure 4B) peptides, the intermediate peptides (compound 3) were most intense, whereas for PEBP-2 (Figure 4C) the heavy peptide (compound 4) isotopomers were by far most intense, nicely in agreement with relative abundances estimated in the label free experiment. Peptide triplets corresponding to PDE10 and to the protein SMCP showed more alike intensities for all isotopomers (Figure 4D and 4E). The total relative abundances, calculated from the summed intensities of all peptides originating from these proteins (Figure 4F), confirmed the

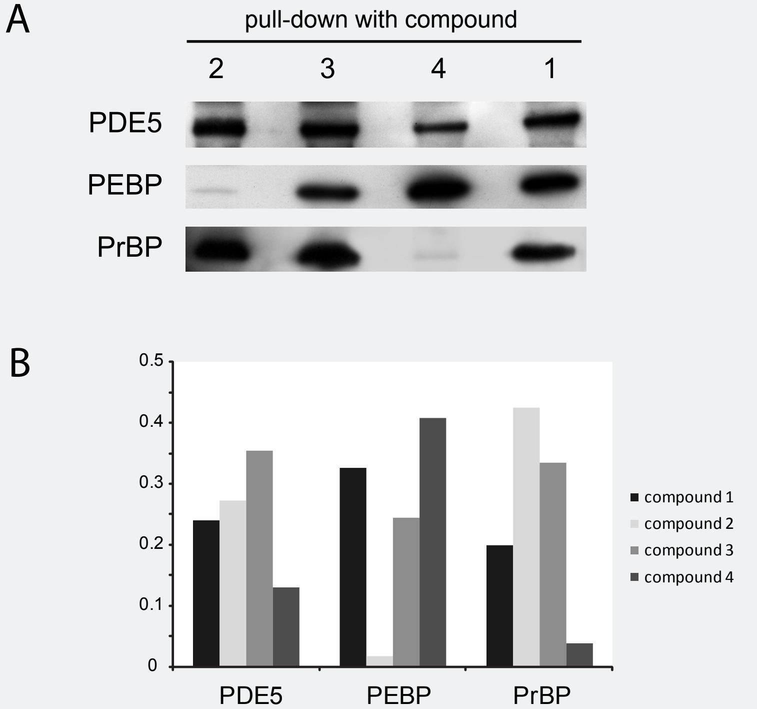

Figure 5. Immunoblotting of pulled down proteins confirms the selectivity profiles. A) Proteins resulting from pull-down experiments with the four compounds were separated by SDS-PAGE and analyzed by immunoblotting using antibodies against PEBP-2, PrBP and PDE5. B) Relative intensities of the three proteins in the immunoblot shown in panel A, as determined by quantitation of the signal intensity.

selectivity profiles obtained in the label free approach. Next, we used antibodies to determine the abundance of PDE5, PEBP-2, and PrBp, after a pull-down from tissue testis lysate with the compounds 1 to 4. Proteins retained by the inhibitor functionalized beads were resolved by gel electrophoresis, subjected to immunoblotting with antibodies against PDE5, PEBP-2 and PrBP (Figure 5A) and the relative protein levels determined by band intensity quantitation. As shown in Figure 5B, PDE5 was present in all pull-downs, but was notably less prominent in the pull-down with compound 4, matching the selectivity profile of PDE5 obtained in the mass spectrometric analyses. PEBP-2 and PrBP were virtually absent in the pull-downs with compounds 2 and 4, respectively and PEBP-2 was most abundantly present when compound 4 was used, clearly confirming the altered selectivity of compound 4 as determined in both quantitative mass spectrometric approaches.

Discussion

Characterizing the interactome of drug molecules and determining their relative selectivity to different interactors is of great importance for the optimization of candidate drugs. Here, we identified and quantified the protein interactome of four different PDE5 inhibitors, all with the same core structural moiety, a pyrazolopyrimidinon structure. All four inhibitors (Figure 2) contain an amine-linker in order to be able to immobilize the chemicals on the activated beads. Based on the crystal structure of PDE5 bound to the structurally related inhibitors sildenafil and vardenafil, this linker was not expected to affect the binding of these types of inhibitors to PDE5.

To characterize the full interactomes of the four PDE5 inhibitors, the immobilized compounds were used in a pull-down with testis tissue lysate to bind their potential targets. Testis tissue lysate is known to contain multiple PDE isoenzymes and is a tissue that conceivably could contain proteins related to erectile dysfunction. The analyses of the interactome of the four different PDE5 inhibitors resulted in the identification of 432 proteins, with 45 proteins shared between the four interactomes. This common interactome included both specific interactors and non-specifically interacting proteins, such as those that bind directly to sepharose beads[39]. Some of the proteins classified as nonspecific interactors included elongation factors, glutathione S-transferases and S100 calcium binding proteins.

Using the emPAI values calculated for each protein in the pull-down experiments with the four inhibitors, we approximated the relative abundance of each interactor in the pull-downs with the four analogues. We hypothesize that the differences in relative abundance of proteins retrieved by different PDE5 inhibitors reflects the differences in affinity of the proteins for these compounds, because the initial abundance in the cell lysate is the same for all pull-downs. Next, we used stable isotope labelling of proteolytic peptides obtained from retrieved proteins, and western blotting to confirm the relative abundances of some specific interactors in the pull-downs. The results obtained with those methods corresponded well with the normalized label-free emPAI peptide counting approach. Where stable isotope labelling requires additional sample handling steps to achieve labelling and western blotting is dependent on the availability of suitable antibodies, the normalized emPAI approach allows a simple method for the relative quantitation of inhibitor/drug interactomes directly from a mass spectrometric analysis.

The quantitative analysis revealed that the different inhibitors had notably different affinities for different proteins, including their main target, PDE5. The main determinant of PDE5 for its substrate cGMP is Gln 817, which also provides a key interaction with PDE5 inhibitors like sildenafil, vardenafil and IBMX. When investigating the co-crystal structure of PDE5-inhibitors complexed with PDE5, this glutamine provides a hydrogen bond with a hydrogen at the (6) N position of the inhibitors[14, 47, 48]. Substitution of Gln 817 by alanine has been shown to markedly decrease the affinity of PDE5 for these inhibitors[48]. Similarly, we observe that the addition of a methyl group at position 6(N) in compound 4 leads to a large decrease in affinity for PDE5.

Substitution at the (1)N and (3)C position of the heterocyclic ring and the ethoxy side chain of the phenyl ring in compound 2 did not affect the binding to PDE5, while just replacing the propyl moiety at (3)C by a methyl group significantly lowered the inhibitory potency of compound 3 towards PDE5. A (3)C-propyl side chain on the pyrazolopyriminone has previously been shown to contribute more to PDE5 binding compared to additional methyl groups on (1)N or on the alkoxy side chain[49]. While showing reduced PDE5 binding, compound 3 had increased affinity for the protein PrBP, an interaction that we described previously and validated using recombinant PrBP[19]. PrBP is a known interactor of some cone and rod PDE6 subunits that may target membrane bound PDE6 to the cytosol[50, 51]. The only other PDE proteins that showed high affinity (nanomolar range) for some of the inhibitors were PDE1A, PDE1C, and PDE6. While the binding of PDE6 to the inhibitors showed a similar profile as PDE5 (Table 1), the binding of both PDE1A and PDE1C was significantly lower for compounds 2-4 compared to compound 1. In total, three isozymes of PDE1 exist. PDE1A and PDE1C have been reported to have high expression levels in developing germ cells, while PDE1B showed a lower expression level[52]. In agreement with the IC50 measurements, compound 1 was the only inhibitor capable of isolating PDE1A from testis cell lysate in our pull-down assays.

One of the most striking differences between the various inhibitors was the change in the selectivity profile of compound 4. While its affinity for PDE proteins was drastically reduced, the compound showed increased affinity for other interacting proteins, most notably PEBP-2. This strongly suggests a different mode of binding of PEBP-2 to these inhibitors compared to most other proteins. PEBP-2 belongs to the highly conserved family of phosphatidylethanolamine binding proteins[53]. While PEBP-2 is only present in rodents, the main family member is the protein PEBP-1, which is also known as the Raf kinase inhibitory protein (RKIP) and is widely expressed in mammals[54, 55]. RKIP plays a role in the MAPK signalling pathways where it binds to Raf-1, causing dissociating of Raf-1 and the protein MEK. As a result, downstream MAPK signalling is interrupted[55]. Because of its role in such an important cellular signalling pathway, RKIP has been implicated in many processes, including membrane biogenesis, spermatogenesis, neural signalling and cardiac output[56]. Although PEBP-2 is a rodent specific protein, human RKIP still has 84% sequence identity with mouse PEBP-2[57] and is also able to bind to certain PDE5 inhibitors, albeit with lower affinity compared to PEBP-2[20]. Although we did detected rat RKIP in our pull-downs, it was generally identified with much lower spectral counts than PEBP-2. Since compound 4 is more selective for PEBP-2 compared to the PDE proteins, this compound potentially provides a chemical scaffold for the development of PEBP/RKIP specific inhibitors.

Conclusion

Here, we used a semi-quantitative label free shotgun proteomics approach to characterize in detail the different selectivity profiles of four PDE5 inhibitors. Following an enrichment step from rat testis tissue lysate with beads functionalized with the four different inhibitors, we used LC-MS/MS to identify all interacting proteins. We semi-quantified the relative abundance of the different proteins by comparing the emPAI values, which are based on the number of unique peptides for each proteins, between the different pull-downs. The observed differences in affinity for various proteins were confirmed using stable isotope labelling followed by mass spectrometric quantification and by immunoblotting. We found significant differences in the binding profiles of the four inhibitors, with one inhibitor showing a shift in affinity from the PDE proteins to another known interacting protein, PEBP-2. This shows that proteomic profiling of the interactome of chemically closely related drugs or inhibitory compounds does not only allow the identification of interacting proteins, but also the relative comparison of binding affinity to find new high affinity protein binders. Our data also nicely illustrate how the interactome of drug molecules can be significantly altered by small chemical modifications. Such modifications can strengthen ideally drug-efficacy, but potentially also reduce side-effects of the drugs caused by interactions with off-target protein binders. Chemical proteomics screens as described here can elucidate new potential targets of established drug molecules, or provide chemical appropriate scaffolds for the development of more specific inhibitors.

Acknowledgements

We would like to thank to dr. A. S. B. Bell (Pfizer Global Research and Development, Sandwich, United Kingdom) for the design and synthesis of the inhibitors and Dr. Toon V. Veen (Department of Medical Physiology, Division of Heart & Lungs, UMCU, Utrecht, The Netherlands) for providing the rat testis tissue. This work is supported by the Netherlands Proteomics Centre, a program embedded in the Netherlands Genomics Initiative.

References

1. A. T. Bender and J. A. Beavo, **Pharmacol Rev**, *2006*, 58, 488-520.
2. K. Omori and J. Kotera, **Circ Res**, *2007*, 100, 309-327.
3. C. S. Lin, S. Chow, A. Lau, R. Tu and T. F. Lue, **Int J Impot Res**, *2002*, 14, 15-24.
4. S. K. Kulkarni and C. S. Patil, **Methods Find Exp Clin Pharmacol**, *2004*, 26, 789-799.
5. R. Zoraghi, E. P. Bessay, J. D. Corbin and S. H. Francis, **J Biol Chem**, *2005*, 280, 12051-12063.
6. S. D. Rybalkin, I. G. Rybalkina, M. Shimizu-Albergine, X. B. Tang and J. A. Beavo, **EMBO J**, *2003*, 22, 469-478.
7. M. A. Blount, R. Zoraghi, H. Ke, E. P. Bessay, J. D. Corbin and S. H. Francis, **Mol Pharmacol**, *2006*, 70, 1822-1831.
8. Y. H. Jeon, Y. S. Heo, C. M. Kim, Y. L. Hyun, T. G. Lee, S. Ro and J. M. Cho, **Cell Mol Life Sci**, *2005*, 62, 1198-1220.
9. T. F. Lue, **N Engl J Med**, *2000*, 342, 1802-1813.
10. R. M. Wallis, J. D. Corbin, S. H. Francis and P. Ellis, **Am J Cardio**l, *1999*, 83, 3C-12C.
11. M. A. Blount, A. Beasley, R. Zoraghi, K. R. Sekhar, E. P. Bessay, S. H. Francis and J. D. Corbin, **Mol Pharmacol**, *2004*, 66, 144-152.
12. J. Corbin, S. Francis and R. Zoraghi, **Int J Impot Res**, *2006*, 18, 251-257.
13. H. Porst, H. Padma-Nathan, F. Giuliano, G. Anglin, L. Varanese and R. Rosen, **Urology**, *2003*, 62, 121-125; discussion 125-126.
14. B. J. Sung, K. Y. Hwang, Y. H. Jeon, J. I. Lee, Y. S. Heo, J. H. Kim, J. Moon, J. M. Yoon, Y. L. Hyun, E. Kim, S. J. Eum, S. Y. Park, J. O. Lee, T. G. Lee, S. Ro and J. M. Cho, **Nature,** *2003*, 425, 98-102.
15. J. D. Corbin, A. Beasley, M. A. Blount and S. H. Francis, **Neurochem Int**, *2004*, 45, 859-863.
16. S. H. Francis, I. V. Turko and J. D. Corbin, Prog **Nucleic Acid Res Mol Biol**, *2001,* 65, 1-52.
17. V. Manganiello, **Mol Pharmacol**, *2003*, 63, 1209-1211.
18. E. Bischoff, **Int J Impot Res**, *2004*, 16 Suppl 1, S11-14.
19. P. Dadvar, M. O'Flaherty, A. Scholten, K. Rumpel and A. J. Heck, **Mol Biosyst**, *2009*, 5, 472-482.
20. P. Dadvar, D. Kovanich, G. E. Folkers, K. Rumprl, R. Raijmakers and A. J. Heck, **in preparation**, *2009*.
21. H. Daub, K. Godl, D. Brehmer, B. Klebl and G. Muller, **Assay Drug Dev Technol**, *2004*, 2, 215-224.
22. M. Bantscheff, D. Eberhard, Y. Abraham, S. Bastuck, M. Boesche, S. Hobson, T. Mathieson, J. Perrin, M. Raida, C. Rau, V. Reader, G. Sweetman, A. Bauer, T. Bouwmeester, C. Hopf, U. Kruse, G. Neubauer, N. Ramsden, J. Rick, B. Kuster and G. Drewes, **Nat Biotechnol**, *2007*, 25, 1035-1044.
23. B. Valsasina, H. M. Kalisz and A. Isacchi, **Expert Rev Proteomics,** *2004*, 1, 303-315.
24. J. R. Freije and R. Bischoff, **J Chromatogr A**, *2003,* 1009, 155-169.
25. Y. Oda, T. Owa, T. Sato, B. Boucher, S. Daniels, H. Yamanaka, Y. Shinohara, A. Yokoi, J. Kuromitsu and T. Nagasu, **Anal Chem**, *2003*, 75, 2159-2165.
26. O. A. Mirgorodskaya, Y. P. Kozmin, M. I. Titov, R. Korner, C. P. Sonksen and P. Roepstorff, **Rapid Commun Mass Spectrom**, *2000*, 14, 1226-1232.
27. Y. Oda, K. Huang, F. R. Cross, D. Cowburn and B. T. Chait, **Proc Natl Acad Sci U S A**, *1999*, 96, 6591-6596.
28. S. P. Gygi, B. Rist, S. A. Gerber, F. Turecek, M. H. Gelb and R. Aebersold, **Nat Biotechnol**, *1999*, 17, 994-999.
29. A. Gilchrist, C. E. Au, J. Hiding, A. W. Bell, J. Fernandez-Rodriguez, S. Lesimple, H. Nagaya, L. Roy, S. J. Gosline, M. Hallett, J. Paiement, R. E. Kearney, T. Nilsson and J. J. Bergeron, **Cell**, *2006*, 127, 1265-1281.
30. H. Liu, R. G. Sadygov and J. R. Yates, 3rd, **Anal Chem**, *2004*, 76, 4193-4201.

31. M. P. Washburn, D. Wolters and J. R. Yates, 3rd, **Nat Biotechnol**, *2001*, 19, 242-247.
32. Y. Ishihama, Y. Oda, T. Tabata, T. Sato, T. Nagasu, J. Rappsilber and M. Mann, **Mol Cell Proteomics**, *2005*, 4, 1265-1272.
33. P. V. Bondarenko, D. Chelius and T. A. Shaler, **Anal Chem**, *2002*, 74, 4741-4749.
34. D. Chelius and P. V. Bondarenko, **J Proteome Res**, *2002*, 1, 317-323.
35. W. Wang, H. Zhou, H. Lin, S. Roy, T. A. Shaler, L. R. Hill, S. Norton, P. Kumar, M. Anderle and C. H. Becker, **Anal Chem,** *2003*, 75, 4818-4826.
36. M. Wang, J. You, K. G. Bemis, T. J. Tegeler and D. P. Brown, **Brief Funct Genomic Proteomic**, *2008*.
37. M. J. Palmer, A. S. Bell, D. N. Fox and D. G. Brown, **Curr Top Med Chem,** *2007*, 7, 405-419.
38. A. Scholten, M. K. Poh, T. A. van Veen, B. van Breukelen, M. A. Vos and A. J. Heck, **J Proteome Res**, *2006*, 5, 1435-1447.
39. L. Trinkle-Mulcahy, S. Boulon, Y. W. Lam, R. Urcia, F. M. Boisvert, F. Vandermoere, N. A.Morrice, S. Swift, U. Rothbauer, H. Leonhardt and A. Lamond, **J Cell Biol**, *2008*, 183, 223-239.
40. J. Gobom, E. Nordhoff, E. Mirgorodskaya, R. Ekman and P. Roepstorff, **J Mass Spectrom**, *1999*, 34, 105-116.
41. P. J. Boersema, T. T. Aye, T. A. van Veen, A. J. Heck and S. Mohammed, **Proteomics,** *2008*, 8, 4624-4632.
42. P. J. Boersema, R. Raijmakers, S. Lemeer, S. Mohammed and A. J. Heck, **Nat Protoc**, *2009*, 4, 484-494.
43. M. W. Pinkse, P. M. Uitto, M. J. Hilhorst, B. Ooms and A. J. Heck, **Anal Chem**, *2004*, 76, 3935-3943.
44. L. Kall, J. D. Storey, M. J. MacCoss and W. S. Noble, **J Proteome Res**, *2008*, 7, 29-34.
45. R. E. Moore, M. K. Young and T. D. Lee, **J Am Soc Mass Spectrom,** *2002*, 13, 378-386.
46. M. Bantscheff, M. Schirle, G. Sweetman, J. Rick and B. Kuster, **Anal Bioanal Chem,** *2007*, 389, 1017-1031.
47. Q. Huai, Y. Liu, S. H. Francis, J. D. Corbin and H. Ke, **J Biol Chem,** *2004*, 279, 13095-13101.
48. R. Zoraghi, J. D. Corbin and S. H. Francis, **J Biol Chem**, *2006*, 281, 5553-5558.
49. A. S. Bell, d. Brown and N. K. Terrett, **GB**, *1995*.
50. S. K. Florio, R. K. Prusti and J. A. Beavo, **J Biol Chem**, *1996*, 271, 24036-24047.
51. P. G. Gillespie and J. A. Beavo, **Proc Natl Acad Sci U S A**, *1989*, 86, 4311-4315.
52. C. Yan, A. Z. Zhao, W. K. Sonnenburg and J. A. Beavo, **Biol Reprod**, *2001*, 64, 1746-1754.
53. F. Schoentgen and P. Jolles, **FEBS Lett**, *1995*, 369, 22-26.
54. G. Odabaei, D. Chatterjee, A. R. Jazirehi, L. Goodglick, K. Yeung and B. Bonavida, **Adv Cancer Res,** *2004*, 91, 169-200.
55. N. Trakul and M. R. Rosner, **Cell Res**, *2005*, 15, 19-23.
56. E. T. Keller, Z. Fu and M. Brennan, **J Cell Biochem**, *2005*, 94, 273-278.
57. P. C. Simister, M. J. Banfield and R. L. Brady, **Acta Crystallogr D Biol Crystallogr,** *2002*, 58, 1077-1080.

Supplementary

Supplementary tables:
http://www.babak-dadvar.com/Thesis/Poupak.html

Chapter 5

Summary/Samenvatting

I. Background

Sexual dysfunction is a major public health concern, which tends to be more prevalent in the older population. The number of males affected by erectile dysfunction (ED), one of the most common forms of sexual dysfunction, is estimated to be more than 100 million people worldwide[1]. An underlying cause of erectile dysfunction can be impaired NO/cGMP signaling which leads to blunted vasodilation. Selective manipulation of the NO/cGMP pathway can induce vasodilation, which promotes erectile function and is therefore of significant pharmacological and therapeutic interest for the treatment of ED[2]. A dominant molecular player in the biology of penile erection and the NO/cGMP pathway is the phosphodiesterase type 5 (PDE5) protein. PDE5 controls the erectile response by degrading 3' ,5' –cyclic guanosine monophosphate (cGMP), the second messenger product of the erection promoting nitric oxide (NO) signaling pathway[3]. An effective pharmacological tool in treatment of ED is the selective inhibition of PDE5. Approved PDE5 inhibitors for the treatment of ED include sildenafil (Viagra), vardenafil (Levira) and tadalafil (Cialis)[4], all of which are considered very specific and ‘safe’ drugs. However, even highly selective, FDA approved, drugs can have the potential to bind to other, unintended, targets, possibly leading to side effects. Some reported side effects observed during ED treatment include headache, flushing and transient visual problems. Understanding the molecular causes of such side effects is an important part of the drug development process and can help in the understanding of the mechanisms of drug action. In the past two decades, a number of new, semi high-throughput technologies have been introduced to identify the protein interactomes of specific inhibitors and/or drugs. Recombinant proteins can be used, for instance using protein arrays, to characterize a drug interactome[5]. However, the production of recombinant proteins on a proteome wide scale is not yet easily feasible and in addition purified recombinant proteins do not necessarily accurately reflect biological levels or isoforms of target proteins. Nowadays, mass spectrometry based proteomic methods are becoming popular to identify specific drug interactomes. One method in chemical proteomics, also applied in this thesis, that uses the immobilization of a drug to an affinity support (e.g. beads). In this strategy it is of central importance that the modified derivative drug molecule retains its biological activity when immobilized to the matrix. The immobilized drugs can then be used to fish for interacting proteins from a complete cellular or tissue lysate. A major challenge for the identification of a drug interactome is to make the distinction between specific and non- or less-specific interactors. There often are high abundant proteins present in a lysate, which can have a relatively low affinity for the drug. Additionally, proteins may also have (so called non-specific) interactions not to the drug, but to the affinity matrixes or a linker molecule used to link the drug to the affinity matrix. For the work described in this thesis, to profile the specific interactors of the sildenafil/vardenafil class of PDE5 inhibitors, we synthesized a number of PDE5 inhibitor derivatives, that we subsequently immobilized on agarose beads. The research initially focused on the optimization of the aforementioned methodology to reduce nonspecific binding to the immobilized PDE5 inhibitor derivatives and improve the dynamic range in the mass spectrometry based analysis. Next, quantitative proteomics was implemented and applied to determine the specificity of the interactions in more detail.

II. Results

The primary goal of the research described in this thesis was profiling the mammalian proteome for proteins that interact with derivatives of clinically used PDE5 inhibitors, of which the structure was based on the known inhibitors sildenafil and vardenafil. An integrated strategy, namely mass spectrometry based chemical proteomics, was the key method used to unravel the protein 'interactome' of these inhibitors. ***Chapter 1*** provides a short overview of NO/cGMP signaling events underlying vasodilation and erectile (dys)function. In particular, the structure-function relationship of the protein PDE5 receives attention here, as it is a very important molecular player in this signaling pathway, and inhibition of PDE5 leads to improved erectile function. PDE5 also is an ideal, challenging, drug target for a proof of concept to show that chemical proteomics can be used to probe the interactome of a drug, because of its the low intracellular concentration and that of its natural substrate cGMP, requiring a very potent inhibitor to compete with the natural substrate[6]. This in turn results in increased specificity of drug-protein interactions with hopefully minimal side effects. Chapter 1 also provides a description and comparison of the three clinically FDA approved PDE5 inhibitors (sildenafil, vardenafil and tadalafil) in terms of their pharmacokinetics and pharmacodynamics. Vardenafil seems to be a more selective inhibitor in comparison with sildenafil, while tadalafil shows a longer half life in vivo[7].

In ***Chapter 2***, the optimization and application of a chemical proteomics approach to limit, and recognize, nonspecific interactors of a PDE5 inhibitor is described. A PDE5 inhibitor (termed PF-4540124) was immobilized on an affinity matrix and used in a pull-down assay with mouse lung tissue. To reduce binding of non-specific proteins, nucleotides (GDP and ADP) were added to the cell lysate, which suppressed the binding of a plethora of generic nucleotide binding proteins (e.g. ATP interacting proteins), which otherwise can bind to the immobilized inhibitor. In addition, only specifically interacting proteins were eluted from the matrix by competition with the soluble inhibitor molecule, meaning proteins nonspecifically interacting with the matrix itself were largely excluded from the analysis. To be able to better differentiate specific interactions, the PF-4540124 interactomes originating from nucleotide treated cell lysates and untreated cell lysates were compared using differential stable isotope labeling. Apart from the expected target, PDE5, several other specifically interacting proteins were identified. These included a PDE5 isoform which was identified based on its modified N-terminus and the PDE6δ subunit delta (also known as prenyl binding protein, PrBP). Intriguingly, PDE6δ/PrBP is not a phosphodiesterase and has no sequence homology with PDE5, but instead is a protein that can bind to the catalytic subunit of the PDE5 related (homologue) enzyme PDE6α or PDEß. To exclude binding of PrBP via PDE5 or PDE6, its specific and direct interaction with PF-4540124 was confirmed with an in vitro pull-down assay using recombinant PrBP as well as by tryptophan fluorescence spectroscopy.

Following the optimization of the pull-down assay, the interactome of another, closely related, PDE5 inhibitor (termed PF-3717842) in rat testis tissue was determined in ***Chapter 3***, as that tissue was hypothesized to contain more proteins potentially related to ED. Using the optimized protocol, also in this tissue PDE5 and PrBP were identified as specific interactors. But, in addition to these now known interactors, another protein, phosphatidyl ethanol amine binding protein-2 (PEBP-2) was found to specifically interact with the PDE5 inhibitor in this tissue. PEBP-2 is a testis specific protein that is only present in rodents and which has been suggested to play a role in spermiogenesis[8]. A closely related protein, PEBP-1, however, is present in many tissues of all mammalian species. This protein is also known as raf kinase inhibitory protein (RKIP) and is an important molecular player in the mitogen activated protein kinase (MAPK) signaling pathways. The specific interaction of mouse PEBP-2 and PEBP-1, as well as that of human PEBP-1/RKIP was confirmed by an in-vitro pull-down assay using PF-3717842 immobilized beads on both recombinant proteins as well as cellular (HeLa) lysate. This interaction was further characterized by tryptophan fluorescence and NMR spectroscopy, revealing an affinity of the phosphatidylenoalamine binding proteins for the inhibitor in the μM range, suggesting a potential use of PF-3717842 or derivatives for the inhibition of RKIP.

The specificity of different analogues of sildenafil and vardenafil is compared in ***Chapter 4***. Four closely related inhibitors, including those used in chapters 2 and 3 were immobilized and the binding proteins from rat testis tissue analyzed by differential quantitative chemical proteomics. Using two different quantitative mass spectrometric approaches, based on unique peptide counts and stable isotope labeling, it is shown that each of these inhibitors has a characteristic selectivity profile, which can be related directly to their affinity (IC50) for PDE5. It is shown that two of the inhibitors display reduced affinity for PDE5, but increased affinity for either PrBP or PEBP-2, showing that slight chemical modifications in the specific binding sites of these PDE5 inhibitors can favor the binding of other specific interacting proteins, opening up the possibility that such compounds could be modified further to be specific inhibitors for these proteins or protein families.

III. Conclusion

In the research described in this thesis, the interactome of several, closely related, PDE5 inhibitors was characterized to obtain further insight in their ability to bind proteins other than PDE5. The pull-down affinity experiments were optimized to decrease binding of non-specific proteins. The optimized pull-down assay was then combined with high resolution quantitative proteomics to get a clear and unbiased insight into the protein interactors of PDE5 inhibitors. Several new specific interacting proteins were identified and verified and it was shown that slight modifications of the inhibitors can alter their specificity to favor these new protein targets. Throughout the work described in this thesis it has become evident that chemical proteomics can be an effective approach to describe the interactome of drugs but that it can also be used to identify potential new targets of known compounds, opening up the possibility to identify new potential therapeutic uses for known and approved drugs.

IV. References:

1. Cheitlin, M.D., et al., Use of sildenafil (Viagra) in patients with cardiovascular disease. *T*echnology and Practice Executive Committee. **Circulation**, *1999*. 99(1): p. 168-77.
2. Lohse, M.J., U. Forstermann, and H.H. Schmidt, Pharmacology of NO:cGMP signal transduction. **Naunyn Schmiedebergs Arch Pharmacol**, *1998*. 358(1): p. 111-2.
3. Burnett, A.L., Molecular pharmacotherapeutic targeting of PDE5 for preservation of penile health. **J Androl**, *2008*. 29(1): p. 3-14.
4. Montague, D.K., et al., Chapter 1: The management of erectile dysfunction: an AUA update. **J Urol,** *2005*. 174(1): p. 230-9.
5. Schofield, M.J., N. Sharma, and H. Ge, The recombinant protein array: use in target identification and validation. **Drug discovery today: targets,** *2004.* 3: p. 246-252.
6. Bender, A.T. and J.A. Beavo, Cyclic nucleotide phosphodiesterases: molecular regulation to clinical use. **Pharmacol Rev**, *2006*. 58(3): p. 488-520.
7. Mehrotra, N., et al., The role of pharmacokinetics and pharmacodynamics in phosphodiesterase-5 inhibitor therapy. **Int J Impot Res**, *2007*. 19(3): p. 253-64.
8. Hickox, D.M., et al., Identification of a novel testis-specific member of the phosphatidylethanolamine binding protein family, pebp-2. **Biol Reprod**, 2002. 67(3): p. 917-27.

I. Achtergrond

Sexuele stoornissen zijn een significant medisch probleem, en blijken voornamelijk voor te komen onder ouderen. Het aantal mannen dat lijdt aan erectiestoornissen, één van de meest belangrijke aandoeningen binnen het gebied van sexuele problemen, wordt geschat op meer dan 100 miljoen personen wereldwijd. Bij personen met erectieproblemen blijkt de NO/cGMP signaalroute, die betrokken is bij vasodilatatie (vaatverwijding), niet goed te functioneren. Door deze signaalroute te manipuleren is het mogelijk om vaatverwijdering te induceren, en daarmee ook een erectie. Er is vanuit de farmaceutische industrie dan ook grote interesse voor het moleculaire mechanisme van de NO/cGMP route.

Een eiwit dat betrokken is bij het tot stand komen van een erectie, en een dominante rol speelt in de NO/cGMP signaalroute, is het fosfodiesterase type 5 (PDE5). PDE5 controleert het erectieproces doordat het 3’,5’-cyclisch guanosine monofosfaat (cGMP) kan afbreken. cGMP is een zogenaamd second messenger, dat wil zeggen dat cGMP de functie van verschillende eiwitten kan beïnvloeden. Zo blijkt ook dat cGMP de NO route aanstuurt. Wanneer er teveel cGMP wordt afgebroken door PDE5, lijdt dat bij mannen tot erectiestoornissen.

Een effectieve behandelingsmethode voor deze problemen is het remmen van PDE5. Toegestane PDE5 remmers, vanuit de farmaceutisch industrie, zijn sildenafil (Viagra), vardenafil (Levira) en tadalfil (Cialis). Deze middelen zijn goedgekeurd door de FDA (Food and Drug Administration) en worden als specifiek gericht voor de kwaal, en veilig beschouwd. Toch is het zeer goed mogelijk dat ook deze “veilige en specifieke” geneesmiddelen bijwerkingen hebben. Dit kan komen doordat het geneesmiddel bijvoorbeeld niet alleen PDE5 herkend maar ook interacties kan aangaan met andere eiwitten. Bekende bijwerkingen van Viagra, Levira en Cialis zijn hoofdpijn, tijdelijk wazig gezichtsvermogen en blozen. Het begrijpen van deze effecten op moleculair niveau is belangrijk bij het maken van nieuwe medicijnen.

In de laatste jaren zijn er verschillende (semi-high througput) technologieën ontwikkeld voor de identificatie van interacterende eiwitten (interactoom) met een bepaald medicijn. Zo kunnen bijvoorbeeld eiwit assays worden gebruikt, waarbij gebruik wordt gemaakt van recombinante eiwitten, om te karakteriseren welke eiwitten met het medicijn binden. Echter het maken van zoveel eiwitten als in het proteoom voorkomen is niet haalbaar. Ook kunnen de recombinant gemaakte eiwitten anders reageren op het medicijn waardoor de resultaten niet de biologische werkelijkheid hoeven te representeren.

Tegenwoordig is massaspectrometrie een veel gebruikte methode binnen de proteomics om eiwitten te identificeren, en daarmee binnen het medicijn onderzoek. Een specifieke methode, die ook in dit proefschrift is toegepast, valt binnen de zogenoemde chemische-proteomics. Hierbij wordt het medicijn van interesse op een drager-materiaal (bead) geïmmobiliseerd. Dit materiaal kan relatief eenvoudig worden gezuiverd, en het medicijn hierop interacteert met eiwitten die aanwezig zijn in het lysaat/weefsel. Hierdoor is het mogelijk de eiwitten van interesse te isoleren en te identificeren. Uiteraard is het bij deze aanpak een vereiste dat de functionele eigenschappen van het medicijn na koppeling aan het drager-materiaal onveranderd blijven. Een grote uitdaging bevindt zich ook in het onderscheid kunnen maken tussen specifiek en niet-specifiek (of minder specifiek) inter-acterende eiwitten met het medicijn. Vaak worden eiwitten die in zeer grote hoeveelheden in cellen voorkomen geïdentificeerd. Ook al is de affiniteit van deze eiwitten erg laag, door de abundantie zullen toch enkele van deze eiwitten blijken te binden, zij het aan het medicijn, ofwel aan het drager-materiaal.

Het werk dat beschreven is in dit proefschrift richt zich op de identificatie van sildenafil/vardenafil (PDE5 remmers) inter-acterende eiwitten. Verschillende derivaten van PDE5 remmers zijn gesynthetiseerd en vervolgens geïmmobiliseerd op agarose-bolletjes (het drager-materiaal). In eerste instantie was het onderzoek gericht op het optimaliseren van de chemische-proteomics methode, en dan met name het verminderen van niet-specifieke interacterende eiwitten. Door deze aspecifieke binding tegen te gaan kunnen de werkelijk specifiek met sidenafil/vardenafil interacterende eiwitten eenvoudiger worden geïdentificeerd met behulp van massaspectrometrie. Tot slot is er ook gebruik gemaakt van kwantitatieve proteomics om de specificiteit van de interacterende eiwitten in meer detail te kunnen bestuderen.

II. Resultaten

Het doel van het beschreven onderzoek was het in kaart brengen van de menselijke eiwitten die interacteren met derivaten van de hedendaags gebruikte PDE5 remmers. Hierbij werd gefocust op de bekende remmers, sidenafil en vardenafil. Gebruik werd gemaakt van reeds bestaande methode, chemische proteomics. In hoofdstuk 1 wordt de NO/cGMP signaalroute beschreven, die betrokken is bij vaatverwijdering en erecties (en erectie-stoornissen). Centraal staat de structuur/functie relatie van het eiwit PDE5. Het is bekend dat remming van PDE5 een erectie mogelijk maakt. Om te bewijzen dat de chemische proteomics strategie geschikt is voor het in kaart brengen van het interactoom van een medicijn, is PDE5 een geschikt en uitdagend target. PDE5, en zijn natuurlijke substraat cGMP, komen beide slechts in zeer lage concentraties voor in de cel. Tevens zullen nieuw te identificeren interactoren van PDE5 moeten competeren met cGMP. Wanneer specifiek interacterende eiwitten worden gevonden kunnen deze verder worden ontwikkeld tot medicijnen. Dit zal hopelijk ook leiden tot een behandeling met weinig bijwerkingen.

Verder worden in dit hoofdstuk de fysische eigenschappen van sildenafil, vardenafil en tadalafil besproken. De meest selectieve PDE5 remmer is vardenafil, en tadalafil heeft de langste halfwaardetijd in vivo.

Hoofdstuk 2 beschrijft de optimalisatie van de chemische proteomics methode, om het binden van niet-specifieke PDE5 remmers te beperken. PF-4540124, een PDE5 remmer, werd geïmmobiliseerd op drager-materiaal en gebruikt in een pull-down experiment op muizen long weefsel. Om de binding van niet-specifieke eiwitten tegen te gaan werden GDP en ADP toegevoegd. Hierdoor bonden de algemeen nucleotide bindende eiwitten niet langer aan de PDE5 remmer. Om de specifiek bindende eiwitten te elueren van de geïmmobiliseerde PDE5 remmer werd deze zelfde remmer (PF-4540124) in oplossing toegevoegd, deze was uiteraard niet gebonden aan het drager-materiaal. De eiwitten die aspecifiek aan dit materiaal bonden worden op deze wijze ook verwijderd. Uiteindelijk werd er nog gebruik gemaakt van differentiële stabiele isotoop labeling om de werkelijk specifieke interactoren van de PDE5 remmer te bepalen. Cel-lysaat van het muizen longweefsel dat was behandeld met GDP en ADP, werd vergeleken met onbehandeld cel-lysaat.

Naast de identificatie van PDE5, werden ook enkele nieuwe targets geïdentificeerd van de PDE5 remmer; waaronder een isovorm van PDE5, waarvan de N-terminus was gemodificeerd, en PDE6δ subunit delta (ook wel bekend als prenyl binding protein, PrBP). Opmerkelijk is dat PrBP geen fosfodiesterase is, en ook geen sequentie homologie heeft met PDE5. PrBP bindt normaal gesproken aan de katalytische subunit van PDE6α (of PDEß), een PDE5 gerelateerd enzym. Uit een in vitro pull down experiment met recombinant PrBP, en tryptofaan fluorescentie spectroscopie experimenten, bleek de interactie tussen PrBP en PF-4540124 direct.

Het in ***hoofdstuk 3*** beschreven onderzoek richtte zich op de identificatie van het interactoom van een andere PDE5 remmer, PF-3717842. In deze studie werd gebruik gemaakt van teelbal weefsel uit een rat. Waarschijnlijk geven de resultaten verkregen met dit weefsel meer inzichten in de eiwitten die tevens zijn betrokken bij humane erectiestoornissen. Ook in deze studie werd naast PDE5, PrBP geïdentificeerd als specifieke interactor. Echter een derde eiwit werd gevonden, namelijk fosfatidyl ethanol amine binding protein-2 (PEBP-2). PEBP-2 is alleen aanwezig in testikel weefsel van knaagdieren, en is mogelijk betrokken bij de vorming van zaadcellen. PEBP-2 is gerelateerd aan het humane PEBP-1, wat voorkomt in verschillende soorten weefsel. PEBP-1 is een raf kinase remmend eiwit (RKIP) en betrokken bij de MAPK kinase signaalroute (welke celdeling stimuleert). Met in vitro pull-down experimenten is de specifieke interactie van muis PEBP-2 en PEBP-1, zowel als die van humaan PEBP-1/RKIP, bevestigd. Hierbij is gebruik gemaakt van recombinante eiwitten en cel-lysaat (HeLa cellen). De interactie tussen deze eiwitten en de PDE5 remmer is verder gekarakteriseerd met NMR spectroscopie en tryptofaan fluorescentie spectroscopie. Fosfatidylenoalamine bindende eiwitten bleken een micromolaire affiniteit voor PF-3717842 te hebben. Mogelijk kan deze PDE5 remmer, of derivaten ervan, worden gebruikt voor de remming van RKIP.

De specificiteit van verschillende sildenafil en vardenafil analogen is vergeleken in ***hoofdstuk 4***. Vier gerelateerde remmers, inclusief PF-4540124 en PF-3717842, werden op drager-materiaal geïmmobiliseerd. Vervolgens werden er differentiële kwantitatieve chemische proteomics studies gedaan op teelbal weefsel van ratten. Twee verschillende kwantitatieve massaspectrometrische methodieken zijn toegepast, de eerste is gebaseerd op het voorkomen van unieke peptide sequenties, de tweede aan de hand van stabiele isotoop labeling. Elke remmer bleek een karakteristiek eigen interactoom te hebben, welke direct gerelateerd was aan de affiniteit (IC50) van de remmers voor PDE5. Twee van de PDE5 remmers bleken lage affiniteit voor PDE5, en een hoge affiniteit voor PrBP of PEBP-2, te vertonen. Relatief kleine chemische modificaties in de specifieke bindings-plaatsen van de remmers hebben dus als gevolg dat de remmers liever andere eiwitten binden dan PDE5. Dit creëert ook mogelijkheden, aangezien op deze wijze specifieke remmers voor andere eiwitten gemaakt kunnen worden.

III. Conclusie

Met het onderzoek beschreven in dit proefschrift is het interactoom van enkele gerelateerde PDE5 remmers bepaald. Hierdoor zijn de mogelijkheden van deze remmers om naast PDE5 ook andere eiwitten te binden in kaart gebracht. De pull-down aanpak (chemische proteomics) is geoptimaliseerd om de identificatie van niet-specifiek bindende eiwitten aan de remmers te voorkomen. Deze aanpak werd vervolgens gecombineerd met kwantitatieve proteomics. Dit heeft geleid tot de identificatie van enkele nieuwe eiwitten die direct interacteren met PDE5 remmers. Kleine veranderingen in deze remmers kunnen de bindings-specificiteit van de remmers veranderen, waardoor PDE5 niet langer met de hoogste affiniteit bindt.

Al het beschreven onderzoek laat zien dat chemische proteomics een effectieve methode is om het interactoom van een medicijn te karakteriseren. Door het identificeren van alle interacterende eiwitten van een bestaand medicijn ontstaan tevens mogelijkheden voor de toepassing van deze middelen voor andere aandoeningen.

Dankwoord

De 4 jaren zijn omgevlogen, jaren van plezier maar ook van bijbehorende frustraties. Plezier vanwege de kennismaking met veel mensen in een wetenschappelijke wereld waarvan je veel kan leren. Niet alleen over de wetenschap maar ook over sociale vaardigheden. De frustraties vanwege niet uitkomende en verwachte resultaten, maar vooral vanwege de strategie van Pfizer, waarvan uiteindelijk bleek dat zij een project hadden voorgesteld waarover niets mocht worden gepubliceerd.

Ik wil hier graag een aantal mensen bedanken, die zonder hun hulp ik dit werk en deze mooie ervaring nooit had kunnen realiseren. Ze weten zelf hoe belangrijk hun aandeel was in dit onderzoek.

Allereerst wil ik mijn promotor bedanken, vooral voor de mooie kans die ik kreeg om in één van de bekendste “proteomics” groepen in Nederland te gaan werken. Bedankt voor jouw enthousiasme en optimisme over dit onderzoek. In het bijzonder deze eigenschappen vind ik heel belangrijk voor een wetenschappelijke leider. Als er uit het onderzoek mooie resultaten kwamen, zat jij meteen achter mijn computer. Je wilde alles weten en kwam met voorstellen die naderhand meestal heel slimme ideeën waren. Ik wil je in het bijzonder ook graag bedanken voor je support, toen bleek dat Pfizer de resultaten niet apprecieerde en onduidelijk was wat er met dit project ging gebeuren.

Reinout, die halverwege het project in onze groep kwam, wil ook ik graag bedanken. Je hebt een hele grote wetenschappelijke waarde aan mijn onderzoek toegevoegd, maar naar mijn mening ook aan de hele groep. Dit onderzoek had waarschijnlijk geen goed einde kunnen krijgen zonder je enorme inzet en begeleiding. Hiervoor bedankt, maar ook voor de vakkundige manier waarop je mij hebt begeleid, terwijl ik weet dat je het altijd al zo druk had. Gelukkig hoefde je de interesse voor de andere projecten niet te verminderen vanwege de capaciteiten die je hebt!

Arjen, ook jou wil ik enorm bedanken voor alles wat ik van je heb geleerd. Je bent in korte tijd een kei geworden in “chemical proteomics”, terwijl je het ook heel druk had met je grote taak als papa. Over de interpretatie van de resultaten heb ik veel van je geleerd, waardoor je op een bepaald moment een groot aandeel in de begeleiding had. Ik vond onze gesprekken over de kinderen erg gezellig. Ik stel het erg op prijs dat je in de promotie commissie zit.

Martijn, de basis van dit vak heb ik van jou geleerd en wil ik je hiervoor graag bedanken. Je kennis over “mass spectrometry” en over alle apparaten is heel breed. Ik ben heel blij dat je een aanstelling als universitair docent bij de Universiteit van Delft hebt gekregen, je hebt het echt verdient.

Veel dank gaat uit naar de mensen die mij dagelijks op de werkvloer omringden en waarmee ups en downs in het werk werden gedeeld. Ik wil graag Martina bedanken voor alle support en begrip die je voor mij hebt getoond. Ik zal altijd met plezier terug kijken op onze gesprekken over de moederschapstaak en de gezellige lunches. Esther, jou wil ik heel erg bedanken voor de vriendschap en het begrip en voor alles dat ik met je deelde. Je hebt ook een wetenschappelijke bijdrage gehad in dit werk, bedankt voor alle metingen die je hebt gedaan. Ook natuurlijk voor de mooie Nederlandse vertaling van de samenvatting die je van dit onderzoek maakte. Simone, met wie ik een groot deel van de tijd de kamer en lief en leed deelde, was altijd aardig. Bedankt voor de leuke tijd en je steun toen ik me even niet goed voelde. Ik hoop dat je altijd zo vrolijk blijft als ik je heb leren kennen. Soenita, die altijd als eerste voor de hele groep zorgde. Die zorgzaamheid en aardigheid vond ik heel bijzonder. Bedankt voor je steun, en heel wijze adviezen.

Nu ik dit dankwoord schrijft merk ik hoe moeilijk ik het vind om de beste woorden te kiezen. Mijn Nederlandse woordenschat is niet zo groot om iedereen op een heel mooie manier te bedanken!

Mirjam, bedankt voor de kennis die je mij het aangereikt bij het gebruik van “MALDI”, het enorme geduld waarmee mij één en ander leerde heb ik erg op prijs gesteld. Bedankt voor je support en alle gezelligheid.

Thin Thin, wat moet ik over jou gaan schrijven. Je kunt heel goed Nederlands lezen, afgezien van de korte tijd waarin je het hebt geleerd. Ik heb een mooie tijd met je gehad en vond de activiteiten die je voor je land doet altijd heel bijzonder, dit terwijl je hier zit en zo bezig bent met je werk. Je kon mij altijd zo goed begrijpen. Nadia, de eerste woorden over jou die in mijn gedachten komen zijn “vrolijk en moedig”. Je positieve uitstraling is heel bijzonder en ik heb leuke herinneringen van je. Paul, in jou zie ik een heel aardige en slimme collega. Je weet hoe je zaken moet aanpakken en hoe je onderzoeken goed kunt publiceren. Bedankt voor het afscheidsfeest en de organisatie hiervan.

Sharon, wat moet ik schrijven dat niet lijkt op wat ik voor anderen al schreef. Je was In korte tijd de expert van de apparaten en je wilde altijd de beste metingen voor iedereen maken. Je aardigheid en vrolijkheid zijn bijzondere aspecten van jou. Ik spreek de wens uit dat we met elkaar in contact blijven.

Shahram, mijn aardige landgenoot die altijd voor me klaar stond. Veel dank voor je steun en de leuke gesprekken.

Bas, Onze slimme bio-informatica deskundige. Ik was altijd verbaasd dat je vader van drie kinderen bent, vooral op die momenten dat je door de gang rende en sprong. Bedankt voor alle support en “alignements” en ook voor de hulp die je me het op het laatste moment gaf.

Mijn aardige collega Onno, de leuke tijd op het lab met jou vergeet ik niet. Je was altijd vroeg op het lab als je iets moest doen en de muziek moest dan meteen aan. Nee hoor, die muziek stoorde mij niet, je mocht het zo hard aanzetten als je wilde. Ik wens je het beste met je grote taak als vader.

Klaus, I don’t think that you can easily find somebody to translate the following for you, thus I write it in English. You were my supervisor in Pfizer that always helped me and gave me suggestions. I have to confess, sometimes I was confused with all your scientific suggestions. But they were indeed worthy for me. Your enthusiasm is very special in the supervision and I do not forget your hospitality when I was in Canterbury. I also like to thank Frank from Pfizer for his support and specially Pfizer company in England for the financial support.

Serena, It was a pleasure to share the office with you at the old building. I like your happy and positive appearance and enthusiasm. Good luck with your project.

Donna, In the beginning of your internship you showed quickly that you were capable to have your own project and afterwards began with the four years journey! Good luck with everything.

It was very nice at the last 4 months to share the office with you, Sara. I wish the best for you and Glen and hope to see as much as possible in this country.
Joost het was gezellig met je de laatste vier maanden op één kamer te werken. Bedankt voor alle hulp bij computer gerelateerde zaken en de wetenschappelijke support vooral in de “MSQUANT”. Veel succes met je grote avontuur in Canada.

Verder zeg ik tegen Maarten, Kees en Arjan (bedankt voor alle metingen), Corine,Monique, Marco, Javier, Jefry, Andrias, Tinieke, Adja, Chhiti, Nikolai, Gideon, Henk, Rebecca en Charlotte; bedankt. Shabaz, the expert in mass spectrometry I have also learned a lot from you and I appreciate all your help and support.

Goede vrienden en familie zijn natuurlijk onmisbaar in een zodanig lang traject.

Cristianne en Maarten, het heeft geen zin om jullie voor onze vriendschap te bedanken, want daar schieten woorden toch tekort voor.
Ik wil het hier niet in de privésfeer gaan schrijven maar, Christianne wat je voor mij hebt gedaan daar blijf ik altijd dankbaar voor en ik vind je heel bijzonder mens. Andere goede vrienden, Marianne en Henk, Marjolein en Leo, ik heb een heel leuke tijd met jullie gedeeld. Marjam, je bent de beste Iranese vriendin

die ik hier heb en ik kon over alles met je praten. Natuurlijk is ons vriendschap heel waardevol voor mij. My good friends in Iran , Poupak, Simin, Shaghayegh and Parisa. I do not forget the nice memories and the fruitful time I have had with you.

Pauline en Hugo, ik wil jullie erg bedanken voor alle steun en de leuke tijd. Pauline je hebt een groot hart en dat maakt je een bijzondere vrouw. Jullie zijn voor ons altijd bijzonder lief. Geniet van al jullie mooie kleinkinderen!
Mijn lieve oom Behrouz, bedankt voor alle steun. Ik kan altijd op jou terug vallen als ik een probleem heb en je staat altijd voor mij klaar. Maar natuurlijk ga ik niet altijd naar alle adviezen van je luisteren! Je bent heel lief voor mij.
Henk, de beste vriend in Nederland, ik wil je graag bedanken voor alle steun vanaf het begin. Je bent aardig en je gastvrijheid en wijze adviezen vind ik heel bijzonder. Je zette alles op alles om mij altijd te helpen. Heel lief vind ik dat.

My dear mother and father thanks for all you have done for me. You did your best and I dedicate, not only this book, but also whole my efforts and life to you. My dear brothers Babak and Siamak , you are the best brothers in the world!

Mijn Lieve echtgenoot Nashwan, er valt niks te bedanken, want tussen ons is de afstand zo klein dat alles wat wij voor elkaar doen er gewoon bij hoort!!!
Als allerlaatste wil ik de naam van het dierbaarste wat ik in de wereld heb in dit boek schrijven,

Nora, zoals de betekenis van je naam ben je het grote licht in mijn leven. Ik hou van je.

Poupak

Curriculum Vitae

Poupak Dadvar was born on 14th September 1976 in Tehran, Iran. In June 1995 she was graduated from high school then began to study chemistry at the University of Gilan. In September 1999 she passed the National Academic Entrance Exam for a master education in organic chemistry which took 2 years. Finally she got the master degree in organic chemistry in 2001. After that in 2002 following continuing her education, she started studying bimolecular sciences at Utrecht University in the Netherlands and in the end succeeded to achieve the diploma in 2004. In February 2005, she started PhD research project in the biomedical analysis group, at Utrecht University and worked on the identification of a drug interactome using the chemical proteomics method, under supervision of Prof. Dr. A.J.R Heck resulting in a thesis entitled
“**probing the drug interactome using chemical proteomics**”.
At this moment she is working at the biological research and development’s group at Solvay Biologicals.

Notes